Dynamical Processes in Crystalline Organometallic Complexes

DARIO BRAGA

Dipartimento di Chimica "G. Ciamician", University of Bologna, 40126 Italy

Received October 29, 1991 (Revised Manuscript Received February 24, 1992)

Contents

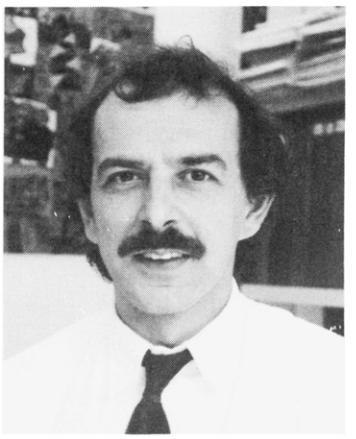

Dario Braga was born in Bologna, Italy, in 1953. After he graduated with a degree in Chemistry in 1977, he obtained a fellowship from the Consiglio Nazionale delle Ricerche to study the structural chemistry of transition metal carbido–carbonyl clusters of the cobalt subgroup. He then spent a year on a postdoctoral position at the Polytechnic of North London working on the structure of high nuclearity clusters of ruthenium and osmium. He joined the Faculty of Science of the University of Bologna in 1982, where he is currently Associate Professor of General and Inorganic Chemistry. He obtained the Raffaello Nasini award from the Inorganic Chemistry Division of the Italian Society of Chemistry in 1988 for his studies on the factors controlling molecular structure and fluxional behavior. His current research interests are focused on the static and dynamic aspects of the structure of mononuclear and polynuclear organometallic molecules and on the relationship between solid-state properties and molecular organization in organometallic crystals.

I. Introduction

Most chemists (and crystallographers) involved in the organometallic chemistry field are accustomed to regarding a crystal as a mere molecular container in which the fundamental component (the molecule) is replicated in the three directions of space by a combination of symmetry operations and translations. With this idea in mind it is difficult to appreciate that some *collective* molecular properties in a crystal may differ substantially from the properties of an *individual* molecular entity ideally present in the gas phase, or from the molecular properties in solution.

A crystal is, undeniably, the most specialized molecular ensemble: an extremely sophisticated process of molecular self-recognition and self-assembling controls the construction of such a "giant supramolecule". The relationship between molecular and crystal properties is, however, a most elusive one: although the molecular "characteristics" (size, shape, chemical bonding, intramolecular nonbonding effects, charge, polarity, etc.) certainly dictate how the crystal is constructed, intermolecular interactions within the lattice ultimately control how the crystalline material reacts, transforms, or behaves with temperature or pressure.

Organic solid-state chemistry has grown rapidly over the last two decades. Solid-state molecular processes and reactivity,[1] intermolecular interactions,[2] and packing modes in organic materials[3] have been the subject of much work and are the matter of continuing investigation. The neighboring organometallic chemistry field has not seen, however, a similar development. In particular, the occurrence of molecular processes and

0009-2665/92/0792-0633$10.00/0

rearrangements in organometallic crystals has not been systematically studied, in spite of the increasing interest in the solid-state behavior of organometallic compounds.

It is by now ascertained that stereochemical changes, which typically occur in solution (ligand fluxionality, isomerizations, reorientations, etc.), are widespread also in organometallic crystals. Phenomena of this kind are intimately related to phase transitions and to reactivity in the solid state.

Dynamic phenomena in organic and organometallic solids are usually investigated by spectroscopic methods, mainly ^1H spin–lattice relaxation time measurements or ^{13}C cross-polarization magic-angle spinning NMR spectroscopy. Diffraction studies provide complementary information on the molecular organization within the crystal and on the atomic or molecular displacements about equilibrium positions.

This review is devoted to an examination of the dynamic behavior shown by molecules or molecular fragments in crystalline organometallic materials. The literature on these aspects of organometallic chemistry, although ample and distributed over about three decades, has never been systematically reviewed.

The aims of this review can be summarized as follows: (i) to provide a broad overview of the typical molecular rearrangements observed in organometallic solids; (ii) to discuss the information of dynamic nature obtainable from diffraction experiments with respect to that derived from spectroscopic sources; (iii) to examine analogies and differences between dynamic processes occurring in organic and organometallic crystals; (iv) to discuss the specific typology of these processes in terms of molecular nonrigidity and of delocalized bonding interactions; (v) to show how information on the molecular organization within the crystalline lattice can be used not only to forecast the possibility of reorientational processes but also to understand (if not predict) the occurrence of lattice modifications and phase transitions.

The main focus will be on the crystallographic and spectroscopic approaches to estimate reorientational barriers and/or activation energies for reorientational processes in the solid state. The results of the various methods will be compared for classes of crystalline complexes containing unsaturated organic fragments. More complicated dynamic processes such as arene ring buckling, diene topomerization, and reorientation of monohapto ligands will be discussed. The dynamic behavior shown by mononuclear and polynuclear metal carbonyl complexes and arene clusters will be analyzed; CO ligand fluxionality in the solid state will be examined and critically evaluated.

II. Dynamic Behavior and Structural Nonrigidity

A. Molecular Rearrangements in Solution and the Solid State

The reorientation of benzene molecules in the crystal was ascertained almost 40 years ago.[4] It is nowadays well understood that rigid disklike or globular organic molecules with a stiff σ-skeleton can undergo reorientational jumping motions in the solid state, usually between orientations undistinguishable by symmetry (such as every 60° for benzene), unless the dynamic process introduces an element of (dynamic) disorder. Phenomena of this kind have been well studied, and there is a large literature available on organic systems.[5,6] Torsional freedom around C–C σ-bonds contributes to conferring structural flexibility in organic molecules. Methyl group rotation is also ubiquitous in organic crystals.[7] Organometallic molecules possess additional degrees of structural freedom with respect to organic ones. Structural nonrigidity arises from two fundamental characteristics of the bonding in organometallic systems: the presence of groups of atoms bound to metal centers through substantially delocalized π-systems (aromatic rings, alkenes, alkynes, etc.) and the availability of geometrically distinct, although nearly isoenergetic, bonding modes for the same ligand (such as terminal, double, and triple bridging CO's, phosphines, arsines, etc.).[8] Molecular rearrangements, conformational changes, and isomerizations are, in general, low-energy processes for such molecules. Many experimental and theoretical studies have shown that, for example, the barrier to *internal* rotation in most polyene–metal complexes is very low, usually of the order of 2–4 kJ mol^{-1}, and that it does not change much with the presence of electron-donating or electron-withdrawing substituents.[9] Similarly the difference in energy between terminal and bridging CO's, for polymetallic systems showing carbonyl "scrambling" in solution, is usually small, in most cases not exceeding 30 kJ mol^{-1}.[10]

These two specific degrees of structural nonrigidity, coupled with the "organic-type" flexibility of other molecular fragments (polyenes, aliphatic chains, polyphosphines, etc.), not only are responsible for the molecular rearrangements that most organometallic molecules undergo in solution but also have strong influence on the dynamic behavior in the solid state.

However, on comparing the dynamic behavior of a molecule in the solid state and in solution, it is of fundamental importance to keep in mind the (far from trivial) difference between the forces experienced by a molecule embedded in the solid lattice (i.e. surrounded by identical entities in well-defined positions) and those experienced by a molecule surrounded by solvent molecules in rapid and chaotic tumbling motion. In general, molecular rearrangements in solution or in the liquid state are controlled by the nature of the chemical bonds and of the intramolecular (steric) contraints. In the solid state, on the other hand, the crystal packing imposes *additional intermolecular constraints*, which can forbid, or limit significantly, the motional freedom. The molecular organization in the lattice is not only responsible for the stability of the entire crystalline edifice but, ultimately, controls the ease of molecular motion. The implication is that *molecular* nonrigidity does not necessarily determine dynamic behavior in the solid state ("crystalline nonrigidity"). However, even if the molecules are blocked at a given temperature, the intramolecular nonrigidity can be liberated if the crystal forces are loosened by an increase in temperature.

Beside an exact knowledge of the molecular geometry, the chemical characteristics of the molecule, and the nature of the solid material under investigation, the characterization of any dynamic phenomenon in the solid state requires information (i) on the behavior of the atoms at the *bottom of the potential energy well*,

in which they are accommodated, and (ii) on the *height of the potential energy barrier* separating two consecutive minima.

Furthermore, the temperature dependence of both the motion about equilibrium and the motion far from equilibrium has to be established. In general, an increase in temperature will not only increase atomic motion about equilibrium position but also decrease the barrier height, as a consequence of the increase in crystal volume.

As discussed above, the geometrical and energetic features of the dynamic processes in organometallic crystals depend not only on the molecular organization within the lattice (crystal structure) but also on the specific structural features of the system under examination (molecular structure). A preliminary discrimination is indeed necessary to distinguish between reorientational jumping motion and large amplitude swinging motion typical of unsaturated fragments bound to metal centers via π-interactions and the "fluxionality" of CO ligands bound to mono- or polymetallic systems.

B. Reorientational Jumping Motion and Large Amplitude Swinging Motion of Unsaturated Ligands

Given that aromatic rings of the type η^n-C_nR_n are essentially free to rotate in the isolated molecule (unless the size of the substituent R causes significant *intramolecular* hindrance),[8,9] the ease of motion in the solid state will be basically a function of the *shape* of the fragment. In general, the more regular the ligand shape, the easier the reorientational phenomenon. This is quite intuitive: ligands with protruding groups (such as toluene, xylene, mesitylene, substituted cyclopentadienyl ligands, etc.) are more easily "locked in place" by the surrounding molecules than ligands with approximate discoidal shape (such as the cyclopentadienyl and benzene ligands, and their permethylated relatives). In order to show the effect of the ligand shape, typical potential energy profiles along the displacement coordinate for the reorientation of various methylated benzene rings are sketched in Figure 1.

Flat disklike fragments are not easily blocked in the lattice. Hence, the most common process in crystalline (η^n-C_nH_n)-metal complexes is the in-plane reorientation. The potential energy profile associated with the jumping motion shows minima every $(2\pi/n)°$ corresponding to the periodicity n of the idealized symmetry axis of the fragment. The intermolecular barrier separating two consecutive minima is usually rather low, seldom exceeding 20–30 kJ mol^{-1} (*see below*).

If the ligand shape is not discoidal (as for 1,3,5-η^6-$C_6H_3Me_3$ in Figure 1) the crystal packing can easily lock in the fragment. The atoms lie at the bottom of a very deep potential energy well. Reorientation is forbidden, any large displacement away from equilibrium leads to short contacts with the surrounding atoms and to strong intermolecular repulsions.

Between these two extremes a whole range of intermediate situation is, obviously, possible. Large amplitude motion is allowed if the ligand (as often observed in complexes containing η^6-C_6H_5Me) lies in a wide and flat potential energy well surrounded by steeply rising walls. The crystal cannot efficiently lock

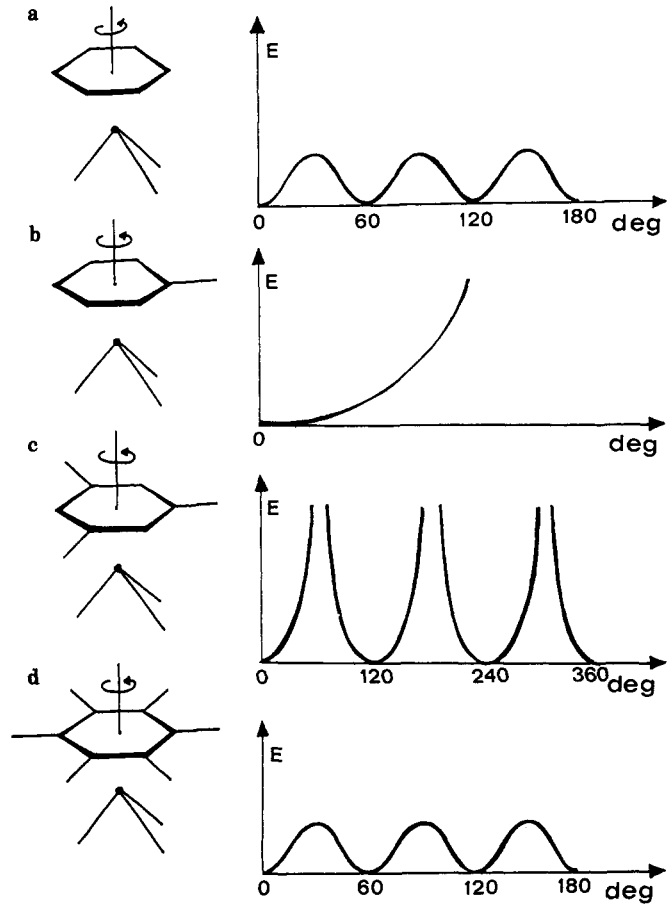

Figure 1. Potential energy wells and barriers: (a) permitted reorientation (the benzene fragment executes $2\pi/6$ jumps between potential energy minima); (b) forbidden reorientation, large amplitude motion (the arene fragment can undergo "swinging" motion at the bottom of a flat potential well, the uprising of strong intermolecular repulsions prevent full reorientational freedom); (c) reorientation forbidden (steeply rising potential energy walls separate the minima corresponding to the symmetry of the mesitylene fragment); (d) permitted reorientation (the diskoidal shape of the hexamethylbenzene fragment allows $2\pi/6$ jumping motion as in the case of benzene).

in the fragment, and large amplitude motion may become true reorientation through a phase transition.

Once the discoidal shape is restored (as in the case of η^6-C_6Me_6) the reorientational barrier drops and jumping motion is no longer forbidden.

It is important to stress that the ligand shape, so relevant in the solid state, has no effect on the ease of motion in solution unless, as mentioned above, the presence of bulky groups on the aromatic rings generates a well-defined conformational preference.

C. Carbonyl Fluxionality in the Solid State

Far more complicated is the relationship between the dynamic behavior shown by mononuclear and polynuclear metal carbonyls in solution and that shown in the solid state.

In solution CO ligand motion is usually studied by ^{13}C NMR spectroscopy.[10] Beside the polytopal rearrangements occurring at a single metal center,[11] "fluxionality" processes in polymetallic systems have been modeled in essentially two ways: (i) intramolecular site exchange over the metal framework (i.e. ligand migration via bridging CO intermediates[12]) and (ii) reorientation of the metal core within the ligand enve-

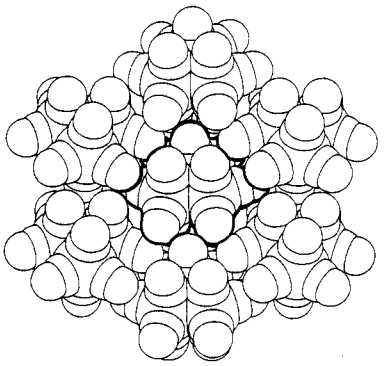

Figure 2. An example of molecular interlocking in the crystal of a binary metal carbonyl cluster. The CO groups packed around the metal core of the central $Ru_3(CO)_{12}$ molecule generate hollow sites over the molecular surface which allow interpenetration of the CO envelopes of neighboring molecules. (For sake of clarity only a layer of molecules is shown, i.e. a two-dimensional crystal.) Reprinted from ref 15; copyright 1991 American Chemical Society.

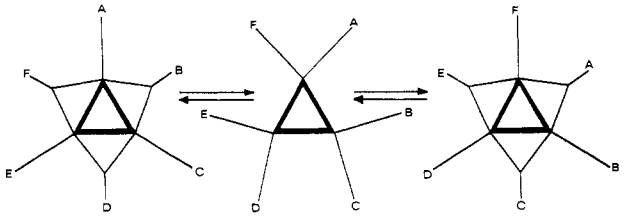

Figure 3. Schematic representation of the "merry-go-round" fluxional process in solution. The CO ligands migrate around the triangular metal framework via bridging intermediates.

lope.[13] These two processes are often undistinguishable in solution, both affording an equilibration mechanism for differently bound CO ligands, such as bridging and terminal ligands, on the NMR time scale.

The situation is rather different in the solid state where the dynamic behavior is governed by the molecular organization within the lattice. In the case of cluster carbonyl species, the crystal packing is based on a tight intermolecular CO···CO interlocking.[14,15] The CO groups protruding from the cluster surface (see Figure 2) generate hollow sites in the ligand coverage that allow interpenetration of carbonyl envelopes of neighboring molecules. Thus no motion of the CO ligands is possible without profoundly affecting all surrounding molecules, and full-scale CO migration of the "merry-go-round" type, i.e. based on bridge–terminal interconversion and site exchange (see Figure 3),[16] is unlikely to occur unless the crystal is close to the melting point. The motion of the metal polyhedron within the CO envelope,[13] on the other hand, does not imply atomic displacements as large as those implied in direct ligand interchange. In the solid state, the relative positions of the CO ligands can remain essentially constant although the type of bond they form with the central unit may change, for example, from terminal to double or triple bridging mode. It has been argued,[17] however, that bridge–terminal equilibration does not necessarily require complete reorientation of the metal frame. Small amplitude oscillations (or "librations", see Figure 4) of both the metal cluster and the CO ligands packed around can lead to rapid bridge–terminal interchange and "apparent" CO exchange on the time scale of the solid-state NMR experiment.[17] The extent of these motions will depend on the efficiency with which the CO groups are packed around the central cluster unit

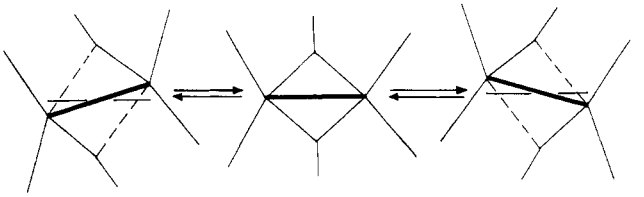

Figure 4. Schematic representation of the librational motion of a dimetallic carbonyl complex. Small amplitude oscillations of both the dimetallic unit and of the CO ligands allow interconversion between symmetric bridging and semibridging bonding; as the amplitude of the motion increases with temperature the all-terminal structure can be attained.

and on the efficiency of the intermolecular interlocking in the lattice. As the temperature increases the amplitude of these motions will increase, leading eventually to bond breaking and more extensive CO rearrangements.

III. Characterization of Dynamic Processes in the Solid State

There are many sources of information on the various aspects of the motion in the solid state. In the following we will compare information of crystallographic nature with that obtained from spectroscopic techniques; the most commonly used experimental approaches to the study of molecular rearrangements in the solid state, namely solid-state NMR, Raman, and infrared spectroscopies and incoherent quasi-elastic neutron scattering (IQENS) will be briefly outlined.

A. Solid-State NMR Spectroscopy

Solid-state NMR can reveal motions with correlation times of 10^{-1}–10^{-9} s. Most molecular and group reorientations fall within this range at room temperature. A number of books and publications dealing with both theory and applications of solid-state NMR spectroscopy are available.[18,19] In the context of this review, we will briefly describe only the NMR experimental approaches most commonly used to detect and quantify motion in solid organometallic complexes. These can be divided in two broad classes: low-resolution "wide-line" and high-resolution "magic-angle" spinning techniques.

In contrast to the highly resolved spectra observed for solutions and liquids, ^1H NMR of solids shows very broad absorptions arising from direct dipole–dipole interactions between nuclei. Measurements of line width and second moment give direct access to the study of motion in the solid state.[20] The second moment is particularly useful since it can be calculated if the crystal structure is known. In the presence of motion the dipolar interactions are partially averaged in the solid state, while, in solution, these interactions are averaged to zero. The extent of such averaging depends on the type of motion and causes narrowing of the spectrum. In variable-temperature experiments, the onset of molecular reorientation is usually revealed by a significant and sudden drop of the second moment parameter. The occurrence of motion can also be detected by measuring the temperature dependence of the spin–lattice relaxation time (T_1). The spin–lattice relaxation time is a function of the correlation time τ_c (the mean time between jumps) which, in turn, depends on

the type of motion. With the assumption that the correlation time obeys an Arrhenius-type law, the activation energy of processes occurring with τ_c in the range 10^{-6}–10^{-9} can be obtained from the slope of the plot of log T_1 versus $1/T$ (in Kelvins). It is important to stress that this activation energy is obtained as a *mean value* measured in a broad temperature range and hence does not refer to a particular dynamic model (compare with Raman and IQENS below). It integrates not only the effect of all possible motions occurring in the solid (such as correlated and uncorrelated jumps) but also all contributions of intramolecular nature arising from chemical bonding and nonbonding interactions.

It should also be mentioned that, although ^{2}H-NMR spectroscopy of solid samples[18,20] is not widely applied in organometallic chemistry, deuterium selective labeling may help to assess the contribution to relaxation due to different molecular fragments, thus overcoming the frequent problem of line assignment in Raman or IQENS (see below).

In the solid the chemical shift is a tensorial property and depends on the actual orientation of the molecule with respect to the magnetic field (giving rise to the anisotropy of the chemical shift, CSA). The motion causes changes in CSA, which for abundant nuclei are obscured by dipolar interactions, while for dilute nuclei (such as ^{13}C) homonuclear dipolar interactions are not present and heteronuclear ones can be suppressed by decoupling at the proton frequency. The three-dimensional shielding of the nuclei (which is averaged to the isotropic value in solution) is sensitive to molecular motions in the solid state and is, therefore, temperature dependent. The changes in the shape of the shielding tensors can be used to gain insights into the nature of the dynamic process.[21]

In recent years the use of cross-polarization magic-angle spinning (CPMAS) experiments to study dynamic processes in the solid state has increased rapidly.[18,19]

The rapid Brownian motion of the molecules in solution (which causes the CSA to be averaged to its isotropic value) can be "simulated" for solid samples by spinning at the "magic angle". The fast rotation of the sample (2–10 KHz) "averages" all orientations of the nuclei with respect to the magnetic field, reduces the shielding to its isotropic value (as in solution), and produces a high-resolution spectrum. For a static sample the resolution could be such as to differenciate all independent nuclei in the structure. If the site symmetry of the molecule in the crystal is lower than the molecular symmetry, nuclei which are *chemically* equivalent in the isolated molecule are no longer equivalent in the crystal so that more signals are usually observed in the solid state than in solution. In the presence of molecular motion, the spectral features are temperature dependent. The degeneracy due to the dynamic process can be removed by decreasing the temperature yielding a spectrum corresponding to the "static" structure. The activation energy for the process can be deduced from the coalescence temperature.

Two-dimensional NMR spectroscopy under CPMAS regime has recently been employed for the study of exchange processes with frequencies of the order of seconds.[18] In the presence of motion (i.e. chemical exchange) the observation of cross-peaks in the 2D frequency plots allows a straightforward assignment of the exchanging resonaces; from their intensities a lower limit of the free energy of activation for the exchange process can be derived.

B. Vibrational Studies and Incoherent Quasi-Elastic Neutron Scattering

Information on reorientational phenomena in the solid state can also be obtained by variable-temperature Raman and infrared spectroscopy.[22] Vibrational spectroscopy is very sensitive to short-range order and to the structural properties of small crystalline domains (which may differ from those of the average structure as seen by X-ray diffraction). Molecular or group reorientations and dynamic disorder have a marked effect on the low-frequency spectra. Broadening of the Raman bands can be interpreted on the basis of torsional modes. In the case of rigid-body reorientation of a molecule or group of atoms the torsional frequencies are usually discussed in terms of intermolecular and intramolecular sinusoidal functions of periodicity depending on the symmetry of the reorientating group. Hence, the interpretation of Raman spectra depends on the precise attribution of the torsional frequencies and on assumptions on the shape of the potential energy curve. In the harmonic approximation, potential barriers can be obtained from the torsional frequencies measured at the various temperatures.

Incoherent quasi-elastic neutron scattering experiments (IQENS) at different resolutions have also proved useful in the characterization of solid-state dynamic processes.[23] In hydrogen-containing materials, the observed spectrum, is dominated by the incoherent scattering from protons. In the presence of reorientational motion the scattering function for a powder sample has been shown to depend from a rotational scattering function which takes into account the proton reorientation. For cyclic systems one must adopt models including rotational jumps between a finite number of sites (a continuous rotational diffusion motion can be described by considering a large number of sites). On the basis of this model the spectrum observed at different resolutions is fitted by a calculated one, yielding information on the correlation time τ_c between two successive rotational jumps. From the slope of the plot of τ_c versus $1/T$ (K), and assuming an Arrhenius type relationship, it is possible to obtain an activation energy for the process.

C. Time-Scale Problem

It is well known that each type of spectroscopic technique delivers information about molecular structure averaged over a characteristic *time scale*, thus giving a measure of the lifetime of the species under investigation.[24] This concept was clearly laid out by Muetterties in 1965,[25] and we need only to stress a few critical aspects of the topic. A correct approach to the time-scale problem becomes essential when a *combination* of spectroscopic and diffraction techniques are used to tackle dynamic phenomena.

In general terms the definition of time scale depends on the characteristic of both the technique employed and the process under investigation. In absorption spectroscopy the time scale is related to the frequency span of the spectral range and to the lifetime of an

absorbing group. As a direct consequence of the Uncertainty Principle, an absorbing group with a limited lifetime gives a broadened spectral line. Structurally inequivalent groups undergoing site exchange at a rapid enough rate cannot therefore be distinguished, because the corresponding spectral lines are not resolved.

In NMR spectroscopy the environment of the individual molecule is probed over a relatively long period (10^{-1}–10^{-9} s), so that a time average of atomic positions is observed in the form of a coalesced spectrum when the exchange rate is near or higher than the separation (in frequency units) between individual resonances. In vibrational spectroscopy (IR, Raman), the combination of a higher radiation frequency and a wider spectral range produces a much shorter time scale (ca. 10^{-13} s). As virtually all molecular rearrangements take much longer than this, IR spectroscopy gives information on the ground-state structure of molecules which are nonrigid on the NMR time scale. Sometimes a superposition of distinct forms is found if there is exchange between isomers. Coalescence is not observed in IR experiments, except in a very few cases. It can be said that it probes the relative population of each potential minimum at a given temperature and so gives thermodynamic information on the energy difference between those minima. On the other hand, NMR coalescence data give information on the rate of exchange between the minima, thus giving kinetic information (i.e. the height of the energy barrier between the minima).

In the case of X-ray diffraction the time required for an X-ray photon to interact with the electrons (ca. $10^{-1}18$ s) is often quoted as the "time scale" for a diffraction experiment.[25] This has led to the widespread belief that the structure determined by diffraction methods is necessarily a representation of a static "lifeless" molecule captured in its ground-state form. The interaction time, however, is not relevant for an experiment in which radiation is not absorbed, but diffracted according to Bragg's law. The whole pattern of the measured diffraction intensities represents a *time average* of all possible atomic displacements *averaged again over the entire crystal* and thus contains information on all atomic motions (vibrations, rotations, librations, diffusion, etc.) that are taking place in the crystal lattice.[26] This averaging process takes place via the Fourier transform of the diffraction intensities. Large displacements, whether associated with oscillatory motions about discrete positions within the harmonic approximation, with freely rotating groups, or with some intermediate type of situation, cause a decrease of long-range order and, via distructive interference from neighboring unit cells, cause a decrease of Bragg's peak intensities (Debye–Waller effect) and a consequent increase of the diffuse background scattering (thermally diffuse scattering, TDS).[27] On these premises, it should be clear that the time scale for a diffraction experiment corresponds to the *entire period of the data collection*. As it will be demonstrated in the following, the widespread idea that diffraction experiments do not give access to dynamic information should be definitely abandoned.

D. Motion about Equilibrium Position from Anisotropic Displacement Parameters

It is well known that the anisotropic displacement parameters (ADP), routinely obtained from X-ray or neutron diffraction experiments, contain information on atomic motion about equilibrium positions in the crystal. The subject has been dealt with in a number of review articles[28] and books[29] and will be only briefly discussed here.

As discussed above, all atomic displacements, whether due to atomic vibrations or to some kind of static disorder arising from random atomic distribution over different sets of equilibrium positions in the crystal, are averaged *over time* during data collection and *over space* throughout the entire content of the crystal. In the case of dynamic disorder, however, no information on the correlation of motion between atoms is contained in Bragg's diffraction intensities, and hence dynamic information is not *directly* accessible from diffraction results. A discrimination between genuine atomic motion and static disorder is indeed possible only if the temperature dependence of the ADP is known and/or if complementary information (mainly of spectroscopic source) on the dynamic nature of the phenomenon under investigation is available.

In many cases, however, even casual inspection of the ADP pictured in ORTEP equiprobability ellipsoids[30] or in PEANUT rms displacement surfaces[31] provides a clear indication of preferential motions in particular directions. In such cases it is not unreasonable to look for correlation between ADP and low activation energy dynamic processes observed by spectroscopic techniques or, at least, to expect some of these dynamic processes to be revealed in the extent and preferential orientations of the mean-square displacement amplitudes of the atoms involved.

The information obtainable from ADP analysis can be succinctly summarized as follows:

(i) Discrimination between static and dynamic disorder. A congruent decrease (increase) of the atomic ADP with decreasing (increasing) temperature reflects a true dynamic phenomenon, otherwise the ADP might be affected by some kind of static disorder.

(ii) Reliability of the atomic ADP from the application of Hirshfield's rigid-bond test.[32] The differences between the mean-square displacement amplitudes along the internuclear separation should approach zero for covalently bonded atom pairs of comparable mass.

(iii) Characterization and quantification of the rigid body motion.[33,34] Thermal motion analysis in terms of the **T**, **L**, and **S** tensors provides information on the extent and direction of molecular librations and translations and on the coupling between these two motions (screw motion). The components of **T**, **L**, and **S** can be obtained by a linear least-squares fit to the observed ADP. The dependence from temperature of these components and the presence of additional motional freedom on top of the rigid body motion can also be estimated.

(iv) Rigid-body motion and presence of fragments with independent motional freedom from application of the *rigid-body* test.[35] If the entire molecule truly behaves as a rigid body in its motion the difference between the mean-square displacement amplitudes of nonbonded atom pairs calculated along the internuclear separation should also approach zero.

(v) Detection of intramolecular contributions to motion. The differences between the observed U's and

those calculated on the basis of the rigid-body motion parameters can be used to describe the internal motions arising from "soft" vibrational and librational modes due to bond bending or other atomic displacements subjected to small restoring forces.[36]

(vi) Estimation of potential energy barriers to reorientation of aromatic rings. The mean-square librational amplitudes, obtained from **T**, **L**, and **S** analysis, can be used in the quadratic approximation of a periodic cosine potential to evaluate the potential barrier to reorientation of flat conjugated polyolefin rings.[37] The potential barrier is calculated from the expression $B = 2RT/n^2\langle\varphi^2\rangle$, where n is the multiplicity of the barrier (5 for cyclopentadienyl ring, 6 for benzene, etc.), and $\langle\varphi^2\rangle$ the mean square librational amplitude about the axis of reorientation.

The success of thermal-motion analysis depends very much on the accuracy of the diffraction data.[38] Accurate measurements of the diffraction intensities are essential to obtain reliable values for the ADP since errors arising from all random and systematic imperfections of the structural model will tend to concentrate in these parameters; in particular, absorption problems can be dramatic when one or more metal atoms are present in the structure. Furthermore, it is well known that ADP may be substantially affected by electron-density contributions,[32] particularly those of the light atoms in metal carbonyls systems.[39] As pointed out by Bürgi et al., however, these problems are less severe when working on *differences* of ADP.[40] Since systematic errors are approximately the same (in absolute terms) for all atoms in the structure, they tend to cancel out in ADP differences, which then become more physically meaningful than the individual atomic ADP. For example, gross violation of Hirshfield's rigid-bond postulate have been successfully exploited to investigate dynamic Jahn–Teller distortions in crystals of Cu^{II} and Mn^{III} complexes[41] and to detect spin cross-over in crystalline Fe^{II} complexes.[40]

E. Motion Far from Equilibrium and Packing Potential Energy Barrier Calculations

As discussed above the rigid-body reorientational motions of the whole molecular unit or of metal coordinated fragments (ligands) is mainly under intermolecular control.

The atom–atom pairwise potential energy method[42] provides an extremely useful tool for the evaluation of how the molecular assemblage in the crystal lattice controls the reorientational phenomena and the height of the potential barriers during reorientation. The basic assumption is that the intermolecular interactions in a molecular crystal can be described as the sum of short-range repulsive and long-range attractive interactions of the kind used to describe the interaction between two isolated atoms in the gas phase. The central problem is that of the choice of an adequate analytical form for the intermolecular potential energy. Many good accounts on the applications of the method to organic crystals are available.[42-45]

The most commonly used expression for the empirical estimate of the packing potential energy (PPE) of a molecular crystal is called *6-exp-1* potential, where $PPE = \sum_i\sum_j(Ae^{-Br_{ij}} - Cr_{ij}^{-6} + q_iq_jr_{ij}^{-1})$. In this expression, index i runs over all atoms of the reference molecule in the lattice and index j over the atoms of the surrounding molecules distributed according to crystallographic symmetry; r_{ij} is an atom–atom intermolecular distance, q_i and q_j are the formal atomic charges if a Coulombic term is included in the calculations. PPE calculations are usually carried out within a preset cutoff distance of 7–10 Å. A number of independent tabulations for the coefficients A, B, and C, for each type of atom–atom contact for organic substances, are available in the literature.[42a,46] They are obtained either by fitting observed crystal properties (heat of sublimation, and known crystal structures) or via ab-initio calculations of the intermolecular potential energy. One of the major limitations in the application of the pairwise atom–atom potential energy method to organometallic crystals is the lack of specific atomic parametrization for metal-containing systems. Hence, for light atoms it is necessary to use potential parameters obtained for organic molecules, while the metal-atom contribution is either neglected or approximated by adopting the parameters available for the corresponding noble gases. It is clear that PPE calculations for organometallic crystals can not be expected to afford a "correct" (or even approximate) estimate of the crystal potential energy, rather they can be used as a convenient tool to investigate the spatial distribution of the molecules within the lattice and/or to compare, on a *relative* basis, the cohesive energy of closely related systems.

The potential energy barrier (PB) to molecular or fragment reorientation can be estimated by calculating the packing potential energy at various rotational steps around a predefined rotation axis (for example, an inertial axis or a ligand-to-metal coordinations axis) and by subtracting the energy corresponding to the observed structure (0° rotation).[5,47] Reorientations can be performed either within the "static environment" approximation (thus yielding an upper limit for the barrier) or within a "cooperating" environment in which molecules of the surroundings are allowed small torsional and translational motions in order to "give way" to the reorientating molecule or fragment.[48]

The calculation of atom–atom potential energy barriers (AAPEB) does not require a priori assumptions on the shape of the potential energy curve (compare with Raman and IQENS). It should be stressed that, since the height of the barrier is essentially determined by the changes in internuclear separation between the outer ligand atoms during reorientation, the problem of a correct parametrization for the inner metal atoms is less severe in AAPEB calculations than in the estimate of the actual PPE values. The height of the potential barrier, on the other hand, depends on the temperature at which the crystal structure is determined. These aspects of the method should be kept always in mind when comparing potential barriers with activation energies obtained from NMR spectroscopy (which are obtained as mean values measured over a temperature range, see above).

In spite of the many limitations and gross approximations required when dealing with organometallic systems, AAPEB calculations have proved extremely useful in evaluating how the crystal packing controls the ease of motion. The method is conceptually and computationally simple, is easily transferable from

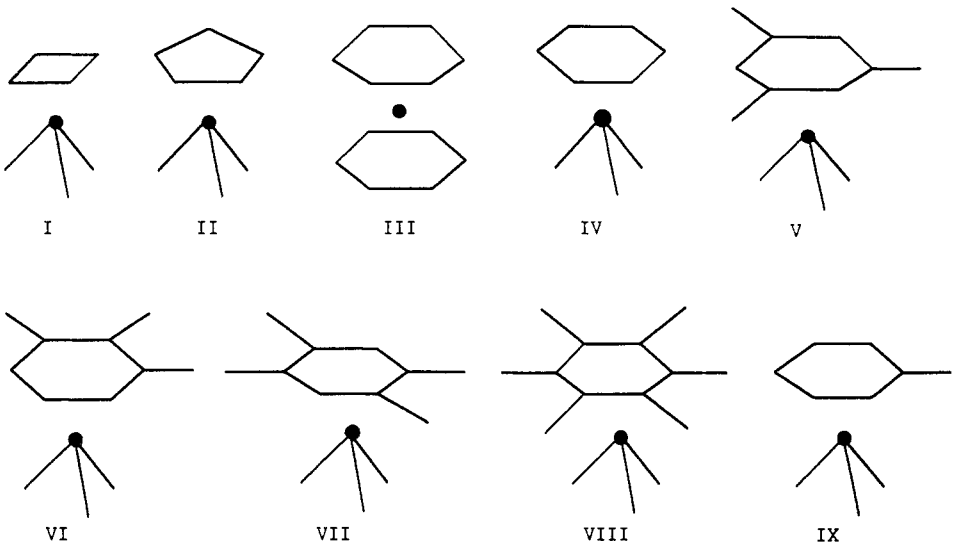

Figure 5. The molecular structures of the most representative complexes listed in Table I: I, $(\eta^4\text{-}C_4H_4)Fe(CO)_3$; II, $(\eta^5\text{-}C_5H_5)M(CO)_3$ (M = Mn, Re); III, $(\eta^6\text{-}C_6H_6)_2Cr$; IV, $(\eta^6\text{-}C_6H_6)M(CO)_3$ (M = Cr, Mo, W); V, $(1,3,5\text{-}\eta^6\text{-}C_6H_3Me_3)Mo(CO)_3$; VI, $(1,2,3\text{-}\eta^6\text{-}C_6H_3Me_3)Cr(CO)_3$; VII, $(1,2,4,5\text{-}\eta^6\text{-}C_6H_2Me_4)Cr(CO)_3$; VIII, $(\eta^6\text{-}C_6Me_6)Cr(CO)_3$; IX, $(\eta^6\text{-}C_6H_5Me)M(CO)_3$ (M = Cr, Mo).

system to system (given the caveat raised on the treatment of the metal atoms in organometallic crystals), and only requires atomic coordinates and crystal lattice parameters, even if known with limited accuracy. These are the reasons why the method has been successfully applied in a large number of cases.

F. Phase Transitions and Calorimetric Measurements

Although a detailed (or even superficial) discussion of phase-transition phenomena is beyond the scopes of this review, it must be mentioned that many dynamic phenomena may introduce disorder in the crystal.[49] In such cases, a phase transition often occurs when the temperature decreases and the dynamic process is slowed down and finally stopped. Phase transitions are generally classified as first order or second order. The Gibbs free energy of a solid remains continuous during a phase transition, but the derivatives of G (T,P) change. The transition is said first order if the first derivatives of G show an abrupt change at a given temperature, while second-order phase transitions show a discontinuity in the second derivatives of G (i.e. volume and entropy show only a change of slope at the transition point). The distinction between the two phenomena is often ambiguous. In general, beside melting, nucleation and growth of a new solid phase is first order, while transformations in which the molecules acquire orientational degree of freedom, but with very limited translational motion, are second order. In such cases, the phase transition is associated with the onset of reorientational phenomena, in which the molecular (or molecular fragment) orientation is distributed between more than one potential energy configuration.

Many organometallic crystals undergo phase transitions as a function of the temperature. In several such cases calorimetric measurements have been used to gain complementary information on the transformations detected by other methods such as X-ray diffraction or NMR reasurements (see below). Both first- and second-order phenomena are accompanied by the appearance of an anomaly in the heat capacity curves, which can be studied by differential thermal analysis (DTA) or differential scanning calorimetry (DSC). DTA affords information on the number of transformations and on the temperatures at which they occur, while information on the transformation enthalpy is usually obtained from DSC experiments.[50]

IV. Dynamic Processes in Organometallic Crystals

The most commonly observed and diffusely studied dynamic processes occurring in organometallic solids will now be reviewed. The various crystalline materials are grouped in classes of similar molecular structure. This is simply an ordering criterion and does not necessarily reflect differences in typology of the dynamic processes. Each section refers to a comparative table containing all essential structural and spectroscopic information, including that relative to single-crystal diffraction studies (when available) and the references to the original papers. Disorder, presence of more than one molecule in the asymmetric unit, polymorphic modifications, and phase transitions are explicitely indicated. All values of the activation energies (AE) and/or potential energy barriers (PB) are given in kilojoule per mole (kJ mol^{-1}). Throughout the following discussion, we will refer to these two quantities collectively as "energy barriers", keeping in mind, however, the differences in underlying assumptions between the various methods used for their estimation. Available information on the temperature or temperature range of measurement is also reported. A list of abbreviations is reported at the end of this review.

A. Reorientational Phenomena in Crystals of Mononuclear Polyene–Metal Complexes

In the following section the reorientational motions of the unsaturated fragments in crystalline polyene–metal complexes[51-91] will be discussed with reference to Table I. Complexes containing heteronuclear cyclic rings are also discussed. The structures of the most representative complexes in this class of compounds are sketched in Figure 5.

TABLE I. Comparison of Potential Energy Barriers and Activation Energies for Ring Reorientation in Crystalline Polyene–Metal Complexes

species diffraction (*T*) ref	method	model: AE/PB (T)[a]	ref
$(\eta^4\text{-}C_4H_4)Fe(CO)_3$	PSLRT	22.6 (120–200 K)	51
X-ray (228 K) 51	AAPEB	25.6 (228 K)	51
	Raman	16.4 (50 K), 19.1 (10 K)	52
$(\eta^5\text{-}C_5H_5)Mn(CO)_3$	PSLRT	7.24 (90–296 K)	55
X-ray (rt) 54a,b	AAPEB	7.9–17.6[b] (rt)	55
	IQENS	16.8 (300 K)	56
	Raman	10 (300 K)	57
$(\eta^5\text{-}C_5H_5)Re(CO)_3$	PSLRT	7.15 (90–296 K)	55
X-ray (293 K) 58	AAPEB	9.2–20.0[b] (rt)	55
	Raman	10 (300 K)	57
$(\eta^5\text{-}C_5H_5)V(CO)_4$	PSLRT	7.07 (90–296 K)	55
X-ray (rt) 59a,b: 2-fold disorder of the C_5H_5 ring	AAPEB	6.5 (rt)	60
$(\eta^5\text{-}C_4H_4S)Cr(CO)_3$	AAPEB	12.1 (rt)	60
X-ray (rt) 61: 3-fold disorder of the C_4H_4S ring,	IQENS	11 (300 K)	62
order-disorder phase transition at 185 K[63,64]	Raman	>12.5 (10 K)	63
$(\eta^5\text{-}C_4H_4N)Mn(CO)_3$ calorimetric measurements: phase transition at 305 K[66]			
$(\eta^5\text{-}C_4H_4P)Mn(CO)_3$ monoclinic–triclinic phase transition at 110 K[67]	Raman	ring reorientation	67
$(\eta^5\text{-}C_4H_2Me_2P)Mn(CO)_3$ order–disorder phase transition at 275 K[68]	Raman	ring reorientation	68
$(\eta^5\text{-}C_5H_5)TiCl_3$ X-ray (295 K) 70	PSLRT	8.8 (90–300 K)	69a
$(\eta^6\text{-}C_6H_6)Cr(CO)_3$	PSLRT	17.6 (77–300 K)	72
X-ray (rt) 71a	AAPEB	19.7 (rt), 31.8 (78 K)	73
Neutron (78 K) 71b	IQENS	15.5 (300 K)	56
X-ray (100 K) 71c	IQENS	27.5 (10 K)	75
	Raman	19.7 (300 K), 25.9 (120 K)	74
$(\eta^6\text{-}C_6H_6)Mo(CO)_3$	PSLRT	16.7 (143–393 K)	77
X-ray (rt, 120 K) 76	AAPEB	24.7 (rt), 33.5 (120 K)	76
	Raman	28.6 (120 K)	74
$(\eta^6\text{-}C_6H_6)W(CO)_3$	Raman	26.8 (120 K)	74
$(\eta^6\text{-}C_6H_6)_2Cr$	PSLRT	19.1 (152–301 K)	80
X-ray (rt, 100 K) 78a,e	AAPEB	19.2 (rt), 31.4 (78 K)	73
$(\eta^6\text{-}C_6Me_6)Cr(CO)_3$	PSLRT	25.9 (217–278 K)	82
X-ray (rt) 81	AAPEB	14.2 (rt)	82
$(1,3,5\text{-}\eta^6\text{-}C_6H_3Me_3)Mo(CO)_3$			
X-ray(293 K) 83	AAPEB	reorientation forbidden at room temperature	84
$(1,2,3\text{-}\eta^6\text{-}C_6H_3Me_3)Cr(CO)_3$	PSLRT	phase transition (ca. 333 K)	82
X-ray (rt) 82	AAPEB	reorientation forbidden at room temperature	82
$(1,2,4,5\text{-}\eta^6\text{-}C_6H_2Me_4)Cr(CO)_3$	PSLRT	phase transition (ca. 333 K)	82
X-ray (rt) 82	AAPEB	reorientation forbidden at room temperature	82
$(\eta^6\text{-}C_6H_5Me)Cr(CO)_3$	CPMAS	$(CO)_3$ rotation, AE = 65[c]	86a
X-ray (rt) 85	AAPEB[d]	reorientations forbidden at room temperature	87
$(\eta^6\text{-}C_6H_5Me)Mo(CO)_3$	CPMAS	$(CO)_3$ rotation, AE = 71[c]	86a
X-ray (rt) 87	AAPEB[d]	reorientations forbidden at room temperature	87
$[(\eta^7\text{-}C_7H_7)M(CO)_3]BF_4$			
M = Cr, tropylium	PSLRT	12.9 (93–296 K)	88a,b
M = Cr, BF_4^-	^{19}FSLRT[e]	6.77	
X-ray (powder) 88a			
M = Mo, tropylium	PSLRT	13.6 (93–296 K)	88a,b
M = Mo, BF_4^-	^{19}FSLRT[e]	12.3	
M = Mo, tropylium	AAPEB	12.6 (rt)	88a,b
M = Mo, BF_4^-	AAPEB	average 12.2 (rt)	
X-ray (rt) 89			
$(\eta^2\text{-}C_{10}H_8)(PP)Ni$[f]	2D-CPMAS	1,2(−)3,4 jumps of (PP)Ni[f] AE > 96 (346 K)	90

[a] Including heterocyclic ligands; activation energies (AE) and potential barriers (PB) in kJ mol^{-1}, temperature or temperature range of experiments reported if available from original papers. [b] Depending on the choice of potential parameters. [c] Obtained for reorientation of the tricarbonyl units. [d] Reorientation of both arene and $(CO)_3$ fragments forbidden at room temperature; large amplitude librational motion of both fragments permitted. [e] ^{19}FSLRT = ^{19}F spin–lattice relaxation time measurements. [f] PP = 1,3-bis(diisopropylphosphino)propane, or 1,2-bis(diisopropylphosphino)ethane.

Cyclobutadieneiron tricarbonyl (η^4-C_4H_4)$Fe(CO)_3$[51] contains the smallest conjugated polyene ring. The cyclobutadiene fragment has been shown to undergo $2\pi/4$ jumping motion about the coordination axis in the solid state.[51-53] Since the barrier to *internal* rotation is negligible,[8,9] the motional freedom of the ligand is exclusively under intermolecular control. The temperature dependence of the proton spin–lattice relaxation times was initially interpreted on the basis of two reorientational processes due to the supposed presence of two crystallographically independent molecules in the unit cell.[52] Following the structural characterization of the complex,[51] this interpretation has been revised in terms of a single jumping process with an activation energy of 22.6 kJ mol^{-1}.[51] This value is in agreement with the PB barrier calculated by the atom–atom potential method on the basis of the X-ray coordinates obtained at 228 K (25.6 kJ mol^{-1}).[51] However the barrier afforded by both Raman[52] and inelastic neutron scattering[53] are somewhat lower (16.4 at 50 K, and 11.0 kJ mol^{-1} at 274 K, respectively). Discrepancies of this kind should not be surprising (and will be encountered often in the following) since the NMR activation energy depends on the rate at which the ring surmounts the barrier, while the Raman torsional frequencies reflect the shape of the potential function at the bottom of the potential well.

(η^5-C_5H_5)$Mn(CO)_3$ and (η^5-C_5H_5)$Re(CO)_3$ are isostructural and their crystals are isomorphous.[54,58] The *internal* barrier obtained from extended Hückel calculations[9] is very small (ca. 0.008 kJ mol^{-1}) as in the previous case. The dynamic behavior of (η^5-C_5H_5)$Mn(CO)_3$ in the solid state has been extensively studied by a combination of spectroscopic methods (PSLRT measurements,[55] IQENS,[56] and IR and Raman spectroscopy[57]) and by AAPEB calculations.[55] Furthermore, the heat capacity has been measured from 10 to 300 K in order to investigate the controversial existence of a phase-transition around 100 K.[56] All these studies (see Table I) concur in indicating that the C_5H_5 ring executes $2\pi/5$ jumps around the ligand–metal coordination axis. The Raman barrier,[57] estimated assuming a 5-fold potential, is ca. 10 kJ mol^{-1} at 300 K in good agreement with the results of NMR measurements and AAPEB calculations. The IQENS study[56] affords a somewhat higher value for the barrier (16.8 kJ mol^{-1}); however, as the authors point out, the IQENS temperture range is too small (260–330 K) with respect to that explored in the PSLRT experiment (90–296 K) to allow direct comparisons. The motion of the tricarbonyl unit, or of the molecule as a whole, is forbidden as shown by the high value of the Raman potential barrier associated with the torsional motion in a 3-fold potential (ca. 100 kJ mol^{-1}).

The small anomaly observed in the heat capacity curve between 75 and 135 K[56] has been explained in terms of a transition from a small to a large amplitude motion of the C_5H_5 rings. For this transition an activation energy of 1.7 kJ mol^{-1} has been estimated from the broadening of the Raman bands.[57]

The activation energy for ring reorientation in crystalline cyclopentadienylvanadium tetracarbonyl, (η^5-C_5H_5)$V(CO)_4$,[59] is only slightly lower than in crystalline (η^5-C_5H_5)$Mn(CO)_3$ and (η^5-C_5H_5)$Re(CO)_3$. However, earlier AAPEB calculations,[55] based on the coordinates reported in ref 59a, indicated the absence of any significant intermolecular barrier. Although the presence of orientational disorder for the C_5H_5 ligand has been confirmed in the more recent structural study,[59b] the new set of coordinates yields a potential barrier[60] that is in good agreement with the PSLRT-derived activation energy (6.5 versus 7.07 kJ mol^{-1}, see Table I).

Crystalline thiophenechromium tricarbonyl, (η^5-C_4H_4S)$Cr(CO)_3$, is isomorphous with (η^6-C_6H_6)$Cr(CO)_3$ (see below), the thiophene ligand showing a 3-fold disorder at room temperature.[61] Both IQENS[62] and Raman[63] experiments indicate that the ligand undergoes reorientational jumping motion with potential barriers of 11.0 and 12.5 kJ mol^{-1}, respectively. In accord with these findings, AAPEB calculations[60] have shown that the molecular environment does not significantly hinder the rotation of the η^5-C_4H_4S ligand, the calculated intermolecular potential energy profile being rather flat with maxima of ca. 5.4 kJ mol^{-1}. Because of the presence of the bulky sulfur atom, intramolecular nonbonding interactions appear to play a more important role in determining the total barrier to reorientation than in the cases discussed above. A 180° reorientation of the ligand requires ca. 11.7 kJ mol^{-1}. Assuming that the intermolecular and intramolecular potential energy terms are additive, a total barrier of 12.1 kJ mol^{-1} is obtained, in good agreement with the spectroscopic results. The total potential energy curve has a roughly sinusoidal profile with minima at about ±110° rotation. These minima correspond to the disordered orientations ascertained by Dahl et al. in the crystal structure at room temperature.[61] A barrier of ca. 63 kJ mol^{-1} has also been estimated, from the torsional frequencies,[63] for the reorientation of the entire molecule.

Differential calorimetry, heat specificity measurements, and X-ray powder diffraction experiments[64] have shown that crystalline (η^5-C_4H_4S)$Cr(CO)_3$ exhibits an order–disorder phase transition from a monoclinic to a triclinic form at 185 K. It has been suggested that the phase transition is required to avoid the upsurge of "localized" repulsive intermolecular interactions on decreasing the temperature: at ambient temperature, when the thermal energy of the crystal is high, short intermolecular S···O contacts are permitted and three orientations of the C_4H_4S cycle are seen, while, below 185 K, all orientations are no longer possible due to intermolecular repulsions and the crystal lattice has to adjust to a new ordered phase. A similar explanation has been put forward to account for the monoclinic–triclinic phase transition in ferrocene (see below).

The crystals of (η^5-C_4H_4N)$Mn(CO)_3$[66] and (η^5-C_4H_4P)$Mn(CO)_3$[67] [both isomorphous with (η^5-C_5H_5)-$Mn(CO)_3$] undergo phase transitions at 305 and 110 K, respectively. Similar behavior is shown by (η^5-$C_4H_2Me_2P$)$Mn(CO)_3$[68] at 275 K just below the melting point (300 K). In all cases the phase transitions imply only small modifications of the crystal packings and are associated either with ring reorientation or with the transition from small to large amplitude motion of the ligands or of the entire molecules. These processes are barely detectable by calorimetric measurements but lead to appreciable broadening of the Raman bands. The behavior of (η^5-C_4H_4N)$Mn(CO)_3$[66] is particularly difficult to interpret. Since the temperature of the

transition is very close to the melting point (315 K), the phenomenon is more likely due to the onset of whole body reorientation or of other translational and librational motions, rather than ring reorientation. Heat capacity and X-ray powder diffraction studies,[65] carried out on crystalline $(\eta^6\text{-}C_6H_6)Cr(CO)_3$, $(\eta^6\text{-}C_6H_6)Cr(CO)_2CS$, and $(\eta^5\text{-}C_4H_4X)Cr(CO)_3$ (X = Se, Te) gave no evidence for phase transitions.

The activation energy[69a] for ring reorientation in crystalline $(\eta^5\text{-}C_5H_5)TiCl_3$[70] (8.8 kJ mol^{-1}) is comparable to the values obtained for the other cyclopentadienyl ligands listed in Table I. A much lower barrier (3.8 kJ mol^{-1}) was, however, obtained in a Raman study.[69b]

Particular attention has been given to the study of benzene reorientation in crystalline $(\eta^6\text{-}C_6H_6)Cr(CO)_3$.[71] This is a prototypical molecule in the vast family of $(\eta^6\text{-arene})M(CO)_3$ (M = Cr, Mo, W) complexes. The barrier to internal rotation has been estimated to be ca. 1.2 kJ mol^{-1} by extended Hückel calculations.[9] All experimental and theoretical approaches concur to indicate that benzene undergoes $2\pi/6$ jumping motion around the molecular coordination axis. The values of the energy barriers obtained by the various methods are in remarkable agreement: at ambient temperature the lowest value for the reorientational barrier is set by the IQENS experiment[56] (15.5 kJ mol^{-1}), while the upper limit is defined by AAPEB calculations[73] (19.7 kJ mol^{-1}) and Raman[74] (19.7 kJ mol^{-1}), with the results of PSLRT measurements[72] falling in between (17.6 kJ mol^{-1}). AAPEB and Raman also show that the barrier increases appreciably on decreasing the temperature (AAPEB, 31.8 kJ mol^{-1} at 78 K; Raman, 25.9 kJ mol^{-1} at 120 K). An independent inelastic neutron scattering study[75] afforded a value of 27.5 kJ mol^{-1} for the barrier at 10 K. In the same study a value of 46.5 kJ mol^{-1} was obtained for ring rotation in the crystalline salt $[(\eta^6\text{-}C_6H_6)Mn(CO)_3]Br$.

The energy barriers for ring jumps in $(\eta^6\text{-}C_6H_6)Mo(CO)_3$[74,76] and $(\eta^6\text{-}C_6H_6)W(CO)_3$[74] are strictly comparable to those discussed above for the chromium derivative (see Table I). On the average, benzene reorientation appears to be slightly "more expensive" in terms of energy, than that of the $(\eta^5\text{-}C_5H_5)$ ligands. The Raman study[74] attributes a barrier between 67 and 78 kJ mol^{-1} to reorientation of the tricarbonyl units or of the entire molecules.

The molecular structure of $(\eta^6\text{-}C_6H_6)_2Cr$ in the solid state has been studied by both X-ray and neutron diffraction.[78] The relationship between the structure of the crystal of $(\eta^6\text{-}C_6H_6)_2Cr$ and those of benzene and $(\eta^6\text{-}C_6H_6)Cr(CO)_3$ has also been investigated (see below). The potential energy barriers[73] for reorientation of the ligand around the molecular axis (19.2 and 31.4 kJ mol^{-1} at room temperature and 78 K, respectively), is in agreement with the activation energy value (19.1 kJ mol^{-1}) obtained in the more recent[80] of the two NMR studies[79,80] carried out on this complex. These values are only slightly lower than those discussed above for benzene reorientation in $(\eta^6\text{-}C_6H_6)Cr(CO)_3$ or $(\eta^6\text{-}C_6H_6)Mo(CO)_3$.

The comparison between the dynamic behavior of the methylated benzene derivatives[81-87] (see Table I) and that of the complexes containing unsubstituted rings shows how the ease of motion depends strictly on the spatial requirements of the unsaturated fragment and not, specifically, on crystalline properties. Disk-like fragments such as benzene and hexamethylbenzene undergo jumping motion with similar energy barriers irrespective of the crystal lattice morphology, while full rotational freedom is prohibited for fragments such as toluene, durene, mesitylene, etc. which are more efficiently "locked in" by the surroundings. As an example, the molecular organization in crystals of $(\eta^6\text{-}C_6H_6)Cr(CO)_3$, $(\eta^6\text{-}C_6Me_6)Cr(CO)_3$, and $(1,3,5\text{-}\eta^6\text{-}C_6H_3Me_3)Mo(CO)_3$ are compared in Figure 6. It can be easily appreciated that, while a rotational motion of the benzene and hexamethylbenzene fragments cannot be efficiently blocked by the surrounding molecules, this is not so for the triangulated mesitylene fragments interacting at almost a right angle with the neighboring molecules.

In all these species rotation of the methyl groups occurs with activation energies in the range 2–6 kJ mol^{-1}.[82]

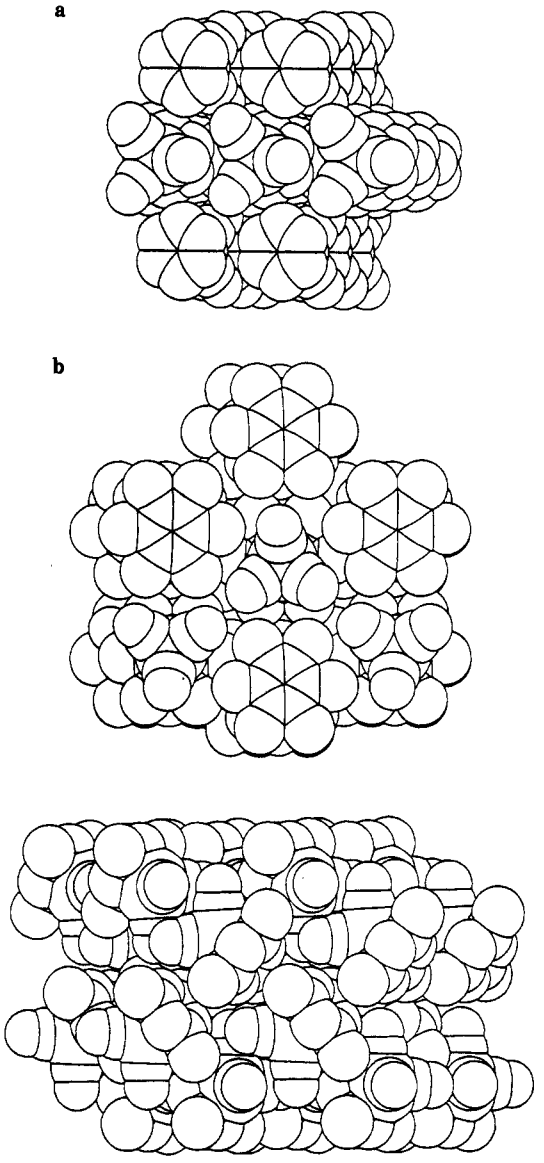

Figure 6. Comparison of the molecular organization in crystalline $(\eta^6\text{-}C_6H_6)Cr(CO)_3$ (a), $(\eta^6\text{-}C_6Me_6)Cr(CO)_3$ (b), and $(1,3,5\text{-}\eta^6\text{-}C_6H_3Me_3)Mo(CO)_3$ (c) (H-atoms are omitted for clarity). In a and b the organic fragments have a roughly diskoidal shape that permits facile reorientation in the solid state, while in c the triangulated mesitylene fragments interact at almost right angle with neighboring arenes; reorientation is forbidden (reprinted from ref 84; copyright 1991 American Chemical Society).

The reorientation of the C_6Me_6 ligand in (η^6-C_6Me_6)$Cr(CO)_3$ requires an activation energy of 25.9 kJ mol^{-1} (from PSLRT measurements[82] in the temperature range 217–278 K), i.e. only slightly larger than for benzene rotation in (η^6-C_6H_6)$Cr(CO)_3$ (17.6 kJ mol^{-1}). The atom–atom potential barrier[82] is instead slightly smaller in (η^6-C_6Me_6)$Cr(CO)_3$ than in (η^6-C_6H_6)$Cr(CO)_3$ (14.2 versus 19.7 kJ mol^{-1} at room temperature).

In (1,2,3-η^6-$C_6H_3Me_3$)$Cr(CO)_3$ and in (1,2,4,5-η^6-$C_6H_2Me_4$)$Cr(CO)_3$ methyl rotation is found to require an activation energy of 5.90 and 5.23 kJ mol^{-1}, respectively.[82] Reorientation of the whole arene fragments in these two species, as well as in (1,3,5-η^6-$C_6H_3Me_3$)$Mo(CO)_3$,[84] is prevented by the upsurge of high potential energy barriers. In (1,2,3-η^6-$C_6H_3Me_3$)$Cr(CO)_3$ and (1,2,4,5-η^6-$C_6H_2Me_4$)$Cr(CO)_3$, however, the combined use of AAPEB calculations, of PSLRT measurements, and of differential scanning calorimetry has allowed the conclusion that, while complete rotation of the arene groups is forbidden up to ca. 333 K,[82] reorientation may be achieved at higher temperatures through a transition to a new phase.

The case of the toluene derivatives (η^6-C_6H_5Me)$M(CO)_3$ (M = Cr,[85] Mo[87]) is more controversial. It has been reported that the rotational motion of the tricarbonyl units is responsible for the broadened features and temperature dependence of the ^{13}CO resonances in the CPMAS spectra of the two—^{13}CO-enriched—crystalline complexes.[86a] The process requires an activation energy of 65 and 71 kJ mol^{-1} for M = Cr and Mo, respectively. Similar behavior has been recently ascertained in tricarbonyl-η^6-[1,2-bis(ethylenedioxy)-cyclobutabenzene]chromium(0),[86b] where the process requires an activation energy of 60 kJ mol^{-1}. It has been argued[87] that rotation of the $(CO)_3$ unit or of the toluene fragment is not possible in the lattice of (η^6-C_6H_5Me)-$M(CO)_3$ (M = Cr, Mo) at room temperature. The broad and flat shape of the potential energy wells accommodating the two fragments suggests an alternative mechanism based on large-amplitude librational motions of both fragments without full rotational freedom.[87] Such motion allows dynamic interconversion between the different rotameric conformations available for the (η^6-C_6H_5Me)$M(CO)_3$ molecule. This is in agreement with the observation of extremely similar spectral features for the two crystalline materials in spite of the substantial difference in solid-state molecular structure between the two complexes (with respect to the arene, the tricarbonyl group is eclipsed for M = Cr, and staggered for M = Mo).

The reorientation of the tropylium ligand and the disorder of the tetrafluoroborate anion in [(η^7-C_7H_7)-$M(CO)_3$][BF_4] (M = Cr, Mo[89]) have been studied by ^{19}F and ^1H spin–lattice relaxation time measurements and AAPEB calculations.[88a,b] The activation energies for tropylium reorientation in the two complexes are similar (12.9 and 13.6 kJ mol^{-1}, for M = Cr and Mo, respectively), AAPEB calculations yield the same value for the two barriers (12.6 kJ mol^{-1}). This barrier is determined mainly by ring-BF_4^- and ring-CO interactions. The barrier calculation for the disordered BF_4^- ions was complicated by disorder. However, the average barrier (ca. 12 kJ mol^{-1}) is comparable to the activation energy obtained from ^{19}F NMR measurements (12.3 kJ mol^{-1}). An incoherent inelastic neutron scattering study[88c] of the two complexes yielded a much higher barrier (22 kJ mol^{-1}) for tropylium rotation.

The results of two-dimensional CPMAS experiments[90] carried out on (η^2-$C_{10}H_8$)(PP)Ni [PP = 1,3-bis(diisopropylphosphino)propane, and 1,2-bis(diisopropylphosphino)ethane] have been interpreted on the basis of a 1,2(−)3,4 jump of the (PP)Ni fragment over the η^2-bound naphthalene ligand occurring without equilibration of the phosphorus atoms. The same mechanism is operating in solution with an activation energy lower than 25 kJ mol^{-1}. In the solid state the activation energy obtained from the intensity of the cross-peaks in the two-dimensional plot has been found larger than 96 kJ mol^{-1} at 346 K.

[(η^6-C_6H_6)$Fe(\eta^5$-C_5H_5)][AsF_6] undergoes phase transition between three different crystal forms.[91a] Variable-temperature CSA measurements indicate that rotation of the entire cation takes place in the cubic phase above 310 K, while in the intermediate β-phase this motion is restricted to a 90° in-plane reorientation. Below 270 K the crystal is in a low-symmetry α-phase, in which whole-body rotation does not take place, although the rings execute jumping motion that persists down to 200 K. Transition from a rotational jumping state to a whole-body reorientation has also been detected from the Mössbauer spectra of the PF_6^- salt of the same complex.[91b] It has been shown that the onset of rapid isotropic motion of the cation is associated with a transition from a tetragonal phase to one of cubic symmetry at 319 K. Activation energies lower than 20 kJ mol^{-1} were estimated for the reorientations around the three rotational axes. If mesitylene is substituted for benzene the rotational process is stopped.[91b] Recently, the effect of substituting fluorobenzene for benzene has been studied.[91c] The temperature dependence of the Mössbauer spectra of the PF_6^- salt has been explained in terms of isotropic reorientation of the cation (AE = 19.6 kJ mol^{-1}). The X-ray diffraction results indicate a primitive cubic cell with totally disordered cations at room temperature, while DSC measurements are consistent with the occurrence of a first-order phase transition at 255 K. Analogous behavior is shown by the AsF_6^- and SbF_6^- salts, while no phase transition is shown by the BF_4^- salt.[91c]

B. Structural and Phase Relationship between Ferrocene, Nickelocene, and Ruthenocene

An extraordinary amount of theoretical and experimental work has been devoted to the study of the metallocenes species $(C_5H_5)_2Fe$, $(C_5H_5)_2Ni$, and $(C_5H_5)_2Ru$. Particular attention has been given to the investigation of the dynamic behavior of these species in the solid state. The structural and phase relationship between the known crystalline forms of ferrocene, nickelocene, and ruthenocene is summarized in Figure 7.

Ferrocene by itself constitutes a textbook example of the "static–dynamic" dualism characteristic of diffraction results.

The first structural study by Dunitz et al.[92] established the familiar sandwich structure with the Fe atom located on an inversion center between two staggered cyclopentadienyl rings. Heat capacity and X-ray diffraction measurements by Edwards et al.[93] gave early indications that an ordered structure was not compatible with the phase transition observed at 163.9 K. The

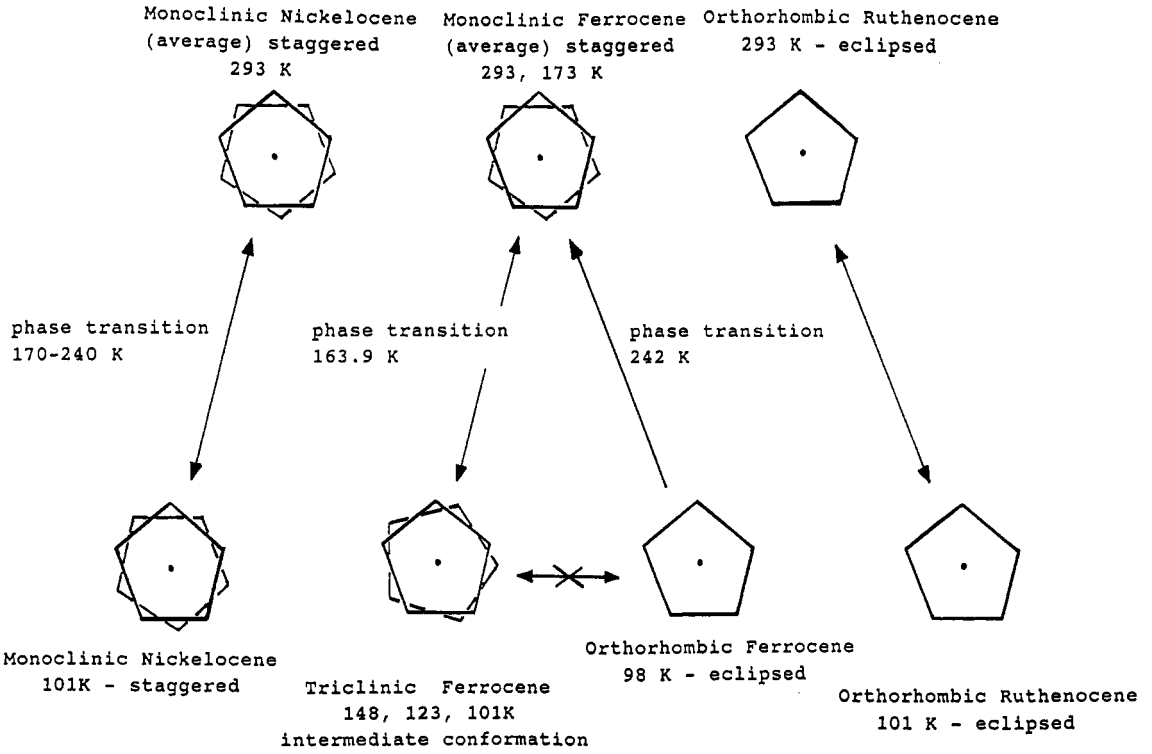

Figure 7. Schematic representation of the phase relationship between ferrocene, nickelocene, and ruthenocene. The temperatures of the various single-crystal X-ray diffraction experiments and of the phase transitions are indicated.

presence of disorder was later confirmed by Willis' neutron diffraction study,[94] while X-ray powder diffraction experiments[95] showed that ferrocene crystals are triclinic below the transition point. Following these studies, the monoclinic form of ferrocene has been studied at 298 and 173 K by neutron diffraction[96] and at 293 and 173 K by X-ray diffraction,[97] while the triclinic modification has been studied by X-ray diffraction at 148, 123, and 101 K.[98]

It is by now well understood that the monoclinic modification contains *average* staggered molecules. On going from 293 to 173 K the major axes of the C atoms ADP do not show a congruent decrease with temperature: the noticeable decrease in atomic displacement perpendicular to the ring plane and in the radial direction is not accompanied by a comparable decrease of the large displacement tangential to the ring. On the basis of these observations it has been concluded that the structural disorder is primarily static in character.[97] The disordered model is based on the *average* image of two superimposed cyclopentadienyl rings differing slightly not only in orientation but also in the position of their centers. In the neutron study[96] the best fit was obtained with rings twisted by ca. 12° from the eclipsed position, although it was pointed out that the disorder more likely involves a continuous range of molecular conformations.

The crystal lattice below the transition point has been described on the basis of a triclinic unit cell obtained by doubling all axes of the monoclinic form.[98] There are two independent ferrocene molecules in the asymmetric unit each deviating ca. 9° from exact eclipsed conformation.

The existence of an orthorhombic phase for ferrocene stable at low temperature and isomorphous with orthorhombic ruthenocene was reported by two independent groups.[99,100] The structure of this phase has been studied by Dunitz and Seiler by X-ray diffraction on crystals grown directly at low temperature.[101] Although the orthorhombic phase is stable below 242 K,[99] its crystals, once formed, can be warmed to ca. 275 K before transformation to the monoclinic phase occurs. The orthorhombic–triclinic transformation has not been observed. Crystals of the triclinic form can be kept indefinitely at temperatures between 100 and 164 K.

Orthorhombic ruthenocene does not undergo phase transition on passing from room temperature to 101 K[102] and down to 15 K,[103] while nickelocene, although retaining the monoclinic structure with staggered molecules between 293 and 101 K,[104] shows an anomalous *negative* expansion coefficient along the *b* axis and an ADP pattern at room temperature similar to that observed for monoclinic ferrocene (i.e. indicative of some degree of static disorder).[97] This behavior is in agreement with the results of a powder diffraction study[105] in the temperature range 5–295 K, which led to the conclusion that nickelocene undergoes an order–disorder transition between 170 and 240 K. At 101 K there is no obvious evidence of static disorder.[104]

The structural and phase relationship between ferrocene, nickelocene, and ruthenocene has been recently investigated by potential energy calculations.[106] The different behavior of ferrocene and nickelocene upon cooling has been attributed to the different inter-ring separation in the nickelocene and ferrocene molecules (3.64 versus 3.30 Å). The larger separation in nickelocene allows easier intermolecular interpenetration on decreasing the temperature. In monoclinic ferrocene, on the other hand, the smaller inter-ring separation cannot prevent the upsurge of C···H and H···H intermolecular repulsions as the crystal volume is decreased. Thus the monoclinic–triclinic phase transition in solid ferrocene (and the consequent torsion from nearly staggered to nearly eclipsed molecular conformation)

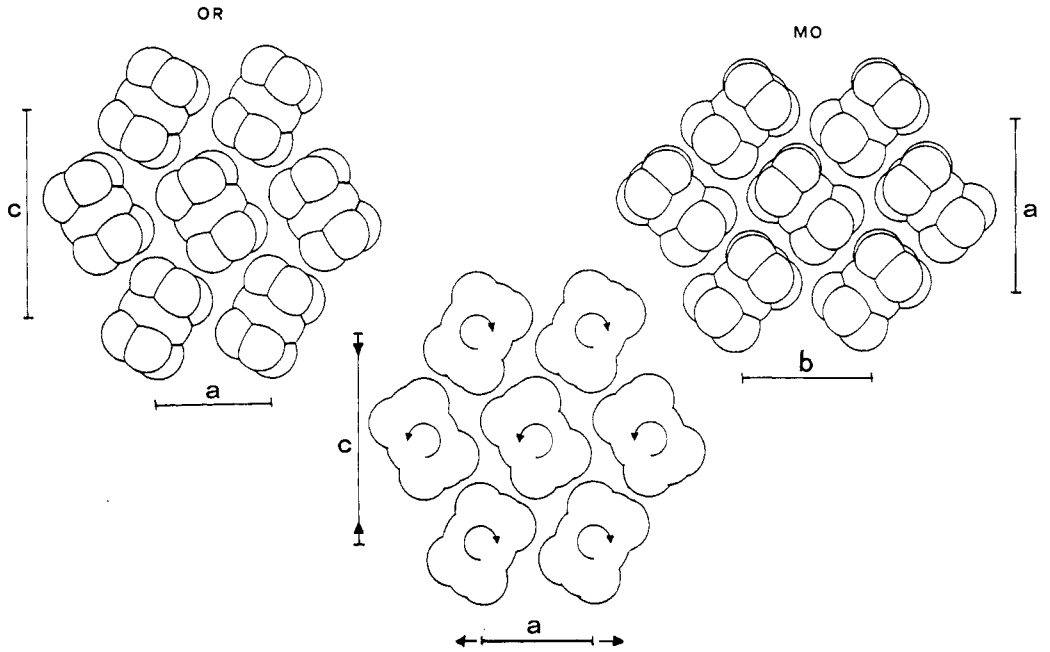

Figure 8. Relationship between the molecular distribution in the lattice layers of the orthorhombic (OR) and monoclinic (MO) crystals of ferrocene. A simple concerted rotation of the molecules within the layer of the orthorhombic form can lead to the monoclinic form. The relationship between the unit cell axes in the two crystals is indicated (reprinted from ref 106; copyright 1991 American Chemical Society).

is needed in order to maintain optimum (i.e. not repulsive) intermolecular contacts and to prevent loss of crystal cohesion. Along this line of thinking, it has been shown that the *b*-axis lengthening in nickelocene follows on the decrease in interlayer separation in the crystal lattice upon cooling (from 5.0 at 293 K to 4.8 Å at 101 K) thus preventing the upsurge of strong H···H repulsions along the *b*-axis direction. It has also been possible to demonstrate that the molecular distribution in orthorhombic ferrocene is related to that in the monoclinic form by a simple rotation of the molecules in the lattice layers (see Figure 8).

C. Motion about Equilibrium in Ferrocene, Nickelocene, and Ruthenocene

In this section the results of thermal motion analysis on the metallocene molecules are reviewed. Attention is focused on the librational motion about the molecular 5-fold axis. The eigenvalues of the librational tensor **L** obtained from the rigid-body treatment of the atomic ADP are reported in Table II (with the exclusion of monoclinic ferrocene because of the disorder discussed above).[97] The homogeneous increase with temperature of the eigenvalues reflects the thermal expansion of the crystal and the decrease in intermolecular hindrance to motion. A comparison of the tensor components indicates a strongly anisotropic motion ($L_1 \gg L_2 \approx L_3$), which, as expected, corresponds to a preferential in-plane libration of the C_5 rings. In all cases the main libration axis is within a few degrees from the idealized molecular axis passing through the middle of the C_5 ring and comprising the metal atoms. It is important to emphasize, however, that thermal motion analysis can not discriminate in-phase libration of the rings (i.e. rigid-body motion) from out-of-phase independent libration of the rings. In triclinic ferrocene, Hirshfeld's rigid-bond test[32] gives values for the differences in mean-square displacement amplitudes along the Fe–C bonds that are all negative (average −0.0034 (6) Å^2 at 101 K) indicating that the C_5 ring is vibrating as a whole relative to the Fe atom and that the rigid-body model is not entirely appropriate to describe the atomic motion about equilibrium.[98] Similar behavior is shown by nickelocene (average −0.0023 Å^2 at 101 K).[104]

TABLE II. Comparison of the Eigenvalues (deg^2) of the Librational Tensors L Obtained from Thermal Motion Analysis of the Ring ADP in Ferrocene, Nickelocene, and Ruthenocene

	L_1	L_2	L_3	R[a]
Nickelocene Monoclinic (ref 104)				
293 K	199.5	17.4	3.6	0.115
101 K	45.08	5.50	1.05	0.076
Ferrocene Triclinic Form (ref 98)[b]				
148 K	58.30	8.46	6.89	0.099
	55.36	10.23	5.77	0.075
123 K	42.76	6.63	6.22	0.078
	41.89	8.28	4.99	0.068
101 K	28.22	5.39	5.00	0.070
	28.59	6.79	4.47	0.059
Ferrocene Orthorhombic Form (ref 101)				
98 K	8.0	*c*	*c*	*c*
Ruthenocene Orthorhombic (ref 102)				
293 K	30.77	14.04	10.50	0.075
101 K	7.33	3.66	3.63	0.104

[a] $R = [\sum(\Delta U)^2/\sum(U^2)]^{1/2}$. [b] Two independent molecules in the asymmetric unit. [c] Not reported in ref 101.

With respect to Table II the following considerations can be made:

(i) In triclinic ferrocene[98] the eigenvalues of the librational tensor **L** show an homogeneous increase with temperature. L_1, in particular, increases from ca. 28 to ca. 58 deg^2 on passing from 101 to 148 K. The difference in librational motion from ring to ring reflects the different packing environments around the two independent molecules present in the asymmetric unit.

(ii) For nickelocene the eigenvalues at both 101 and 293 K are larger than for the other molecules (the large

value of L_1 at 293 K can be an artifact due to static disorder).[104]

(iii) In orthorhombic ferrocene[101] at 98 K the eigenvalue of **L** for the principal librational axis is only 8 deg^2, i.e. markedly smaller than in the triclinic crystal at 101 K (it has been pointed out[28b] that this value is so small that can be due mainly to zero-point motion).

(iv) Similarly, in orthorhombic ruthenocene[102] the ADP at 101 K are smaller than those obtained for triclinic ferrocene and for nickelocene at the same temperature; L_1 is only 7 deg^2 at 101 K (compare with 28 deg^2 for triclinic ferrocene, and 45 deg^2 for nickelocene).

(v) The possibility that the two rings do not have the same librational motion has been investigated in detail for orthorhombic ruthenocene[102] where the two rings are not related by crystallographic symmetry and might show different rigid-body motion parameters. This possibility has been explored by applying **T**, **L**, and **S** analysis to the two rings taken separately and, alternatively, by allowing nonrigid libration in addition to the rigid-body motion.[102] Both tests confirmed that ruthenocene does not behave as a rigid body in the crystal: one ring undergoes an additional libration with respect to the other ring of ca. 6 deg^2.

D. Ring Reorientation in Ferrocene, Nickelocene, and Ruthenocene

The values of the potential energy barriers and activation energies for ring reorientation in crystalline ferrocene, nickelocene, and ruthenocene are summarized in Table III. Potential energy barriers (PBADP) calculated, as discussed above, from the mean square librational amplitudes obtained from thermal motion analysis are also available for comparison.[37]

All sources of dynamic information[37,80,106-113] collected in Table III are in agreement in indicating that facile ring reorientation is a general feature of the metallocene crystals. A single crystal NMR study[114a] of ferrocene also confirmed that ring reorientation leads to an axially symmetric shielding tensor for the C nuclei.

The activation energies obtained from PSLRT measurements fall in the range 7.5–24.7 kJ mol^{-1}, showing a tendency toward higher values than for the cyclopentadienyl complexes discussed in section A (compare Table III with Table I). The reorientational barriers calculated by means of the atom–atom potential energy method[106] (AAPEB) are found in good quantitative agreement with the values of the energy barriers obtained by spectroscopic techniques. AAPEB, as well as PBADP calculations,[37] give separate barriers for crystallographically independent rings, which are not discriminated by other methods. In some cases AAPEB calculations appear to overestimate slightly the reorientational barriers (probably because of the "static environment" approximation[48]). PBADP calculations, on the other hand, tend to underestimate the barriers, this effect being particularly noticeable in the case of monoclinic ferrocene where the C atoms ADP are anomalously large because of disorder.[37] On the basis of lattice-energy calculations,[114b] it has been argued that, while the C_5H_5 rings in ferrocene can undergo a smooth geared motion, in nickelocene the motion leads to high energy clashes. This conclusion is in contrast with the variety of evidence reported in Table III that ring reorientation is slightly less expensive in nickelocene than in ferrocene.

TABLE III. Comparison of Potential Energy Barriers and Activation Energies for Ring Reorientation in Crystalline Ferrocene, Nickelocene, and Ruthenocene

species diffraction (TK) ref	method	AE/PB (*T*)	ref
ferrocene, monoclinic form			
neutron (298, 173 K) 96	PSLRT	7.5 (68–380 K)	107
X-ray (293, 173 K) 97	PSLRT	9.6 (78–415 K)	108
	PSLRT	7.9	109
	IQENS	4.6	110
	AAPEB	8.4 (298 K)	106
	PBADP	4.7 (293 K)	37
	AAPEB	9.2 (173 K)	106
	PBADP	2.7 (173 K)	37
	AAPEB[a]	11.0, 8.1, 4.9 (95, 135, 298 K)	80
ferrocene, triclinic form			
X-ray (148, 123, 101 K) 98	PSLRT	8.4 (296–90 K)	80
	PSLRT	10.5	111
	IQENS	9.2	110
	AAPEB[b]	10.9, 18.4, 10.0, 14.2 (101 K)	106
	PBADP[b]	7.6, 12, 8.4, 9 (101 K)	37
	PBADP[b]	6.4, 10.2, 6.8, 8.5 (123 K)	37
	PBADP[b]	5.9, 10, 7.0, 8 (148 K)	37
ferrocene, orthorhombic form			
X-ray (98 K) 101	PSLRT	24.7	111
	AAPEB[c]	21.7, 41.3	106
	PBADP[c]	23., 33.	37
nickelocene	Raman	5.0 (300 K)	112
X-ray (293, 101 K) 104	IQENS	6.3 (300 K)	113
	AAPEB	6.3 (293 K)	106
	PBADP	5.2 (293 K)	37
	AAPEB	13.8 (101 K)	106
	PBADP	6.5 (101 K)	37
ruthenocene	PSLRT	9.6 (380–68 K)	107
X-ray (293, 101 K) 102	PSLRT	18.9 (301–152 K)	80
Neutron (298, 78, 15 K) 103	AAPEB[c]	14.2, 33.9 (293 K)	106
	PBADP[c]	24, 38 (293 K)	37
	AAPEB[c]	17.2, 47.7 (101 K)	106
	PBADP[c]	25, >50 (101 K)	37

[a] Calculated on the basis of the monoclinic structure at room temperature and of the cell dimensions at 95, 135, and 298 K reported in ref 93. [b] Four independent cyclopentadienyl rings. [c] Two independent cyclopentadienyl rings.

It is also worth noting that ring reorientation in the orthorhombic crystals of ferrocene and ruthenocene is associated with higher energy barriers than in the other crystals. The comparison between the "average" energy barriers in the two crystals (AAPEB 13.4; PBADP 9.5; PSLRT 9.5, in the triclinic form; AAPEB 31.5; PBADP 20.0; PSLRT 24.7 kJ mol^{-1}, in the orthorhombic form), beside constituting an interesting "sensitivity test" for the AAPEB and PBADP methods, affords a nice demonstration of how small modifications in molecular organization within the lattice can have marked influence on the ease of motion. In this respect, it is worth stressing that in all these crystals the barriers to cyclopentadienyl reorientation, and the activation energies for the jumping process, appear to be essentially due to intermolecular interactions. As a matter of fact, the barrier to *internal* rotation in both ferrocene and nickelocene are known to be very small (in the gas phase ferrocene is eclipsed with an internal barrier of 3.8 kJ mol^{-1},[115a] the barrier is probably lower in nickelocene[115b]) while a theoretical study gives a barrier of ca. 2 kJ mol^{-1} for ruthenocene.[115c] In view of the small

TABLE IV. Activation Energies for Ring Reorientation in Crystalline Substituted Ferrocenes

species diffraction (*T*) ref	method	model: AE/PB (*T*)	ref
$(\eta^5\text{-}C_5Me_5)_2Fe$	CPMAS	13.5	117
X-ray (rt) 116	AAPEB	10.0 (rt)	60
$(\eta^5\text{-}C_5H_4Et)Fe(\eta^5\text{-}C_5H_5)$	WLNMR[a]	unsubstituted ring 14.2 substituted ring 34.3	120
$(\eta^5\text{-}C_5H_4{}^iPr)Fe(\eta^5\text{-}C_5H_5)$	WLNMR[a]	unsubstituted ring 33.0 substituted ring 39.7	120
$(\eta^5\text{-}C_5H_4{}^tBu)Fe(\eta^5\text{-}C_5H_5)$	WLNMR[a]	unsubstituted ring 35.1 substituted ring 39.7	120
$(\eta^5\text{-}C_5H_4{}^tBu)_2Fe$	WLNMR[a]	substituted rings 28.5	120
$(\eta^5\text{-}C_5H_4COMe)_2Fe$	WLNMR[a]	substituted rings >46	120
$(\eta^5\text{-}C_5H_4COMe)Fe(\eta^5\text{-}C_5H_5)$	WLNMR[b]	unsubstituted ring 19.2	108
	WLNMR[a]	unsubstituted ring 23.0 substituted ring >46	120
X-ray (297 K) 121: phase transition at 356 K			
$(\eta^5\text{-}C_5H_4COH)Fe(\eta^5\text{-}C_5H_5)$	WLNMR[c]	unsubstituted ring 16.3	108
	IQENS	(135–374 K) 17	124
X-ray (rt) 122a,b: disorder of the C_5-rings, phase transition at 316.5 K X-ray (333 K) powder, 123: face centered cubic phase X-ray (318–343 K), 122b: orthorhombic phase			

[a] Second moment measurements in the temperature range 4.2–300 K at 27.5 MHz. Activation energies for methyl group rotation also reported [range 6.3–19.2 kJ mol^{-1}]. [b] In the temperature range 78–298 K; an activation energy of 15.5 kJ mol^{-1} also reported for methyl group rotation. [c] In the temperature range 78–300 K.

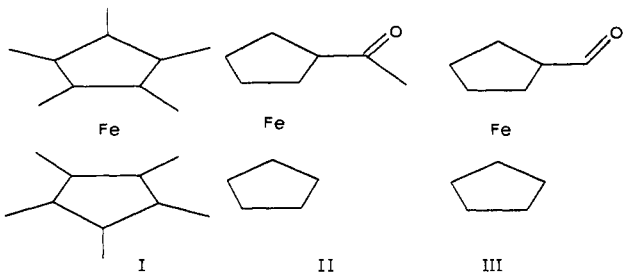

Figure 9. The molecular structures of the most representative complexes listed in Table IV: I, $(\eta^5\text{-}C_5Me_5)_2Fe$; II, $(\eta^5\text{-}C_5H_4COMe)Fe(\eta^5\text{-}C_5H_5)$; III, $(\eta^5\text{-}C_5H_4COH)Fe(\eta^5\text{-}C_5H_5)$.

differences in internal barriers, the reason for the different conformational preference in the solid state of nickelocene (staggered) and ruthenocene (eclipsed) remains an open question.

E. Motion and Phase Transitions in Substituted Metallocenes

The information on the structure, dynamic behavior, and phase transition phenomena for some substituted ferrocene derivatives is collected in Table IV.[116-124] Representative structures are shown in Figure 9.

The dynamic behavior of the permethylated rings in crystalline $(\eta^5\text{-}C_5Me_5)Fe$[116] does not differ significantly from that of the unsubstituted rings in the metallocene species. CPMAS experiments[117] yield an activation energy of 13.5 kJ mol^{-1} for the $2\pi/5$ jumping motion of the C_5Me_5 ligands, i.e. only slightly larger than required for ring reorientation in monoclinic and triclinic ferrocene (see Table III). AAPEB calculations[60] allow one to see that this difference arises mainly at the intramolecular level. In fact, while the calculated intermolecular barrier is quite low (6.3 kJ mol^{-1}), the intramolecular contribution, which is negligible in the nonmethylated system, is appreciable (3.8 kJ mol^{-1}). The total reorientational barrier is ca. 10 kJ mol^{-1}, i.e. only slightly lower than the NMR activation energy. The barrier to internal rotation has been estimated to be ca. 4 kJ mol^{-1} from gas-phase electron diffraction studies.[118]

The similarity in reorientational motion between $(\eta^5\text{-}C_5Me_5)_2Fe$ and ferrocene is reminiscent of that observed between crystalline $(\eta^6\text{-}C_6H_6)Cr(CO)_3$ and $(\eta^6\text{-}C_6Me_6)Cr(CO)_3$ and confirms that, in general, the permethylated rings behave very much the same as the unsubstituted ones. Molecular reorientation has also been invoked to account for the CPMAS ^{29}Si, ^{119}Sn, and ^{207}Pb spectral features of solid $(\eta^5\text{-}C_5Me_5)_2X$ (X = Si, Sn, Pb).[119]

Molecular motions in the ferrocene derivatives $(\eta^5\text{-}C_5H_4R)Fe(\eta^5\text{-}C_5H_5)$ [R = C_2H_5 (Et), *i*-C_3H_7 (^{i}Pr), *t*-C_4H_9 (^{t}Bu), CH_3CO], $(\eta^5\text{-}C_5H_4{}^tBu)_2Fe$, and $(\eta^5\text{-}C_5H_4COMe)_2Fe$ has been investigated mainly by WLNMR measurements.[108,120] In these crystals the activation energy for methyl proton rotation falls in the range 6.3–19.2 kJ mol^{-1}, while reorientation of the unsubstituted ring requires from 14.2 $[(\eta^5\text{-}C_5H_4Et)Fe(\eta^5\text{-}C_5H_5)]$ to 35.1 kJ mol^{-1} $[(\eta^5\text{-}C_5H_4{}^tBu)Fe(\eta^5\text{-}C_5H_5)]$. Reorientation of the substituted rings is generally a much higher energy process (with activation energies from 34.3 to larger than 46 kJ mol^{-1} at ambient temperature).[120] In the cases of formylferrocene, $(\eta^5\text{-}C_5H_4COH)Fe(\eta^5\text{-}C_5H_5)$ and acetylferrocene, $(\eta^5\text{-}C_5H_4COMe)Fe(\eta^5\text{-}C_5H_5)$, reorientation of the substituted ring is associated with phase-transition phenomena.[121-123]

The asymmetric unit in crystalline acetylferrocene at room temperature contains two independent molecules both showing methyl group orientational disorder.[121] Methyl rotation occurs with an activation energy of 15.5 kJ mol^{-1}, while reorientation of the unsubstituted C_5H_5 rings requires 19.2 kJ mol^{-1}.[108] Acetylferrocene undergoes a phase transition at ca. 356 K just below the melting point (359 K). This transition is accompanied by an abrupt change in the diffraction pattern,[120] that has been modeled by a simultaneous and cooperative jumping motion of *pairs* of adjacent molecules. The transformation is reversible.

Formylferrocene has been thoroughly studied by means of X-ray diffraction,[122] calorimetry, IQENS,[124] Mössbauer,[123] and NMR spectroscopy.[108] The solid shows a mesophase between 316.5 K and the melting

TABLE V. Dynamic Models, Activation Energies, and Potential Energy Barriers for Molecular Rearrangements in Crystalline "Bent" Metallocenes[a] and Monohapto Cyclopentadienyl Complexes

species diffraction (*T*) ref	method	model: AE/PB (*T*)	ref
$(\eta^5\text{-}C_5H_5)_2TiS_5$	PSLRT	axial ligand, AE = 9.0 equatorial ligand, AE = 7.7	69a
X-ray (rt) 125: first monoclinic form, one independent molecule X-ray (rt) 126: second monoclinic form, two independent molecules X-ray (rt) 126: orthorhombic form, perhaps disordered			
$(\eta^5\text{-}C_5H_5)_2MoCl_2$	PSLRT	four ring rotations, AE = 12.76, 8.64, 8.64, 1.47	129
X-ray (rt) 128: two independent molecules			
$(\eta^5\text{-}C_5H_5)_2TiCl_2$	PSLRT	ring rotation, AE = 2.1	107
X-ray, 130: two independent molecules			
$(\eta^5\text{-}C_5H_5)_2ZrCl_2$	CPMAS	ring rotation	131a
	AAPEB	four independent barriers, PB = 10.8, 6.7, 6.7, 6.3 (rt)	132
X-ray (rt) 128: two independent molecules			
$(\eta^5\text{-}C_5H_4Me)_2ZrCl_2$	2D-CPMAS	ring rotation, AE = 70.7	131b
$(\eta^5\text{-}C_5H_4Et)_2ZrCl_2$	CPMAS	ring rotation forbidden	131a
$(\eta^5\text{-}C_5H_4{}^tBu)_2ZrCl_2$	CPMAS	ring rotation forbidden	131a
X-ray (rt) 133	AAPEB	PB >200 (rt)	132
$(\eta^5\text{-}C_5H_5)_2Zr(\eta^4\text{-}C_4H_6)$	2D-CPMAS	ring rotation	131a
		diene flip, AE = 58.6 (300 K)	131
$(\eta^5\text{-}C_5H_5)_2Zr(\eta^4\text{-}C_4H_4Me_2)$	CPMAS	ring rotation	131b
X-ray (rt) 134	AAPEB	two independent barriers, PB = 15.5, 7.1 (rt)	132
$(\eta^5\text{-}C_5H_5)_2Zr(\eta^4\text{-}C_4H_5Me)$	CPMAS	two ring rotations, AE = 23.0, 16.7	131a
$(\eta^5\text{-}C_4H_4{}^tBu)_2Zr(\eta^4\text{-}C_4H_6)$	CPMAS	ring rotation forbidden	131b
X-ray (rt) 135	2D-CPMAS	diene flip, AE = 58.6 (300 K)	131a
	AAPEB	nondegenerate motion	132
$(\eta^1\text{-}C_5H_5)(\eta^5\text{-}C_5H_5)Fe(CO)_2$	WLNMR	(68–320 K), AE = 19.2[b]	137a
X-ray (rt) 138a			
$(\eta^1\text{-}C_5H_5)_2Hg$	PSLRT	(304–185 K), AE = 25.7	137b
X-ray (100 K) 139			
$(\eta^1\text{-}C_5H_5)HgCl$	PSLRT	(330–268 K), AE = 41.2	137b
$(\eta^1\text{-}C_5H_5)HgBr$	PSLRT	AE = 34.4	137b
$(\eta^1\text{-}C_5H_5)HgI$	PSLRT	AE = 42.3	137b
$(\eta^1\text{-}C_5H_5)_2(\eta^5\text{-}C_5H_5)_2Ti$	CPMAS	(182–369 K), AE = 33.2[b]	140
X-ray (rt) 138b			

[a] ^tBu = *tert*-butyl, Et = ethyl, ^iPr = isopropyl. [b] Activation energy for reorientation of the $(\eta^1\text{-}C_5H_5)$ ligand.

point (396 K). At room temperature, formylferrocene is orthorhombic showing an 85–15% disorder in the rotameric positions of both the substituted and unsubstituted rings.[122b] Two different models for the structure of the high-temperature (plastic) phase have been put forward: (i) a face-centered cubic lattice with a unit cell axis of 9.99 Å, resulting from the superposition of 24 orientations of local domains having the structure of the low-temperature phase,[122b] and (ii) a second orthorhombic phase with *a* and *c* axes of similar length and a *b* axis which is $^3/_2$ of the room temperature one.[123]

IQENS[124] yields an energy barrier of 17 (4) kJ mol^{-1} for the reorientation of the unsubstituted C_5H_5 ligand in the low-temperature phase in accord with the value of the activation energy obtained by WLNMR spectroscopy (16.3 kJ mol^{-1}).[108] Although the substituted ring has no reorientational freedom at room temperature, the phase transition appears to be associated with a change in orientation of this group and by a reorganization of intermolecular H bonding.

F. "Bent" Metallocenes and Monohapto Cyclopentadienyl Complexes

In "bent" metallocene complexes of general formula $(\eta^5\text{-}C_5R_5)_2M(L)_2$ (M = Ti, Mo, Zr) the nature of the ligand(s) $(L)_2$ can render the two cyclopentadienyl ligands electronically not equivalent (with respect to typical metallocenes). If this electronic difference is coupled with differences in lattice environment, the two ligands show an appreciably different dynamic behavior in the solid state. Structural and dynamic information on the species examined in this section are reported in

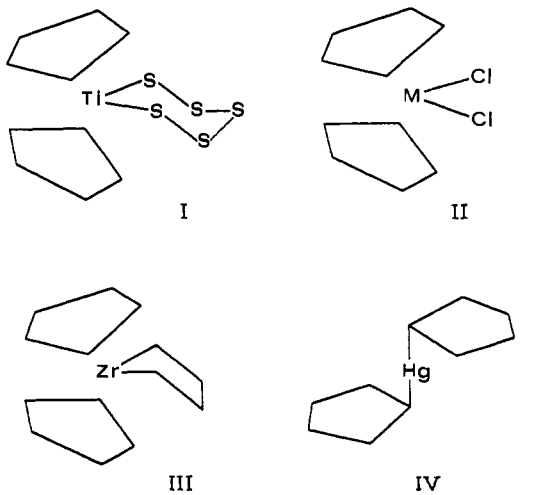

Figure 10. The molecular structures of the most representative complexes listed in Table V: I, $(\eta^5\text{-}C_5H_5)_2TiS_5$; II, $(\eta^5\text{-}C_5H_5)_2MCl_2$ (M = Ti, Mo, Zr); III, $(\eta^5\text{-}C_5H_5)_2Zr(\eta^4\text{-}C_4H_6)$; IV, $(\eta^1\text{-}C_5H_5)_2Hg$.

Table V.[69a,125-139] Representative structures are shown in Figure 10.

The two C_5H_5 ligands in $(\eta^5\text{-}C_5H_5)_2TiS_5$ occupy axial and equatorial positions with respect to the TiS_5 system and are, therefore, electronically not equivalent. PSLRT measurements[69a] show that the two rings have different activation energies for reorientation (9.0 and 7.7 kJ mol^{-1} for the axial and equatorial ligands, respectively). The attribution is based on the study of the ADP in the monoclinic form[125] where the two rings display different mean-squares librational amplitudes (20° and 5°, respectively). The existence of three polymorphic modifications[125,126] for this complex has been related to the flexibility of the cyclohexane-like TiS_5 chair,[69a] although it has been shown that the ring undergoes flipping motion in solution only above 361 K.[127]

Crystalline $(\eta^5\text{-}C_5H_5)_2MoCl_2$ is interesting because the asymmetric unit contains both a staggered and an eclipsed molecule.[128] Four different reorientational processes should be, in principle, observed. PSLRT has indicated one process of very low energy (AE = 1.47 kJ mol^{-1}), two intermediate ones (AE = 8.64 kJ mol^{-1}), and a third high energy process (AE = 12.76 kJ mol^{-1}).[129] Only one process with an activation energy of 2.1 kJ mol^{-1} has been otherwise observed in $(\eta^5\text{-}C_5H_5)_2TiCl_2$[107] although the asymmetric unit also contains two independent molecules.[130]

CPMAS results[131] for zirconocene complexes of general formula $(\eta^5\text{-}C_5H_4R)_2Zr(M)_2$ [R = H, Me, ^{t}Bu; M = Cl, $(M)_2$ = η^4-C_4H_6, η^4-$C_4H_4Me_2$, η^4-C_4H_5Me] have recently become available (see Table V). Some of these complexes have also been studied by AAPEB calculations.[132]

The unsubstituted C_5H_5 rings in $(\eta^5\text{-}C_5H_5)_2ZrCl_2$ and $(\eta^5\text{-}C_5H_5)_2Zr(\eta^4\text{-}C_5H_4Me_2)$ undergo reorientational motion in the solid state at 300 K. Only one resonance is observed for the ring C atoms in the former molecule, while two distinct resonances are observed in the spectrum of $(\eta^5\text{-}C_5H_5)_2Zr(\eta^4\text{-}C_4H_4Me_2)$.[131a] Although no estimate of the activation energies for these processes has been given, a higher rotational barrier for the ring closer to the butadiene methyl groups in $(\eta^5\text{-}C_5H_5)_2Zr(\eta^4\text{-}C_4H_4Me_2)$ has been proposed on the basis of the T_1 (^{13}C) values for the two rings. This assignment has been confirmed in the case of $(\eta^5\text{-}C_5H_5)_2Zr(\eta^4\text{-}C_4H_5Me)$, the activation energies for reorientation of the C_5H_5 rings being 23.0 and 16.7 kJ mol^{-1}, respectively.[131a]

Since the crystal structures of $(\eta^5\text{-}C_5H_5)_2ZrCl_2$ and $(\eta^5\text{-}C_5H_5)_2Zr(\eta^4\text{-}C_4H_4Me_2)$ are available, a detailed examination of the reorientational phenomena has been possible via AAPEB calculations.[132] In agreement with the presence of two independent molecules in the asymmetric unit of the triclinic cell of $(\eta^5\text{-}C_5H_5)_2ZrCl_2$,[128] the four independent rings experience different reorientational barriers (from 6.3 to 10.8 kJ mol^{-1}, see Table V). Due to the "bent" coordination, *intramolecular* contributions to the barriers are not negligible (from 2.5 to 5.4 kJ mol^{-1}). In the case of $(\eta^5\text{-}C_5H_5)_2Zr(\eta^4\text{-}C_4H_4Me_2)$ the total reorientational barriers for the two ligands differ appreciably (15.5 versus 7.1 kJ mol^{-1}). It has been shown that the two rings are not truly independent in their motion: intramolecular repulsions are minimized if asyncronous rotational jumps take place (one ligand is in a jump state, while the other is in a minimum).[132]

Both CPMAS experiments[131] and AAPEB calculations[132] indicate that in crystalline $(\eta^5\text{-}C_5H_4{}^tBu)_2ZrCl_2$[133] and $(\eta^5\text{-}C_5H_4{}^tBu)_2Zr(\eta^4\text{-}C_4H_6)$[135] ring reorientation does not take place even at 360 K. The two-dimensional exchange spectrum of $(\eta^5\text{-}C_5H_4Me)_2ZrCl_2$[131b] is, however, indicative of a slow rotational motion (not necessarily a complete rotation) of the C_5H_4Me rings occurring with an activation energy of 70.7 kJ mol^{-1}.

The most interesting feature of the two-dimensional CPMAS spectra of $(\eta^5\text{-}C_5H_4{}^tBu)_2Zr(\eta^4\text{-}C_4H_6)$ and $(\eta^5\text{-}C_5H_5)_2Zr(\eta^4\text{-}C_4H_6)$ is the "flip" of the diene ligand. The activation energy for the process in the solid state has been estimated to be 58.6 kJ mol^{-1}, only slightly higher than in solution.[131] On the basis of AAPEB calculations,[132] it has been argued that the molecular organization in crystalline of $(\eta^5\text{-}C_5H_4{}^tBu)_2Zr(\eta^4\text{-}C_4H_6)$ does not prohibit the flip of the diene ligands given that the two ligands, belonging to the two independent molecules in the asymmetric unit,[135] do not move simultaneously. It has been proposed that the process detected by the CPMAS experiment should be better described as a rapid clicking motion, with very little residence time in the second orientation in agreement with the fact that the solid-state structure of $(\eta^5\text{-}C_5H_4{}^tBu)_2Zr(\eta^4\text{-}C_4H_6)$ does not show positional disorder for the diene atoms over two sites. AAPEB calculations have also shown that in $(\eta^5\text{-}C_5H_5)_2Zr(\eta^4\text{-}C_4H_4Me_2)$ topomerization requires either that the motion of the $C_4H_4Me_2$ group is accompanied by a synchronous "clicking" motion of the neighboring molecules, or that a more substantial lattice modification, such as an order–disorder phase transition, takes place above 300 K.

CPMAS experiments have revealed hindered rotation of the W=C(carbene) bond in crystalline $(\eta^5\text{-}C_5H_5)_2Zr[OC[=W(CO)_5]\ CH_2CH=CHCH_2CMe(CMe_3)O]$ with an energy barrier at ca. 69 kJ mol^{-1} at 350 K.[136] In the corresponding nine-membered complex $(\eta^5\text{-}C_5H_5)_2Zr[OC[=W(CO)_5]CH_2CH=CHCH_2CMe_2O]$ the barrier is 54.5 kJ mol^{-1} at 260 K.[136]

Another family of complexes that exhibits an interesting dynamic behavior in the solid state is that of the monohapto cyclopentadienyl derivatives also listed in Table V. These crystalline materials have been extensively studied by Fyfe and co-workers by means of WLNMR, PSLRT and continuous wave solid state NMR measurements.[137] Contrary to most complexes discussed thus far, these molecules contain localized metal–carbon σ-bonds. Nonetheless, they are highly fluxional in solution and undergo reorientational jumping motion in the solid state. The motion of the monohapto ligand involves breaking of the M–C σ-bond and simultaneous reorientation and distortion of the ring as it jumps between potential energy minima.

In crystalline $(\eta^1\text{-}C_5H_5)(\eta^5\text{-}C_5H_5)Fe(CO)_2$[138a] the motion of the monohapto ligand in solution is frozen out at 198 K.[137a] In the solid state two reorientational processes are detected: reorientation of the η^5-ligand above 120 K and at 323 K, close to the melting point, reorientation of the η^1-ligand with an activation energy of 19.2 kJ mol^{-1}. Similar behavior is shown by $(\eta^1\text{-}C_5H_5)_2Hg$[139] and by $(\eta^1\text{-}C_5H_5)HgX$ (X = Cl, Br, I). The activation energies (see Table V), taken from the more reliable PSLRT measurements[137b] for reorientation of the η^1-ligand range from 25.7 to 42.3 kJ mol^{-1} and increase in the order η^1-C_5H_5 < Br < Cl ≈ I. It has been

TABLE VI. Dynamic Models, Activation Energies, and Potential Energy Barriers for Ring Reorientation in Crystalline Dinuclear Cyclopentadienyl Complexes

species diffraction (T) method(s)	model: AE/PB (T)	ref
cis-$(\eta^5\text{-}C_5H_5)_2Fe_2(\mu\text{-}CO)_2$		
X-ray (rt):	site symmetry C_1, two independent rings	141a
CPMAS (rt):	C_5H_5 reorientation, two resonances (5:5) CO ligands static, two resonances	142
PSLRT (147–300 K):	C_5H_5 reorientation, AE_1 = 7.2; AE_2 = 15.8	143
AAPEB (rt):	C_5H_5 reorientation, PB_1 = 7.9; PB_2 = 17.6	144
trans-$(\eta^5\text{-}C_5H_5)_2Fe_2(\mu\text{-}CO)_2(CO)_2$		
X-ray (rt):	site symmetry C_i, one independent ring	141b
X-ray/neutron (74 K)		145
CPMAS (rt):	C_5H_5 reorientation, one resonance (5) CO ligands static, two resonances	142
DSLRT[a] (100–300 K):	C_5H_5 reorientation, AE = 12.5	146
PSLRT (147–300 K):	C_5H_5 reorientation, AE = 10.5	143
AAPEB (rt, 74 K):	C_5H_5 reorientation, PB_1 = 15.1, PB_2 = 25.0[b]	144
trans-$(\eta^5\text{-}C_5H_5)_2Mo_2(CO)_6$		
X-ray (rt):	site symmetry C_i, one independent ring	147a,b
CPMAS (rt):	C_5H_5 reorientation, one resonance (5)	142
PSLRT	C_5H_5 reorientation, AE = 13.5	69a

[a] Deuterium spin–lattice relaxation time measurements. [b] Values calculated for the room temperature and 74 K determinations.

pointed out that, if the motion were under intramolecular control, the activation energy should follow the order of increasing electronegativity of the second ligand, i.e. $\eta^1\text{-}C_5H_5 < I < Br < Cl$. The change in order suggests that the processes are controlled mainly by intermolecular forces.[137b]

A recent CPMAS study[140] of crystalline $(\eta^1\text{-}C_5H_5)_2(\eta^5\text{-}C_5H_5)_2Ti$[138b] has provided clear evidence that the monohapto ligands undergo 1,2 shifts in the solid state above 183 K. Line-shape analysis yields an AE value of 33.2 kJ mol^{-1} similar to the value obtained for the same process in solution. On the contrary, interchange between the η^1 and η^5 ligands reaches the fast exchange limit in solution above 330 K, while in the solid state becomes significant only at high temperature (>369 K) and close to thermal decomposition.[140]

G. Dinuclear Cyclopentadienyl and Arene Complexes

We have seen that jumping motion of the C_5H_5 ligand in mononuclear complexes requires relatively small activation energies (2–16 kJ mol^{-1}). Similar behavior is observed in crystals of dimetallic system, such as *trans*- and *cis*-$(\eta^5\text{-}C_5H_5)_2Fe_2(\mu\text{-}CO)_2(CO)_2$ and *trans*-$(\eta^5\text{-}C_5H_5)_2Mo_2(CO)_6$ (see Table VI).[69a,141-146]

Both *cis*- and *trans*-$(\eta^5\text{-}C_5H_5)_2Fe_2(\mu\text{-}CO)_2(CO)_2$ have been studied by CPMAS[142] and by PSLRT measurements.[143] The dynamic behavior shown by the two complexes in the solid state is different: in crystals of the trans isomer only one process is observed in agreement with the location of the molecule on a crystallographic center of symmetry.[141b] The activation energy for ring reorientation, obtained from PSLRT measurements[143] in the temperature range 147–300 K, is 10.5 kJ mol^{-1}, in good agreement with the results of deuterium spin–lattice relaxation time measurements (DSLRT, AE = 12.5 kJ mol^{-1}).[146] In crystals of the cis isomer two T_1 minima are observed:[143] one at 210 K, then a plateau between 175 and 165 K, and a new decrease from 163 to 147 K, affording two activation energy values (7.2 and 15.8 kJ mol^{-1}) for the reorientation of the two crystallographically independent C_5H_5 ligands.[141a] These findings are in good agreement with the results of a study of the two crystals by thermal motion analysis and AAPEB calculations.[144] In qualitative and quantitative agreement with the spectroscopic results, two barrier values are calculated for the cis isomer (7.9 and 17.6 kJ mol^{-1}). The two independent structural characterizations of the trans isomer allow the estimation of the temperature dependence of the barrier to reorientation of the crystallographically independent ring (15.1 at room temperature and 25.0 kJ mol^{-1} at 74 K).[144] Thermal motion analysis shows that the rather different motional freedom of the two C_5H_5-rings in the cis isomer is reflected in the different mean-square librational amplitudes for rigid-body motion of the ligands around their coordination axes (302.8 and 62.4 deg^2, respectively), indicating that a flatter potential energy well is associated with a smaller potential energy barrier (see Figure 11). In the case of the trans isomer analogous correlation exists between the two potential energy barriers and the mean square librational amplitudes at room temperature and at 74 K (349.7 versus 7.3 deg^2, respectively).

In crystalline $(\eta^5\text{-}C_5H_5)_2Mo_2(CO)_6$ the site symmetry is also C_i,[147] so that only one resonance for two reorientating C_5H_5 groups is observed in CPMAS regime at room temperature.[142] The activation energy obtained by PSLRT measurements[69a] (13.5 kJ mol^{-1}) is strictly comparable to the values discussed above, although the two additional CO's present in $(\eta^5\text{-}C_5H_5)_2Mo_2(CO)_6$ (three terminal CO's bound to each Mo atom) with respect to the iron complexes (two CO's in bridging position and one terminally bound to each Fe atom) could be expected to increase the intramolecular contribution to the barrier heights.

One of the first examples of temperature-dependent dynamic disorder investigated by sole X-ray diffraction is that of the dinuclear sandwich complex $[PdAl_2Cl_7(C_6H_6)]_2$.[148]

The room temperature structure shows a rather diffuse electron density ring which could be refined by assuming two disordered orientations of nearly equivalent occupancy for the benzene ligands. On going to 263 K there is a transition from a disordered structure

TABLE VII. Dynamic Models, Activation Energies, and Potential Energy Barriers for Ring Reorientation in Crystalline Cyclooctatetraene Complexes

species diffraction (*T*) ref	method	model: AE/PB (*T*)	ref
$(C_8H_8)_2Fe$	WLNMR	ligand tautomerism	151
X-ray (rt) 150: two nonequivalent molecules, disorder			
$(C_8H_8)_2Zr$	CPMAS (298–123 K)	ring whizzing, AE < 23	153
X-ray (198 K) 153		ring equilibration, AE > 56.5	
$(C_8H_8)_2U$	WLNMR	ring reorientation	79
X-ray (rt) 154	WLNMR (298–90 K)	ring reorientation	155
$(\eta^4\text{-}C_8H_8)Fe(CO)_3$	PSLRT (350–250 K)	reorientation, AE = 37.9	157
X-ray (rt) 156	WLNMR (330–70 K)	reorientation, AE = 34.7	158
$(\mu_2\text{:}\eta^3\text{:}\eta^3\text{-}C_8H_8)Fe_2(\mu\text{-}CO)(CO)_4$			
X-ray (rt) 159	PSLRT (130–77 K)	reorientation, AE = 7.9	157
$(CO)_3Fe(C_8H_8)Fe(CO)_3$			
X-ray (rt) 156	PSLRT (306–77 K)	static	157
	WLNMR (430–77 K)	static	158
$(\mu_2\text{-}C_8H_8)_2Ru_3(CO)_4$			
X-ray (rt) 160	PSLRT (400–191 K)	reorientation, AE = 21.5	157
	WLNMR (300–80 K)	reorientation, AE = 21.5	162
	CPMAS (300 K)	reorientation, 1 resonance	161
	CPMAS (93 K)	static, 6 resolved lines	161

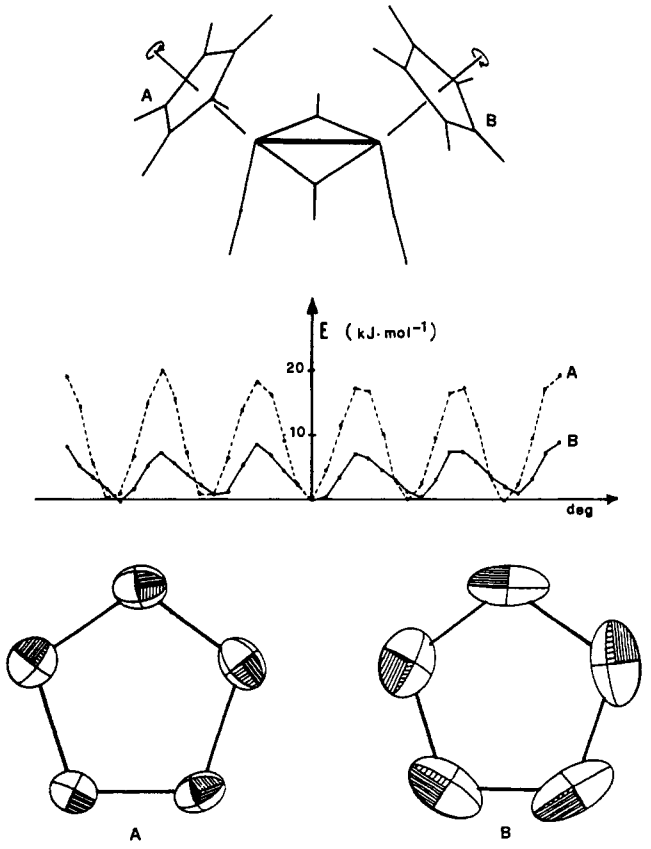

Figure 11. Ring reorientation in crystalline *cis*-$(\eta^5\text{-}C_5H_5)_2Fe_2(\mu\text{-}CO)_2(CO)_2$. Relationship between the reorientational barriers obtained by AAPEB calculations and the C-atom ADP patterns for the two crystallographically independent cyclopentadienyl rings.

to an ordered one in which the orientation of the benzene ring is close to one of the two coexisting orientations found at room temperature. This behavior was taken as an indication that the energy difference between the two orientations is very small (on the order of 2 kJ mol^{-1}), i.e. the barrier to internal rotation is low and the Pd–benzene interactions are highly delocalized. Interestingly, the analogous complex $[PdAlCl_4(C_6H_6)]_2$[149] is not affected by disorder; the benzene orientation does not correspond to either orientations observed in $[PdAl_2Cl_7(C_6H_6)]_2$ at room temperature, thus suggesting that the benzene fragments in complexes of this kind lie in a rather flat bonding and nonbonding potential energy well.

H. Cyclooctatetraene Complexes

The dynamic behavior of the cyclooctatetraene (C_8H_8) derivatives[150–162] listed in Table VII are described together in this section, irrespective of the complex nuclearity. The structures of the most representative compounds are sketched in Figure 12. Cyclooctatetraene is an extremely flexible ligand, the extent of ring buckling depending on the ability of the ligand to donate from four up to eight electrons to the coordinate metal atom(s).

$(C_8H_8)_2Fe$ undergoes internuclear tautomerism between two different coordination modes both in solution and the solid state.[151,152] The complex crystallizes with two nonequivalent molecules (one of which is affected by disorder) in the asymmetric unit.[150] The dynamic nature of the positional disorder affecting one of these molecules has been ascertainded by WLNMR experiments.[151] The NMR spectra reveal an overlap of two lines arising from two different types of molecular motions. These findings agree not only with the results of the diffraction study[150] but also with those of high-resolution NMR which showed that the molecule undergoes internuclear tautomerism in solution.[152]

A combined diffraction and CPMAS study of the related complex $(C_8H_8)_2Zr$ has been recently carried out.[153] In solution, both ^1H and ^{13}C NMR experiments show that the molecule is highly fluxional: the 16 C atoms and H atoms are equivalent even at 173 K; the fluxionality process occurs with an exchange barrier lower than 31 kJ mol^{-1}. The solid-state structure, on the other hand, reveals that the two rings are bound in η^8- and η^4-mode, respectively, with the C atoms showing extensive in-plane displacement.[153] Two processes have been revealed by the CPMAS experiment in the temperature range 123–298 K: a lower energy 1,2 shift ("ring whizzing") occurring with AE < 23 kJ mol^{-1} and a higher energy process involving interconversion of the two rings which requires at least 56.5 kJ mol^{-1}.

Ring reorientation is also a low-energy process in crystalline $(C_8H_8)_2U$[154] as shown by early WLNMR measurements.[79] ^1H NMR line-shape analysis[155] on both $(C_8H_8)_2U$ and $(C_5H_5)_3UCl$ powders confirmed that

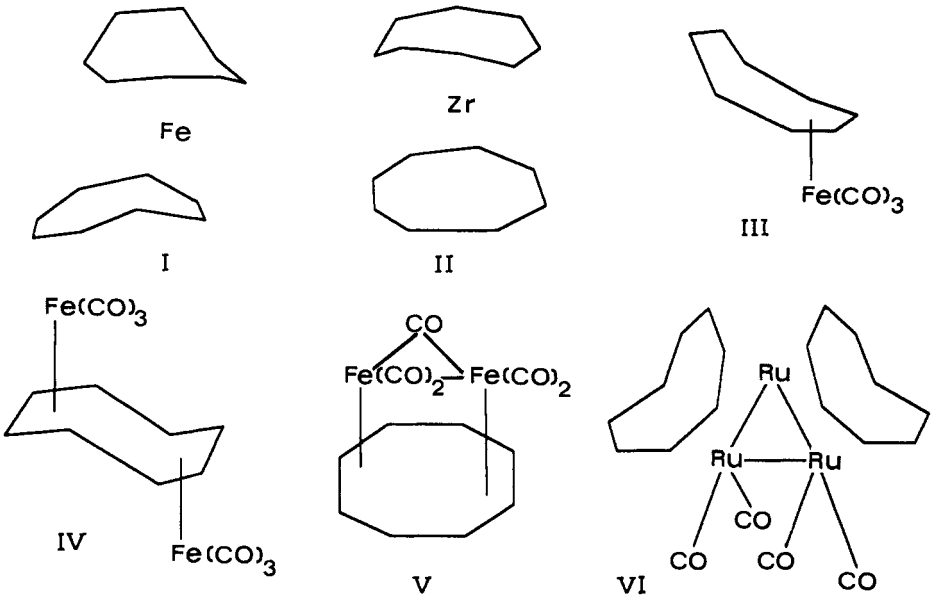

Figure 12. The molecular structures of the most representative complexes listed in Table VII: I, $(C_8H_8)_2Fe$; II, $(C_8H_8)_2Zr$; III, $(\eta^4\text{-}C_8H_8)Fe(CO)_3$; IV, $(CO)_3Fe(C_8H_8)Fe(CO)_3$; V, $(\mu_2{:}\eta^3{:}\eta^3\text{-}C_8H_8)Fe_2(\mu\text{-}CO)(CO)_4$; VI, $(\mu_2\text{-}C_8H_8)_2Ru_3(CO)_4$.

ring reorientation in the former complex takes place even at 90 K, while for the latter a more complicated process (perhaps a tumbling motion) has to be invoked to account for the spectral features, a spectrum corresponding to a static solid is obtained only at 140 K.

$(\eta^4\text{-}C_8H_8)Fe(CO)_3$[156] has been shown to be nonrigid in the solid state.[157,158] PSLRT measurements in the range 250–350 K showed that the T_1 are very temperature dependent.[157] The rather high value of the activation energy (37.9 kJ mol^{-1}) is in agreement with a motion that involves simultaneous rotation and distortion of the ring. No disorder is observed in the crystal structure[156] so that the jumping motion between the positions of minimum energy "observed" in the diffraction experiment requires simultaneous rotation and rearrangement of the localized C–C bonds within the ligand.

Similarly, T_1 measurements in crystalline $(\mu_2{:}\eta^3{:}\eta^3\text{-}C_8H_8)Fe_2(\mu\text{-}CO)(CO)_4$[159] between 130 and 77 K afforded a much smaller activation energy for reorientation of the ligand (7.9 kJ mol^{-1}),[157] in accord with the observation that the C_8H_8 ring in this molecule is much flatter and discoidal than in $(\eta^4\text{-}C_8H_8)Fe(CO)_3$.[156] Again no disorder is present so that the reorientation has been described as a jumping of the C_8H_8 ring between positions of equivalent (or nearly equivalent) potential energy.

Both WLNMR[158] and PSLRT[157] experiments have shown that the C_8H_8 ligand is otherwise "static" in $(CO)_3Fe(C_8H_8)Fe(CO)_3$.[156]

$(\eta^8\text{-}C_8H_8)Ru_3(CO)_4$ has also been investigated by WLNMR,[162] PSLRT,[157] and CPMAS spectroscopy.[161] The proton NMR experiments yielded an activation energy of 21.5 kJ mol^{-1} for reorientation of the ligands. The CPMAS experiments[161] confirmed facile ring reorientation at ambient temperature by showing the presence of one-carbon resonance for the 16 C atoms of the two rings; six resolved lines could be observed only in the spectrum at 93 K. As in the cases discussed above, the two rings are nonplanar so that the averaging process must imply quite substantial ring buckling and dynamic distortion during reorientation.

I. Mononuclear and Polynuclear Binary Carbonyls

In the previous sections we have shown that molecular motion is common in crystalline organometallic compounds. It is not so for crystalline transition metal carbonyl complexes and clusters where the solution–solid analogy breaks down as far as dynamic behavior is concerned. A very few of the species that are termed "highly fluxional" in solution do show dynamic behavior in the condensed state. Out of a large number of binary carbonyls studied up to now[163–189] (see Table VIII and Figure 13) only the behavior of $Fe(CO)_5$, $Co_2(CO)_8$, $Fe_3(CO)_{12}$, and $Co_4(CO)_{12}$ has been discussed in terms of solid state "fluxionality" (and not without some controversy).

The study of $Ni(CO)_4$ and $Fe(CO)_5$ constitutes one of the first attempts to obtain information about motion in the solid state by means of ^{13}C NMR experiments on powder samples.[164] Both species have low melting point (248 and 253 K, respectively), and their solid-state structures have been determined at 218 K and 193 K, respectively.[163,165] From an analysis of the chemical shift anisotropy (CSA) and from spin–lattice relation time measurements it has been proposed that, while $Ni(CO)_4$ is static, molecular motion appears in solid $Fe(CO)_5$.[164] The spectral features observed between 213 and 4.2 K were fitted by a model in which intramolecular axial–equatorial CO exchange takes place via Berry pseudorotation,[11a] with an apparent activation energy (from T_1 measurements) of about 4 kJ mol^{-1}. The exchange frequency was measured to be 2.4×10^4 s^{-1} at 213 K, i.e. much slower that in the liquid state (1.1×10^{10} s^{-1} at 253 K). These findings were later questioned by Gleeson and Vaughan.[166] More recently, the results of CPMAS experiments[167] on $Fe(CO)_5$ in the temperature range 155–250 K have been reported: below 235 K the spectrum reveals two resonances of relative integrated intensities 2:3 in agreement with the presence of two axial and three equatorial CO's in the static structure. A rotational motion about the molecular 3-fold axis rather than an axial–equatorial ex-

TABLE VIII. Dynamic Behavior in Crystalline Binary Carbonyls

species diffraction (T) ref	method	model	ref
$Ni(CO)_4$	^{13}C NMR CSA	static	164
X-ray (218 K) 163			
$Fe(CO)_5$	^{13}C NMR CSA	CO exchange	164
X-ray (163 K) 165	CPMAS	equatorial CO exchange	167b
$Fe_2(\mu\text{-}CO)_3(CO)_6$	CPMAS	static	142
X-ray (rt) 86			
$Co_2(\mu\text{-}CO)_2(CO)_6$	two independent "half" molecules		
X-ray (rt) 169a	CPMAS (313–139 K)	CO exchange[a] (AE = 48.9)	170
X-ray (100 K) 169b	CPMAS	CO exchange	167a
	AAPEB	libration	171
$Fe_3(\mu\text{-}CO)_2(CO)_{10}$	disorder		
X-ray (rt) 173a,b	^{13}C NMR CSA	CO exchange[c]	166
	CPMAS	CO exchange[c] (AE = 41.8)	174
	CPMAS	CO exchange[c]	175
	AAPEB	libration	171, 172
$Ru_3(CO)_{12}$	^{13}C NMR CSA	static	166
X-ray (296 K) 179	CPMAS	static	175
	CPMAS	static	180
$Os_3(CO)_{12}$	^{13}C NMR CSA	static	166
X-ray (RT) 183	CPMAS	static	175, 180, 184
$Co_4(\mu\text{-}CO)_3(CO)_9$	disorder		
X-ray (rt) 185a,b	CPMAS (336–211 K)	CO exchange[d]	186
	CPMAS	static	187
	AAPEB	libration	171, 172
$Ir_4(CO)_{12}$	disorder		
X-ray (rt) 188	^{13}C NMR CSA	static	166
	CPMAS	static	175
$Rh_6(CO)_{16}$	^{13}C NMR CSA	static	166
X-ray (rt) 189	CPMAS	static	175

[a] Model: ligand equilibration via bridge-terminal exchange. [b] Model: formation of "trapped" $Co(CO)_4$ radicals, reorientation, and recombination. [c] Model: reorientation of the Fe_3 triangle within the ligand shell (see text). [d] Model: reorientation of the Co_4 tetrahedron within the ligand shell.

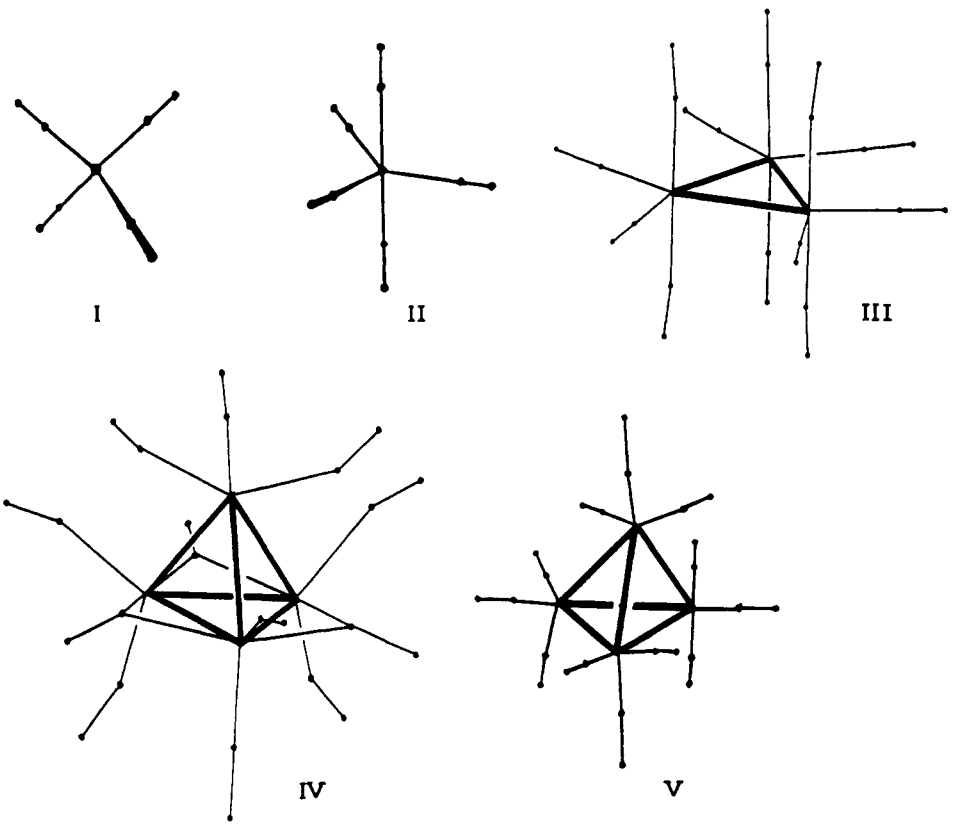

Figure 13. The molecular structures of some representative binary carbonyls listed in Table VIII (see also Figure 14): I, $NI(CO)_4$; II, $Fe(CO)_5$; III, $Ru_3(CO)_{12}$; IV, $Co_4(\mu\text{-}CO)_3(CO)_9$; V, $Ir_4(CO)_{12}$.

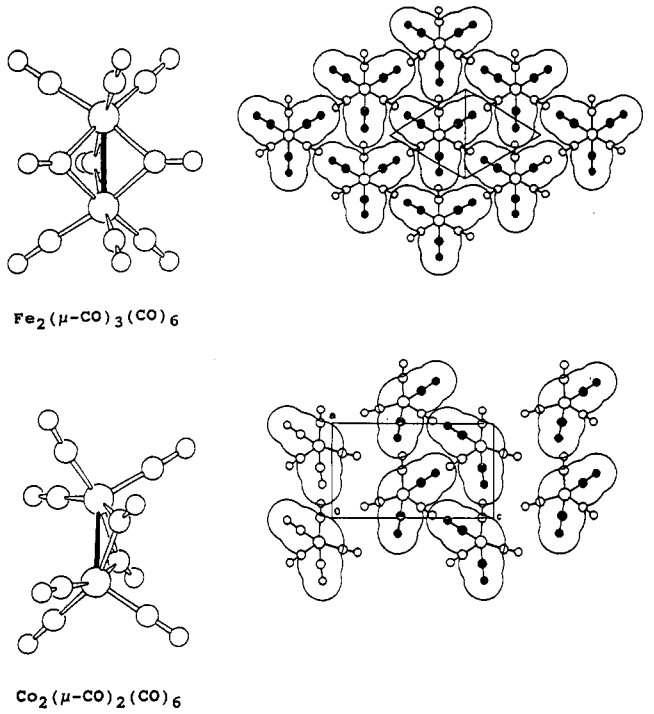

Figure 14. The relationship between molecular and crystal structure of $Fe_2(CO)_9$ and $Co_2(CO)_8$. The "missing ligands" generate large parallel channels in the packing of $Co_2(CO)_8$ with respect to the otherwise extremely similar packing of $Fe_2(CO)_9$. The two packing sections are projected along the molecular M–M axes and cut along the crystallographic mirror planes (space-filling outlines) of the space groups $P6_3/m$ [$Fe_2(CO)_9$] and $P2_1/m$ [$Co_2(CO)_8$]. Filled CO groups identify the bridging ligands.

change has been invoked to explain the presence of three signals in the CO region in the spectra measured between 250 and 243 K.[167b,c]

The CPMAS spectrum[167c] of the $[N(C_2H_5)_4]^+$ salt of the hydridocarbonyl anion $[HFe(CO)_4]^-$ shows only one signal in the CO region at room temperature, while two resonances are resolved (1:3 ratio) below 213 K, consistent with the presence of one axial and three equatorial CO's. To account for this behavior, pseudorotation or other fluxional mechanisms were discarded in favor of an hydride tunneling process requiring an activation energy of ca. 29 kJ mol^{-1}. In the $[PPN]^+$ salt of the same anion, however, all four carbonyl resonances are equivalent. A simultaneous occurrence of hydride tunneling and 3-fold rotation has been invoked to account for the degeneracy.[167c]

The crystal and molecular structures of $Fe_2(CO)_9$[168] and $Co_2(CO)_8$[169] are closely related: at the *molecular* level the two complexes differ essentially by the "absence" of one bridging CO in $Co_2(CO)_8$ with respect to $Fe_2(CO)_9$; in the *crystal*, the main difference is again due to the absence of the "ninth carbonyl" which leads to the formation of large "channels" throughout the lattice of $Co_2(CO)_8$; otherwise the packing is quite similar to that of $Fe_2(CO)_9$ (see Figure 14).[171b] In spite of their close similarities the two species show totally different CPMAS spectra. $Fe_2(CO)_9$ shows a typical "static" pattern of signals,[142] while $Co_2(CO)_8$ shows only one resonance at high temperature (>293 K), which splits into an increasingly complex system of signals below 233 K.[170] The low-temperature spectra reveal the presence of two signals of relative intensity 4:1 (not 3:1 as expected on the basis of the crystal structure[169]), whose chemical shifts have been attributed to terminal and bridging C atoms, respectively. The exchange process was initially interpreted as an interchange between terminal and bridging CO's via simultaneous movement of all ligands with an activation energy of 48.9 kJ mol^{-1}.[170] More recently, a different interpretation has been proposed: a homolitic cleavage of the Co–Co bond in the solid state would generate "trapped" $Co(CO)_4$ radicals which would be able to reorientate and then, eventually, recombine in the bridged structure leading to CO exchange on the NMR time scale.[167a]

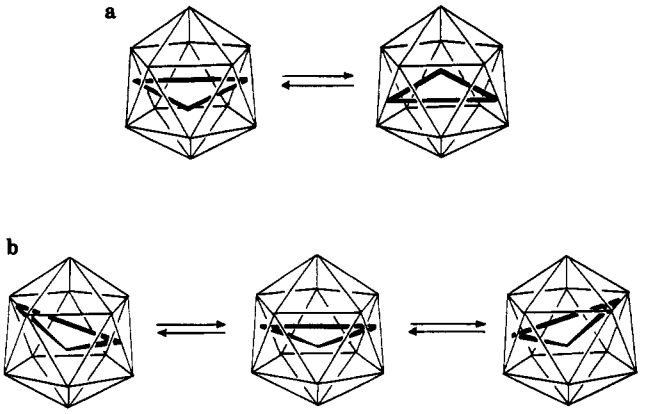

Figure 15. Dynamic behavior in crystalline $Fe_3(CO)_{12}$: model a, reorientation of the Fe_3 triangle within the CO envelope via $2\pi/6$ jumps; model b, librational motion of the Fe_3 triangle within the quasi-icosahedral ligand polyhedron.

Alternatively, it has been suggested that a mechanism based on a limited (a few degrees) librational motion of the Co–Co axis about its center of mass allow partial CO equilibration without major reorganization of the ligand envelope.[171,172]

$Fe_3(CO)_{12}$ shows orientational disorder in the solid state.[173] In the molecular structure two carbonyls are in asymmetric bridging positions along one edge of the iron triangle. The molecule has formal C_2 symmetry with a pseudo-2-fold axis passing through the middle of the bridged Fe–Fe bond and the opposite Fe atom. The disorder is due to the high regularity of the outer, almost icosahedral, peripheral polyhedron described by the O atoms which does not appreciably differ whether the iron triangle is in one orientation or its inverse. CPMAS measurements[174] have shown that, at temperatures below 178 K, the NMR spectrum is consistent with the crystal structure,[173] indicating two bridging and ten terminal carbonyls. At 297 K there are three pairs of resonances of similar integrated intensities, but none of the observed chemical shifts are consistent with either bridging or semibridging carbonyls. Rapid in-plane 60° jumps of the Fe_3 triangle within the ligand envelope (see Figure 15) has been invoked to explain the intensity pattern and the temperature dependence of the spectra. An activation energy of 41.8 kJ mol^{-1} has been estimated for bridge–terminal exchange from the coalescence temperature of 218 K.[174]

A qualitative inspection of the thermal motion features of the Fe atoms casts some doubt on this mechanisms. It has been pointed out[172] that the ADP orientation[173b] shows no indication of preferential in-plane motion of the metal triangle, rather, the thermal ellipsoids for the iron atoms indicate a preferred librational motion of the triangle about the molecular pseudo-2-fold axis (see Figure 15). This motion, provided the amplitude is sufficiently large, might suffice to bring

about partial isomerizations between the limiting C_2 (with two symmetric bridging CO's) and D_3 (all terminal) molecular conformations without need for a complete rotation of the metal framework.

A further interpretation of the dynamic behavior of $Fe_3(CO)_{12}$ has been put forward:[178] it has been argued that the lowest energy process in solution implies shifts of the bridging CO's along the triangle edges without full-scale ligand migration.[178] This mechanism would be still operating in the solid state at 180 K, thus accounting for the differences between the positions of the signals observed in the CPMAS spectra and those predicted on the basis of the behavior in solution of a number of $Fe_3(CO)_{12}$ derivatives. Finally the Mossbauer study[177] of $Fe_3(CO)_{12}$ should be mentioned. The spectral changes observed between 4.2 and 295 K have been explained on the basis of changes in Fe–Fe and Fe–C bond lengths arising from some kind of solid-state dynamic process.

The solid-state dynamics of $Fe_2Os(CO)_{12}$[176] has not been studied. It is, however, worth mentioning in the context of this discussion, that this molecule is isostructural with $Fe_3(CO)_{12}$ although the orientational disorder of the metal frame over the two alternative sites is only 12:1 in $Fe_2Os(CO)_{12}$ with respect to the 1:1 in $Fe_3(CO)_{12}$.[173] This difference has been attributed to the higher contribution of the inner metal core to the crystal potential in the species containing osmium with respect to the homonuclear complex.[15] The metal core appears to favor an ordered molecular distribution in the lattice, this effect is "obscured" in $Fe_3(CO)_{12}$ where the outer CO ligand polyhedron (invariant to inversion) dominates the intermolecular interactions.

Contrary to $Fe_3(CO)_{12}$, no equilibration mechanism operates in crystalline $Ru_3(CO)_{12}$,[179] $Os_3(CO)_{12}$,[183] $Ir_4(CO)_{12}$,[188] and $Rh_6(CO)_{16}$[189] as shown by several independent CPMAS and CSA studies.[166,175,180,184] In the case of $Ru_3(CO)_{12}$, however, the resonances attributed to the axial CO's show a marked narrowing on increasing the temperature from 293 K to 318 K, while those of the equatorial CO's remain almost unchanged.[175,180] This behavior has been attributed to the occurrence of "local" motion involving the axial ligands.[180] Finally, the extensive vibrational studies carried out by high-resolution infrared and Raman spectroscopy[181,182] should be mentioned.

The crystal of $Co_4(CO)_{12}$ is also disordered.[185a,b] The molecule has three carbonyl groups in edge-bridging positions around a tetrahedral face, the remaining carbonyls being terminally bound. The peripheral polyhedron described by the O atoms is again approximately icosahedral, and the molecular symmetry is very close to C_{3v}. The CPMAS spectrum of $Co_4(CO)_{12}$ has been recorded over a wide temperature range (211–336 K).[186] Above 308 K only one broad signal can be seen, but below 297 K four peaks appear. No other changes occur on cooling to 211 K. Similarly to $Fe_3(CO)_{12}$, these spectral features have been initially interpreted assuming reorientation of the Co_4 core within the ligand envelope.[186] More recently, the high-field CPMAS spectrum of $Co_4(CO)_{12}$ at room temperature has been reinvestigated.[187] It has been concluded that the presence of (at least) three signals and of (at least) one signal unambiguously attributable to terminal and bridging CO's, respectively, can be justified either on the basis of a "static", poorly resolved, spectrum or by invoking a rotational motion of the Co_4 frame exclusively around the crystallographic 2-fold axis that relates the two disordered orientations of the cluster.

It has been argued, however, that the librational model applied to $Co_2(CO)_8$ and $Fe_3(CO)_{12}$ can also account for the (controversial) behavior of $Co_4(CO)_{12}$: a librational motion of the Co_4 tetrahedron accompanied by small concerted motions of the carbonyl shell could lead to partial averaging of the CO resonances at room temperature.[172] This model is in agreement with the preferential oscillation of the metal frame around the tetrahedron axis indicated by the ADP pattern of the cobalt atoms.[185b]

J. High Nuclearity Transition Metal Arene Clusters

In the preceding sections, it was shown by many examples that unsaturated organic fragments coordinated to metal centers with substantial bonding delocalization can undergo rotational jumping motion in the solid state as a function of the shape of the fragment: i.e. the more regular the shape the lower the reorientational barrier.

More recently it has been demonstrated that the relationship between fragment shape and ease of reorientation can be transferred to larger polymetallic systems. Differences between mononuclear and polynuclear species arise mainly at the *intramolecular* level as it will be briefly discussed in the following.

For all cases[190–199] listed in Table IX the possible occurrence of reorientational motions, similar to those observed in mononuclear crystalline complexes, has been explored by means of AAPEB calculations.[191,197] The structures of the most representative clusters listed in Table IX are shown in Figures 16–18.

CPMAS experimental results are available only for solid $Os_3(CO)_8(\eta^2\text{-}C_2H_4)(\mu_3{:}\eta^2{:}\eta^2{:}\eta^2\text{-}C_6H_6)$.[193] The CPMAS spectra recorded in the range 220–335 K indicate the occurrence of exchange processes involving both the face-capping C_6H_6 and the terminally bound C_2H_4 fragments: reorientation of the two fragments (over the triangular metal frame and about the $Os\text{–}C_2H_4$ coordination axis, respectively) gives rise to two resonances between 245 and 296 K for the two groups of C atoms. Multiple resonances are resolved on cooling from 245 to 220 K. Above 270 K and up to 335 K progressive broadening of the CO resonances is also observed suggesting that the CO ligands within the $Os(CO)_3$ units can interchange by "turnstile" rotation. Benzene and ethene reorientational motions have the same activation energy (55 kJ mol^{-1}).[193] A discrimination between fortuitous coincidence and correlated motions has not been possible on the basis of the CPMAS experiment alone. Insights into this problem have been afforded by AAPEB calculations.[191] While *intermolecular* interactions do not oppose significantly the two motions, reorientation of the C_2H_4 fragment is possible only if accompanied by benzene jumps over the cluster surface. The two reorientational processes are, therefore, correlated, i.e. C_2H_4 can reorientate only if benzene "gives way". The calculated intramolecular barrier for this process is about 50 kJ mol^{-1}, thus suggesting that the motion in the solid state is almost exclusively under intramolecular control.

TABLE IX. Dynamic Behavior in Crystalline Transition Metal Arene Clusters

species diffraction (T) ref method(s)	model; AE/PB (T)	ref
$Ru_3(CO)_9(\mu_3:\eta^2:\eta^2:\eta^2\text{-}C_6H_6)$		
X-ray (rt, 193 K) 190		
AAPEB, benzene reorientation	PB = 18.8 (rt), 26.4 (193 K)	190
$Os_3(CO)_8(\eta^2\text{-}CH_2CH_2)(\mu_3:\eta^2:\eta^2:\eta^2\text{-}C_6H_6)$		
X-ray (rt) 192		
AAPEB, benzene reorientation, static C_2H_4	PB = 20.1[a]	191
AAPEB, C_2H_4 reorientation, static benzene	forbidden[a]	
AAPEB, concerted benzene and C_2H_4 motion	PB = 50.2[b]	
AAPEB, $(CO)_3$ rotation	forbidden	
CPMAS,[c] benzene and C_2H_4 reorientation[d]	AE = 55	193
CPMAS,[c] CO's turnstile rotation	AE > 66, AE < 44[e]	
$Os_3(CO)_7(\mu_3:\delta:\eta^2:\delta\text{-}C_2Me_2)(\eta^6\text{-}C_6\text{-}H_6)$		
X-ray (rt) 194		
AAPEB, benzene reorientation, static C_2Me_2	PB = 8.8[a]	191
AAPEB, C_2Me_2 reorientation	forbidden	
$Ru_3(CO)_7(\eta_3:\delta:\eta^2:\delta\text{-}PhC_2PhCO)(\eta^6\text{-}C_6H_6)$		
X-ray (rt) 195		
AAPEB, benzene reorientation	PB = 10.9[a]	195
$H_2Os_4(CO)_{10}(\eta^6\text{-}C_6H_6)$		
X-ray (rt) 196		
AAPEB, benzene reorientation	PB = 36.0[a]	197
$H_2Os_4(CO)_{10}(\eta^6\text{-}C_6H_5Me)$		
X-ray (rt) 197		
AAPEB, toluene reorientation	forbidden	197
$H_2Os_4(CO)_{10}(\eta^6\text{-m-}C_6H_4Me_2)$ and $H_2Os_4(CO)_{10}(\eta^6\text{-o-}C_6H_4Me_2)$		
X-ray (rt) 197		
AAPEB, xylene reorientation	forbidden	197
$Ru_6C(CO)_{14}(\eta^6\text{-arene})$ (arene = C_6H_5Me, $C_6H_3Me_3$)		
X-ray (rt) 198 (C_6H_5Me); 197 ($C_6H_3Me_3$)		
AAPEB, arene reorientation	forbidden	197
$Ru_6C(CO)_{11}(\mu_3:\eta^2:\eta^2:\eta^2\text{-}C_6H_6)(\eta^6\text{-}C_6H_6)$		
X-ray (rt) 199		
AAPEB, η^6-benzene reorientation	PB = 11.7[a]	197
AAPEB, μ_3-benzene reorientation	PB = 20.5[a]	

[a] Total barrier resulting from the sum of intermolecular and intramolecular terms. [b] Intramolecular barrier only. [c] In the temperature range 220–335 K. [d] The NMR data do not allow one to ascertain if the motion of the two ligands is correlated. [e] Activation energies for turnstile rotation of the two $Os(CO)_3$ units in the molecule (labeled Z and Y in ref 193).

AAPEB calculations have shown that benzene reorientation can occur also in the other crystalline benzene clusters. From Table IX it can be seen that, irrespective of the cluster nuclearity and of the mode of bonding of benzene (whether $\mu_3:\eta^2:\eta^2:\eta^2$ or η^6), reorientation of C_6H_6 fragments is invariably permitted at room temperature with potential barriers between 9 and 36 kJ mol^{-1}. No systematic differences can be detected between face-capping and terminal-bonding modes. This is in agreement with the highly fluxional behavior of these species in solution: irrespective of the mode of coordination, the ring protons invariably show a broad singlet resonance in ^{1}H NMR spectra at room temperature. The averaging processes can be frozen out only at low temperatures (below 180 K).[192,193]

On the contrary, reorientation of toluene, xylene, and mesitylene ligands appears to be prevented by strong intermolecular and intramolecular repulsions. In fact, these ligands are tightly "locked in place" both by the neighboring ligands belonging to the same molecule ("intramolecular locking") and by those belonging to the surrounding molecules ("intermolecular locking").

Interestingly, the crystal packings of the benzene and toluene derivatives have much in common. In spite of the differences in cluster nuclearity and in type of arene ligand, the crystals of $H_2Os_{10}(CO)_{10}(\eta^6\text{-}C_6H_6)$, $H_2Os_{10}(CO)_{10}(\eta^6\text{-}C_6H_5Me)$, and $Ru_6(CO)_{14}(\eta^6\text{-}C_6H_5Me)$ show arene fragments grouped together in "ribbons" in order to optimize CO···CO interlocking.[197] A schematic representation of the molecular organization in the lattice of the two tetranuclear osmium clusters is shown in Figure 17. In this respect, it is worth recalling that in crystalline $Ru_6(CO)_{11}(\eta^6\text{-}C_6H_6)(\mu_3:\eta^2:\eta^2:\eta^2\text{-}C_6H_6)$ the benzene ligands have been found to establish graphitic-like interactions (see Figure 18).[197] In this crystal the reorientational barrier of the face-capping benzene is almost twice as large as that of the terminal ligand (20.5 versus 11.7 kJ mol^{-1}).

An example of the application of thermal motion analysis to transition metal clusters is offered by the species $Ru_3(CO)_9(\mu_3:\eta^2:\eta^2:\eta^2\text{-}C_6H_6)$ whose structure has been studied at room temperature and 193 K by X-ray diffraction.[190] Figure 19 shows a pictorial representation of the mean-square librational amplitudes for a dynamic model in which different atomic groups are supposed to possess additional motion with respect to the rigid-body motion of the entire molecule. These independently moving groups are the face-capping C_6 fragment, the radial CO's, and the $(CO)_3$ "cones" carried by the three ruthenium atoms (see Figure 19). Furthermore, the O atoms are allowed independent motion with respect to the C atoms of the carbonyl groups. It can be seen that the molecule behaves as a rigid body in its motion about equilibrium only in first approximation since both benzene and CO groups have appreciable additional motion with respect to the metal frame. Both rigid-body and additional motions increase with temperature. It can also be noted that the librational freedom of benzene around the idealized molecular 3-fold axis is larger than that of the equatorial CO's and

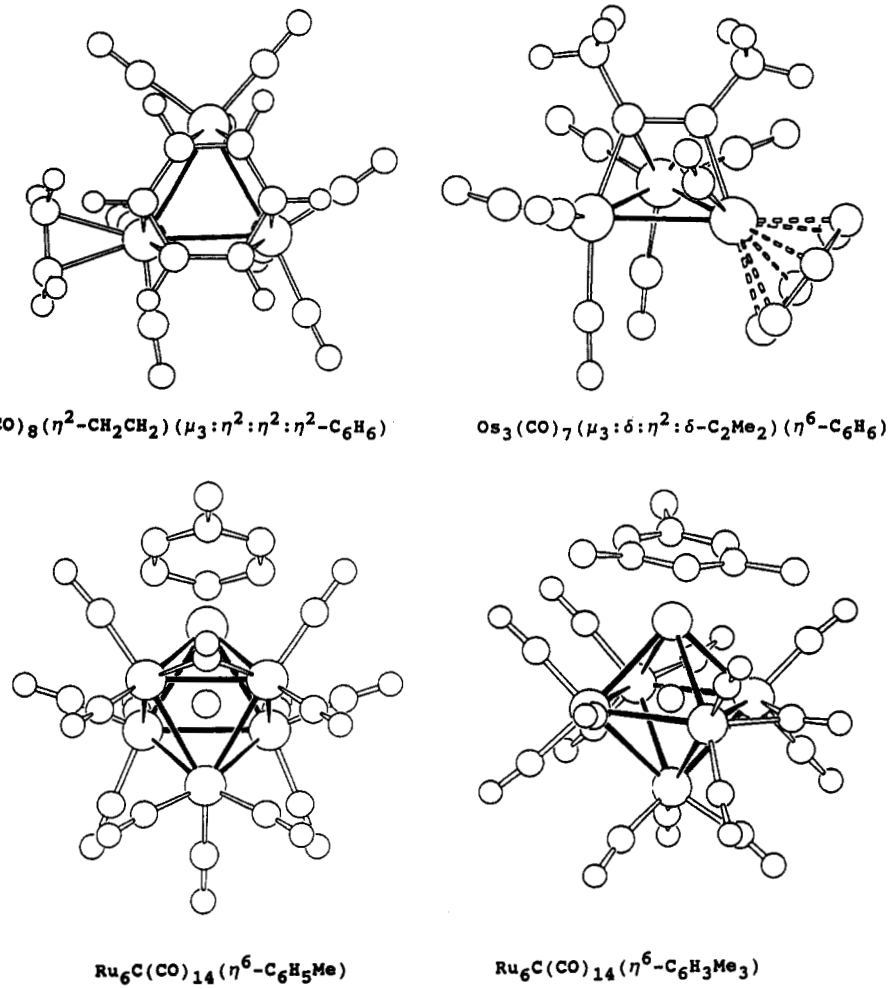

Figure 16. The molecular structures of some arene carbonyl clusters listed in Table IX (see also Figures 17 and 18).

that the extra motion of the $(CO)_3$ cones is larger than that of the equatorial ligands. In general, however, in the carbonyl groups the additional motion of the O atoms is larger than that of the C atoms, indicating that some bending motion of the M–C–O axes is convoluted in the observed ADP.

V. Conclusions and Outlook

Molecules are mobile in their crystals. This idea is fairly commonplace in the organic solid-state chemistry field, but it is, perhaps, less obvious for inorganic and organometallic chemists and crystallographers. Only a few of the very large number of structural organometallic papers published yearly address the problem of motion in the solid state directly. In most cases, diffraction studies result in the description (although accurate) of the structure of an individual molecule *extracted* from its environment. The anisotropic refinement of the atoms, when carried out, is regarded more as a convenient way to increase the number of parameters in the structural model and achieve better agreement indices, than as a way to explore atomic motion about equilibrium positions. Unless extraordinary features appear, this information is relegated to rather unaccessible depositories if not totally lost.

The information on the structure of the crystal (although *invariably* and *necessarily* contained in the results of any structural analysis of reasonable quality) does not face a better fate. The molecular organization in the lattice, the distribution of intermolecular interactions (apart for comments on "van der Waals contacts within the expected range"), and the intimate relationship between molecular and crystal structure are, in most cases, simply neglected.

We have seen, in this review article, that a large variety of molecular rearrangements take place in the crystal lattice of organometallic molecules. These processes are *identified* mainly by spectroscopic techniques, but their *interpretation* is usually based on the knowledge of the crystallographically determined structure. Hence, when studying molecular rearrangements in the solid state, spectroscopy and crystallography are complementary and mutually dependent. Only an exact knowledge of the molecular organization within the lattice and, possibly, of the factors which determine the choice of the packing mode, is the ground on which dynamic phenomena detected spectroscopically (and, more generally, the whole range of crystal properties) can be modeled and (perhaps) understood.

The results of this survey can be summarized as follows:

Molecules containing π-bonded conjugated cyclic polyolefins without ring substituents easily rearrange in the solid state. The simplest process is ring jumping of the ligand between symmetry undistinguishable positions. The activation energies for the jumping motion are invariably very low, rarely exceeding 20–25 kJ mol^{-1}. There is no direct relationship between en-

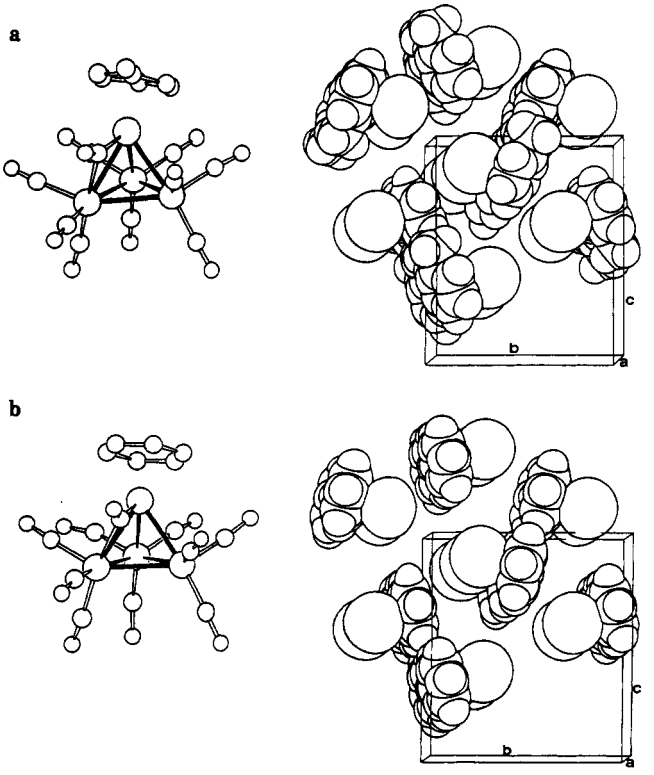

Figure 17. Relationship between molecular and crystal structures of $H_2Os_4(CO)_{10}(\eta^6\text{-}C_6H_5Me)$ (a) and $H_2Os_4(CO)_{10}(\eta^6\text{-}C_6H_6)$ (b). For sake of clarity the metal frame and the CO ligands in the packing drawings are represented by large spheres. Note that the arenes form "ribbons" throughout the lattice. In spite of these similarities, reorientation of benzene is permitted at room temperature, while toluene is blocked in its motion.

ergy barriers and the *size* of the ring. If the contribution of the internal barrier (arising from chemical bonding and/or intramolecular nonbonding interactions) is small, the energy barriers to reorientation are a function solely of the molecular organization in the lattice.

Each fragment appears to have specific packing requirements and motional characteristics, which are *transferable* from crystal to crystal. As a matter of fact, a simple comparison of the activation energies associated to ring reorientation in crystalline benzene, thiophene, and hexamethylbenzene (from PSLRT measurements, benzene, 17.4;[200a] thiophene, 15.5;[200b] hexamethylbenzene,[20b] 26.8 kJ mol^{-1}) with the values reported in Table I for the crystalline complexes containing these fragments as ligands provides a clear indication that the intermolecular interactions due to crystal packing exert a similar control on the dynamic behaviors of these fragments *whether as free molecules or coordinated to metal centers.* This is a natural consequence of the principles of close packing.[3a] Since the packing of organometallic complexes is governed mainly by the shape of the outer fragments, it should not surprise that the same organic fragments in organic and organometallic crystals are found often to pack in a similar way, and hence to reorient under similar intermolecular constraints. An example of how closely related the structures of organic and organometallic *crystals* can be is given in Figure 20, where the distribution of the first neighboring molecules in the lattice of benzene and of dibenzenechromium is compared.[84] In both crystals the polyhedron described by the centers of mass of the first neighboring molecules is nearly

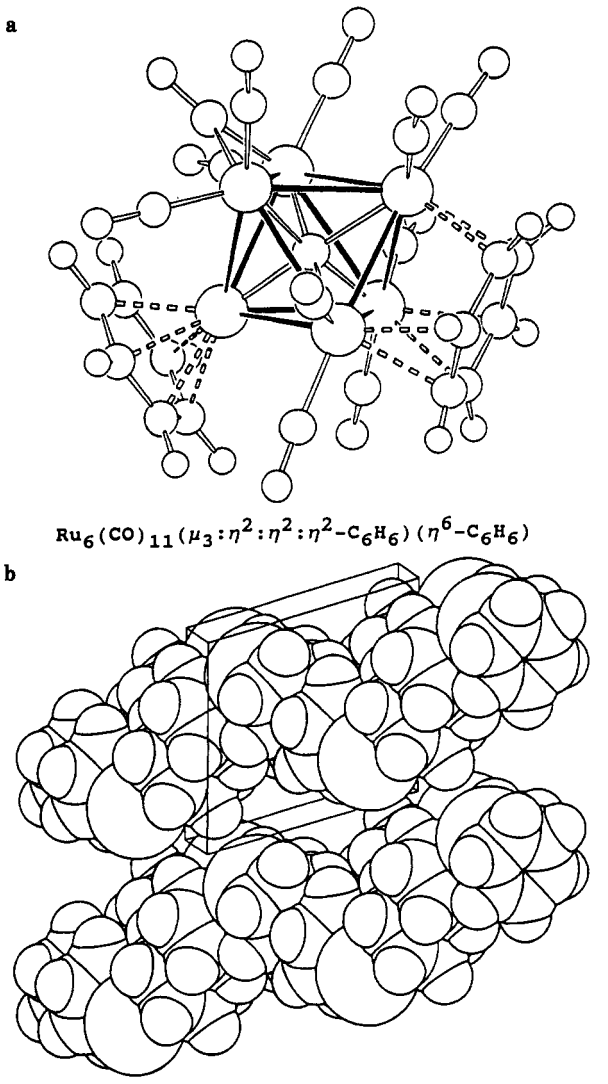

Figure 18. Relationship between the molecular structure (a) of $Ru_6C(CO)_{11}(\eta^6\text{-}C_6H_6)(\mu_3:\eta^2:\eta^2:\eta^2\text{-}C_6H_6)$ and its crystal structure (b). For sake of clarity the metal frame and the CO ligands in the packing diagram are represented by large spheres. Note the graphitic-like interaction between the benzene ligands. Both ligands can undergo reorientational jumping motion in the solid state.

cubooctahedral and the benzene fragments have similar relative orientations in spite of the *apparent* differences in space group symmetry (benzene crystallizes in the space group *Pbca*,[201] while $(C_6H_6)_2Cr$ crystallizes in the space group $Pa\bar{3}$[78]).

We have also shown that benzene can undergo reorientational jumping motion in crystals of large polymetallic systems irrespective of the molecular complexity (i.e. nuclearity, presence of other ligands beside CO's, etc.), of the crystal features (site symmetry, space-group symmetry etc.), and of the mode of coordination (terminal or face capping). Similar behavior can be safely predicted for all other rigid and planar conjugated cyclic polyolefin ligands.

Upon substitution of bulky groups for the H atoms, the ease of motion becomes a direct function of the ligand shape. If the ligand shape deviates from discoidal, the jumping motion (at least at room temperature) is restricted, if not altogether forbidden. In some cases, even if jumping motion is not allowed, large amplitude oscillatory motions can still afford isomerization mechanisms, which are detected in the NMR experi-

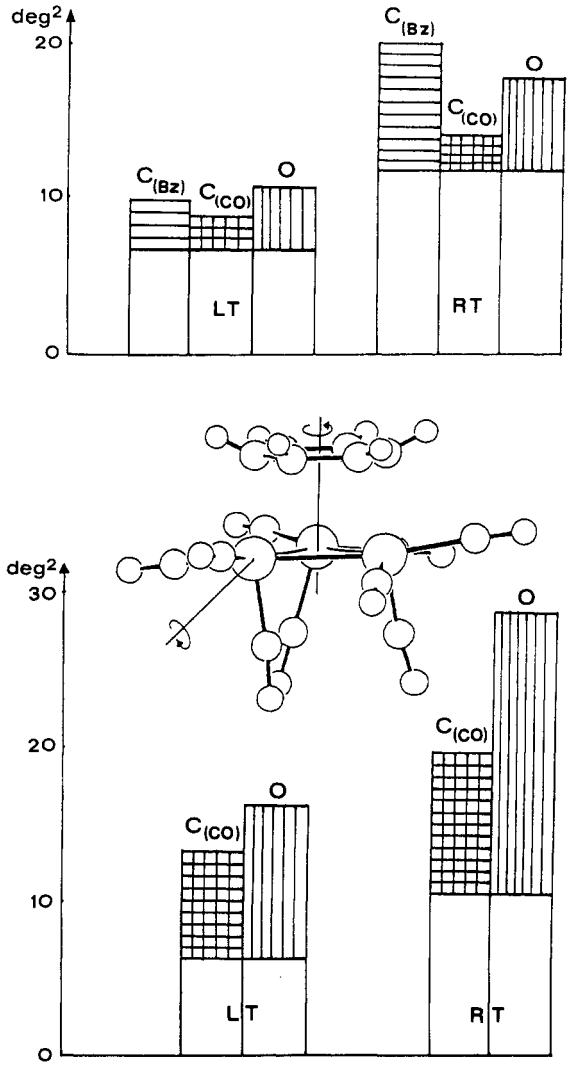

Figure 19. Schematic representation of the temperature dependence of the mean-square librational amplitudes (deg^2) obtained from the "nonrigid" treatment of the thermal motion in $Ru_3(CO)_9(\mu_3{:}\eta^2{:}\eta^2{:}\eta^2\text{-}C_6H_6)$; RT = 298 K, LT = 193 K: top, rigid-body and additional motion of the benzene ligand and of the radial C and O atoms of the CO ligands; bottom, (average) rigid-body and additional motion of the C and O atoms of the tricarbonyl units.

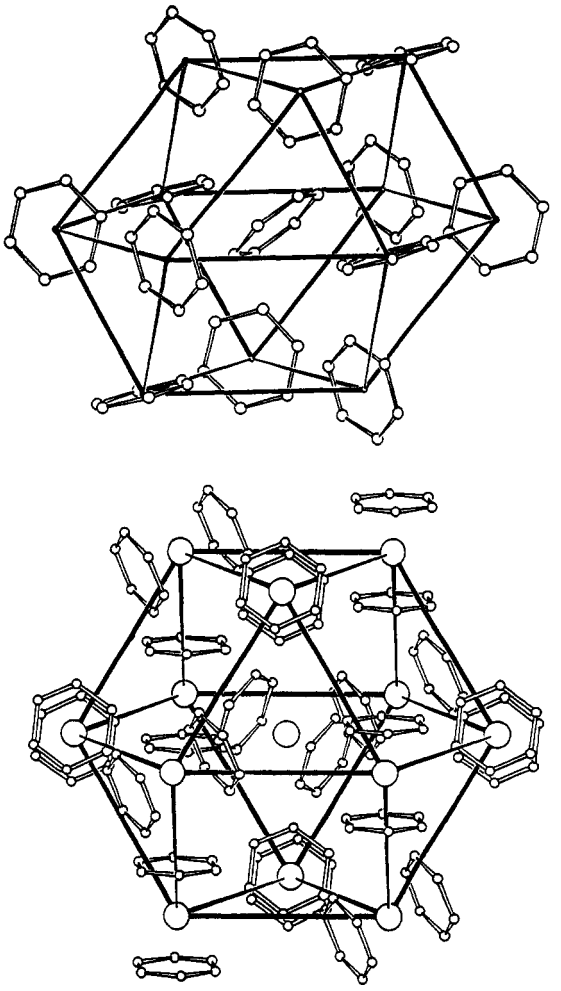

Figure 20. Relationship between the molecular organization in crystalline benzene and $(\eta^6\text{-}C_6H_6)_2Cr$. Note the cubooctahedral molecular distribution in the two crystals. The benzene fragments have similar relative orientation and can undergo reorientational jumping motion with similar values of energy barriers (reprinted from ref 84; copyright 1991 American Chemical Society).

ments in the form of partially averaged spectra or of a superposition of signals due to the simultaneous presence in the lattice of several molecular conformations. On increasing the temperature, the amplitude of the librational motions increases leading, eventually, to complete reorientation.

In most $(\eta^n\text{-}C_nH_n)M(CO)_3$, bis-arenes, and metallocenes species intramolecular nonbonding interactions give a negligible contribution to the reorientational barrier. This is not so when the molecular geometry brings closer together the organic fragments ("bent" metallocenes and cyclooctatetraene derivatives). In such cases, the total barrier is the sum of intramolecular and intermolecular contributions. Intramolecular repulsions become particularly effective as the molecular complexity is increased to the extent that, in some transition metal clusters, the reorientational processes are actually *controlled* primarily at the intramolecular level.

Ring buckling is observed when the conjugated cyclic polyolefin ligand is very flexible, as in the case of cyclooctatetraene. The activation energy for reorientation of this ligand is substantially higher than for other rigid rings, indicating that the complicated motion of the ring between minimum energy lattice positions is more hindered than simple ring jumps. Diene topomerization and reorientation of monohapto cyclopentadienyl rings are also higher energy processes with respect to ring jumps.

On the experimental side there is a generally good agreement between the results of the various experimental methods, and between these and the results of calculations based on the atom–atom potential energy method or on thermal motion analysis, at least for low-energy reorientational processes. This is quite remarkable in view of the many different assumptions behind the various kinds of analysis.

In some cases, indications of low-energy atomic and molecular motions are directly provided by an analysis of the atomic ADP. In general (although not necessarily), low-energy barriers are associated with a motion pathway easily recognizable from the pattern of preferential atomic displacements around equilibrium positions, as revealed by the atomic ADP.

When the dynamic phenomena become more complicated than simple rigid body reorientations, the interpretations of the various experimental results tend to diverge. In this respect, carbonyl fluxionality in the

solid state is definitely a controversial phenomenon. One may argue, however, that the "way of thinking" to CO motion in solution (in terms of ligand migration or metal framework reorientation) cannot be simply "transferred" to the solid state. Fluxionality processes imply extensive molecular reorganization and extremely large atomic displacements that contrast with the presence of tight molecular interlocking in the lattice due to the interpentration of the CO envelopes. Perhaps a different approach should be put to test: the motional features both in the solid state *and* solution might be explained on the basis of processes that do not involve full scale ligand migration but only limited displacements of the CO ligands (such as opening and closing of CO bridges and torsional motions of tricarbonyls groups) accompanied by librational motions of the metal frameworks. These processes take full advantage of the intrinsic "plasticity" of the CO polyhedra around the metal cores. The extent to which such processes occur will depend on the temperature and on the extent of intermolecular interactions. Thanks to the drastic decrease in motional freedom with respect to solution, solid-state studies allow, in principle, direct investigation of the dynamic processes of lowest energy that are often impossible to freeze out in solution or in the liquid state. We believe that much work needs to be done before the solid-state dynamic behavior of binary carbonyls is fully understood.

Phase transitions in organometallic crystals are more common than usually thought. Although these phenomena have not been systematically studied (with the notable exception of the metallocene family) the evidence collected here clearly shows that phase transitions are often associated with the onset of reorientational processes. If the reorientational motion occurs *via* jumps between positions undistinguishable by symmetry, the transition is usually undetected by X-ray diffraction, since the atoms spend "most of their time" at the bottom of isoenergetic potential wells. In many other cases, phase-transition phenomena are seen to involve transition metal complexes containing either heteroatomic rings (such as thiophene) or partially substituted rings (such as durene and acetyl- and formylcyclopentadienyl ligands, etc.). The "irregular shape" of these fragments seems to prevent optimum intermolecular organization and introduce some degree of "instability" in the crystal. Crystals of this kind are, thus, very likely to undergo transformations toward disordered (or plastic) phases as the lattice loses cohesion on increasing the temperature.

While there has been no report of temperature-dependent phase transitions for metal carbonyl crystals, Raman spectroscopy studies have recently shown that a number of solid metal carbonyl complexes undergo phase transition under high pressure.[202] This behavior has been ascertained for $(\eta^5\text{-}C_5H_5)Re(CO)_3$[202c] and for several carbonyl and cyanide complexes.[202d] A particularly interesting observation is that the phase transition occurring between 7 and 13 kbar in crystalline $Mn_2(CO)_{10}$ and $Re_2(CO)_{10}$ is accompanied by a change from staggered to eclipsed conformation of the two $M(CO)_5$ units.[202e]

Solid-state reactions are still regarded as mere chemical curiosities in this field. Very few, well-understood, examples have been described and this area of organometallic research is almost totally unexplored. In the context of this review it can only be pointed out that molecular motion is a prerequisite for reactivity. In the case of the extensively studied crystal-to-crystal racemization reactions of cobalt oxime complexes[203] it has been shown that the reaction rate depends critically on the volume of the reactive cavity in which the racemization takes place. Analogously, the solid-state dimerization of $(\eta^5\text{-}C_5H_5)Co(S_2C_6H_4)$[204] implies displacement of two monomers toward each other and 45° tilt of the cyclopentadienyl ligands, while the recently described solid–vapor reaction of $[P(CH_2CH_2PPh_2)_3Co(N_2)][BPh_4]$ with HCCH, H_2CCH_2, CH_2O, MeCHO, and CO has been discussed in terms of motional freedom of the phosphine ligand to permit elimination of N_2 and access to the small organic molecules through the crystal lattice.[205]

Conformational polymorphism and transformation between polymorphic forms are well documented in the organic solid-state chemistry field,[206] while they have been given, thus far, very little attention in the organometallic area. The X-ray stimulated, irreversible, phase transition of a bis(terpyridyl)cobalt(II) salt[207a] and the solid-state rearrangement of (phenylazophenyl)palladium hexafluoroacetonate[207b] constitute two examples of crystallographically characterized solid-state transformations between two polymorphic modifications. In the latter case, in particular, it has been shown that the two phases differ markedly in crystal packing patterns, and that their interconversion implies extensive molecular reorganization in the solid state.

These seminal studies demonstrate that solid-state organometallic chemistry is full of potentialities. It can be anticipated that, as the interest in exploring new synthetic paths and in designing new materials with predefined properties will increase, this area of chemistry will become a fruitful field of new discoveries in the near future.

VI. Acknowledgments

It is a pleasure to acknowledge the help and encouragement received from a number of collegues during the preparation of this review. I am particularly indebted with S. Aime, A. Gavezzotti, and F. Grepioni for their continuous scientific support and for many helpful comments and constructive criticisms. I also thank R. Gobetto and H. B. Bürgi for many valuable suggestions and discussions. I have been greatly assisted by M. Gandolfi, A. Mondini, and D. Chrysostomou during the preparation of the manuscript. Financial support by Ministero dell' Università e della Ricerca Scientifica is acknowledged.

VII. Abbreviations

AAPEB	atom–atom potential energy barrier calculations
ADP	anisotropic displacement parameters
AE	activation energy
CPMAS	^{13}C cross-polarization magic-angle spinning NMR spectroscopy
CSA	chemical shift anisotropy
IQENS	incoherent quasi-elastic neutron scattering
PB	potential barrier

PBADP potential energy barrier calculations from mean-square librational amplitudes obtained by thermal motion analysis
PSLRT ^1H spin–lattice relaxation time measurements
WLNMR ^1H wide-line NMR spectroscopy

VIII. References

(1) (a) Gavezzotti, A.; Simonetta, M. *Chem. Rev.* **1981**, *82*, 1. (b) *Organic Solid State Chemistry*; Desiraju, G. R., Ed.; Elsevier: Amsterdam, 1987. (c) *Structure and Properties of Molecular Crystals*; Pierrot, M., Ed.; Elsevier: Amsterdam, 1990.
(2) (a) Desiraju, G. R.; Harlow, R. L. *J. Am. Chem. Soc.* **1989**, *111*, 6757. (b) Addadi, L.; Berkovitch-Yellin, Z.; Weissbuch, I.; van Mil, I.; Shimon, L. J. W.; Lahav, M.; Leiserowitz, L. *Angew. Chem., Int. Ed. Engl.* **1985**, *24*, 466. (c) Desiraju, G. R.; Parthasarathy, R. *J. Am. Chem. Soc.* **1989**, *111*, 8725. (d) Etter, M. C.; MacDonald, J. C.; Bernstein, J. *Acta Crystallogr., Sect. B* **1990**, *B46*, 256.
(3) (a) Kitaigorodsky, A. I. *Molecular Crystals and Molecules*; Academic Press: New York, 1973. (b) Gavezzotti, A. *J. Am. Soc.* **1989**, *111*, 1835. (c) Gavezzotti, A. *Acta Crystallogr., Sect. B* **1990**, *B46*, 275. (d) Gavezzotti, A.; Desiraju, G. R. *Acta Crystallogr., Sect. B* **1988**, *B44*, 427. (e) Sarma, J. A. R. P.; Desiraju, G. R. *J. Am. Chem. Soc.* **1986**, *108*, 2791. (f) Bernstein, J.; Sarma, J. A. R. P.; Gavezzotti, A. *Chem. Phys. Lett.* **1990**, *174*, 361. (g) Desiraju, G. R. *Crystal Engineering. The Design of Organic Solids*; Elsevier: Amsterdam, 1989.
(4) (a) Andrew, E. R.; Eades, R. G. *Proc. Soc. London* **1953**, *A218*, 517. (b) Andrew, E. R. *J. Chem. Phys.* **1950**, *18*, 607.
(5) (a) Boyd, R. K.; Fyfe, C. A.; Wright, D. A. *J. Phys. Chem. Solids* **1974**, *35*, 1355. (b) Fyfe, C. A.; Harold-Smith, D. *J. Chem. Soc. Faraday Trans. 2* **1975**, 967. (c) Fyfe, C. A.; Harold-Smith, D. *Can. J. Chem.* **1976**, *54*, 783. (d) Fyfe, C. A.; Dunell, B. A.; Ripmeester, J. *Can. J. Chem.* **1971**, *49*, 3332. (e) Fyfe, C. A.; Gilson, D. F. R.; Thompson, K. H. *Chem. Phys. Lett.* **1970**, *5*, 215.
(6) Gavezzotti, A.; Simonetta, M. *Acta Crystallogr., Sect. A* **1975**, *A31*, 645. (b) Shmueli, U.; Goldberg, I. *Acta Crystallogr., Sect. B* **1973**, *B29*, 2466.
(7) (a) Durig, J. R.; Craven, S. M.; Mulligan, J. H.; Hawley, C. W.; Bragin, J. *J. Chem. Phys.* **1973**, *58*, 1282. (b) Allen, P.; Cowking, A. *J. Chem. Phys.* **1967**, *47*, 4286. (c) Afonina, N. N.; Zorkii, P. M. *J. Struct. Chem.* **1976**, *17*, 13. (d) Eguchi, T.; Chilara, H. *J. Magn. Reson.* **1988**, *76*, 143.
(8) (a) Muetterties, E. L.; Bleeke, J. R.; Wucherer, E. J.; Albright, T. A. *Chem. Rev.* **1992**, *82*, 499. Cotton, F. A.; Wilkinson, G. *Advances Inorganic Chemistry*; Wiley: New York, 1988.
(9) (a) Albright, T. A. *Acc. Chem. Res.* **1982**, *15*, 149. (b) Albright, T. A.; Hofman, P.; Hoffman, R. *J. Am. Chem. Soc.* **1977**, *9*, 7546.
(10) (a) Cotton, F. A.; Hanson, B. E. *Rearrangements in Ground and Excited States*; De Mayo, P., Ed.; Academic Press: New York, 1980; p 379. (b) Aime, S.; Milone, L. *Prog. Nucl. Magn. Reson. Spectrosc.* **1977**, *11*, 183.
(11) (a) Berry, S. *J. Chem. Phys.* **1960**, *32*, 933. (b) Muetterties, E. L. *Tetrahedron* **1974**, *30*, 1595. (c) Muetterties, E. L.; Guggenberger, L. J. *J. Am. Chem. Soc.* **1974**, *96*, 1748.
(12) (a) Evans, J. W. *Adv. Organomet. Chem.* **1979**, *16*, 319. (b) Faller, J. W. *Adv. Organomet. Chem.* **1978**, *16*, 211. (c) Band, E.; Muetterties, E. L. *Chem. Rev.* **1978**, *78*, 639.
(13) (a) Benfield, R. E.; Johnson, B. F. G. *J. Chem. Soc., Dalton Trans.* **1980**, 1743. (b) Johnson, B. F. G.; Benfield, R. E. *Organomet. Stereochem.* **1981**, *12*, 253. (c) Johnson, B. F. G.; Benfield, R. E. *Transition Metal Clusters*; Johnson, B. F. G., Ed.; Wiley: New York, 1980; p 471.
(14) (a) Braga, D.; Grepioni, F. *Acta Crystallogr., Sect. B* **1989**, *B45*, 378. (b) Braga, D.; Grepioni, F. *Polyhedron* **1989**, *8*, 2237. (c) Braga, D.; Grepioni, F.; Sabatino, P. *J. Chem. Soc., Dalton Trans.* **1990**, 3137.
(15) Braga, D.; Grepioni, F. *Organometallics* **1991**, *10*, 1254.
(16) (a) Cotton, F. A. *Inorg. Chem.* **1966**, *5*, 1083. (b) Bullit, J. G.; Cotton, F. A.; Marks, T. J. *J. Am. Chem. Soc.* **1970**, *92*, 2155.
(17) (a) Johnson, B. F. G.; Bott, A.; Benfield, R. E.; Braga, D.; Marseglia, E. A.; Rodger, A. *Metal-Metal Bonds and Clusters in Chemistry and Catalysis*; Fackler, J. P., Ed.; Plenum: New York, 1989. (b) Braga, D.; Anson, C. E.; Bott, A.; Johnson, B. F. G.; Marseglia, E. *J. Chem. Soc., Dalton Trans.* **1990**, 3517.
(18) Fyfe, C. A. *Solid State NMR for Chemists*; CFC Press: Guelph, Ontario, Canada, 1983.
(19) (a) Yannoni, C. S. *Acc. Chem. Res.* **1982**, *15*, 201. (b) Lyerla, J. R.; Yannoni, C. S.; Fyfe, C. A. *Acc. Chem. Res.* **1982**, *15*, 208. (c) Fyfe, C. A.; Wasylishen, R. E. *Solid State Chemistry Techniques*; Cheetham, A. K., Day, P., Eds.; Clarendon Press: oxford, 1987; p 190. (d) Etter, M. C.; Hoje, R. C.; Vojta, G. M. *Crystallogr. Rev.* **1988**, *1*, 281. (e) Bryant, R. G.; Chacko, V. P.; Etter, M. C. *Inorg. Chem.* **1984**, *23*, 3580.
(20) (a) Fyfe, C. A.; Kupferschmidt, G. J. *Can. J. Chem.* **1973**, *51*, 3774. (b) Rothwell, W. P.; Waugh, J. S. *J. Chem. Phys.* **1981**, *74*, 2721. (c) Haeberlen, U.; Waugh, J. S. *Phys. Rev.* **1969**, *185*, 420. (d) Vold, R. R.; Vold, R. L. *J. Chem. Phys.* **1988**, *88*, 1443. (e) Ok, J. H.; Vold, R. R.; Vold, R. L.; Etter, M. C. *J. Phys. Chem.* **1989**, *93*, 7618.
(21) (a) Pines, A.; Gibby, M. G.; Waugh, J. S. *J. Chem. Phys.* **1973**, *59*, 569. (b) Pausak, S.; Pines, A.; Waugh, J. S. *J. Chem. Phys.* **1973**, *59*, 591. (c) Wemmer, D. E.; Pines, A. *J. Am. Chem. Soc.* **1981**, *103*, 34.
(22) Howard, J.; Waddington, T. C. *Advances in Infrared and Raman Spectroscopyl* Hester, R. E., Clark, R. J. H., Eds.; Heyden: London, 1980; p 86.
(23) (a) Schlaak, M. *Mol. Phys.* **1977**, *33*, 125. (b) Dianoux, A. J.; Volino, F. *Mol. Phys.* **1977**, *34*, 1263. (c) Dianoux, A. J.; Volino, F.; Hervet, H. *Mol. Phys.* **1975**, *30*, 1181. (d) Springer, T. *Quasielastic Neutron Scattering for the Investigation of Diffusive Motions in Solid and Liquids*; Springer-Verlag: New York, 1972. (e) Gardner, A. B.; Howard, J.; Waddington, R. M.; Richardson, R. M.; Tomkinson, J. *Chem. Phys.* **1981**, *57*, 453.
(24) (a) Ebsworth, E. A. V.; Rankin, D. V. H.; Cradock, S. *Structural Methods in Inorganic Chemistry*; Blackwell: Oxford, 1987. (b) Bryant, R. G. *J. Chem. Ed.* **1983**, *60*, 933.
(25) Muetterties, E. L. *Inorg. Chem.* **1965**, *4*, 769.
(26) Benfield, R. E.; Braga, D.; Johnson, B. F. G. *Polyhedron* **1988**, *7*, 2549.
(27) Amorós, J. L.; Amorós, M. *Molecular Crystals: their Transform and Diffuse Scattering*; Wiley: New York, 1968.
(28) (a) Dunitz, J. D.; Schomaker, V.; Trueblood, K. N. *J. Phys. Chem.* **1988**, *82*, 856. (b) Dunitz, J. D.; Maverick, E. F.; Trueblood, K. N. *Angew. Chem., Int. Ed. Engl.* **1988**, *27*, 880.
(29) Willis, B. T. M.; Pryor, A. W. *Thermal Vibration in Crystallography*; Cambridge University Press: Cambridge, 1975.
(30) Johnson, L. H. ORTEP. Report ORNL-3794; Oak Ridge National Laboratory: Oak Ridge, TN, 1965. The well known graphic program ORTEP allows to represent atomic ADP in terms of equiprobability (thermal) ellipsoids.
(31) Hummel, W.; Hauser, J.; Bürgi, H. B. *J. Mol. Graphics* **1990**, *8*, 214. The graphic program PEANUT provides for alternative representations of the atomic ADP, such as surfaces of mean square or root mean square displacements. These representations are especially convenient when dealing with ADP differences (see also ref 36).
(32) Hirshfeld, F. L. *Acta Crystallogr., Sect. A* **1976**, *32*, 239.
(33) Schomaker, V.; Trueblood, K. N. *Acta Crystallogr., Sect. B* **1968**, *24*, 63.
(34) Bürgi, H. B. *Acta Crystallogr., Sect. B* **1989**, *B45*, 383.
(35) (a) Dunitz, J. D.; White, D. N. J. *Acta Crystallogr., Sect. A* **1973**, *A29*, 93. (b) Rosenfield, R. E.; Trueblood, K. N.; Dunitz, J. D. *Acta Crystallogr., Sect. A* **1978**, *A34*, 829. (c) Trueblood, K. N. *Acta Crystallogr., Sect. A* **1978**, *A34*, 950.
(36) Hummel, W.; Raselli, A.; Bürgi, H. B. *Acta Crystallogr., Sect. B* **1990**, *B46*, 683.
(37) Maverick, E.; Dunitz, J. D. *Mol. Phys.* **1984**, *62*, 451.
(38) *Accurate Molecular Structures*; Domenicano, A., Harghittay, I., Eds.; Oxford University Press: Oxford, 1991.
(39) (a) Braga, D.; Koetzle, T. F. *J. Chem. Soc., Chem. Commun.* **1987**, 144. (b) Braga, D.; Koetzle, T. F. *Acta Crystallogr., Sect. B* **1988**, *B44*, 151.
(40) Chandrasekhar, K.; Bürgi, H. B. *Acta Crystallogr., Sect. B* **1984**, *B40*, 387.
(41) (a) Ammeter, J. H.; Bürgi, H. B.; Gamp, E.; Meyer-Sandrin, V.; Jensen, W. P. *Inorg. Chem.* **1979**, *18*, 733. (b) Stebler, M.; Ludi, A.; Bürgi, H. B. *Inorg. Chem.* **1986**, *25*, 4743.
(42) (a) Pertsin, A. J.; Kitaigorodsky, A. I. *The Atom-Atom Potential Method*; Springer-Verlag: Berlin, 1987. (b) Kitaigorodsky, A. I. *Chem. Soc. Rev.* **1978**, *7*, 133. (c) Kitaigorodsky, A. I. *Acta Crystallogr.* **1965**, *18*, 585.
(43) (a) Williams, D. E. *Acta Crystallogr., Sect. A* **1972**, *A28*, 629. (b) Williams, D. E.; Cox, S. R. *Acta Crystallogr., Sect. B* **1984**, *B40*, 404. Williams, D. E. *Acta Crystallogr., Sect. A* **1974**, *A30*, 71.
(44) (a) Cox, S. R.; Hsu, L. Y.; Williams, D. E. *Acta Crystallogr., Sect. A* **1981**, *A37*, 293. (b) Gavezzotti, A. *Tetrahedron* **1987**, *43*, 1241.
(45) (a) Berkovitch-Yellin, Z.; Leiserowitz, L. *J. Am. Chem. Soc.* **1982**, *104*, 4052. (b) Dahl, T. *Acta Crystallogr., Sect. B* **1990**, *B46*, 283.
(46) Gavezzotti, A. *Nouv. J. Chim.* **1982**, *6*, 433.
(47) (a) Mirsky, K. *Computing in Crystallography, Proceedings of the International Summer School on Crystallographic Computing*; Delft University Press: Twente, 1978; p 169. (b) Mirsky, K. *Chem. Phys.* **1980**, *40*, 445.
(48) Gavezzotti, A.; Simonetta, M. *Acta Crystallogr., Sect. A* **1976**, *A32*, 997.

(49) Parsonage, N. G.; Staveley, L. A. K. *Disorder in Crystals*; Clarendon Press: Oxford, 1978.
(50) Wendlandt, W. Wm. *Thermal Analysis*; Wiley: New York, 1986.
(51) Harvey, P. D.; Schaefer, W. P.; Gray, H. B.; Gilson, D. F. R.; Butler, I. S. *Inorg. Chem.* **1988**, *27*, 57.
(52) Harvey, P. D.; Butler, I. S.; Gilson, D. F. R. *Inorg. Chem.* **1986**, *25*, 1009.
(53) Howard, J.; Waddington, T. C. *Spectrochim. Acta* **1978**, *34A*, 445.
(54) (a) Bernd, A. F.; Marsh, R. E. *Acta Crystallogr.* **1963**, *16*, 118. (b) Fizpatrick, P. J.; Le Page, Y.; Sedman, J.; Butler, I. S. *Inorg. Chem.* **1981**, *20*, 2852.
(55) Gilson, D. F. R.; Gomez, G.; Butler, I. S.; Fitzpatrick, P. J. *Can. J. Chem.* **1983**, *61*, 737.
(56) Lucazeau, G.; Chhor, K.; Sourisseau, C.; Dianoux, A. J. *J. Chem. Phys.* **1983**, *76*, 307.
(57) Chhor, K.; Lucazeau, G. *Inorg. Chem.* **1984**, *23*, 462.
(58) Fizpatrick, P. J.; Le Page, Y.; Butler, I. S. *Acta Crystallogr., Sect. B* **1981**, *B37*, 1052.
(59) (a) Wilford, J. B.; Whitla, A.; Powell, H. M. *J. Organomet. Chem.* **1967**, *8*, 495. (b) Hoch, M.; Rehder, D. *Chem. Ber.* **1988**, *121*, 1541.
(60) Braga, D.; Grepioni, F.; Sabatino, P. Unpublished results.
(61) Bailey, M. F.; Dahl, L. F. *Inorg. Chem.* **1985**, *4*, 1306.
(62) Chhor, K.; Bocquet, J. F.; Lucazeau, G.; Dianoux, A. J. *Chem. Phys.* **1984**, *91*, 471.
(63) Chhor, K.; Lucazeau, G. *Spectrochim. Acta* **1982**, *38A*, 1163.
(64) Calvarin, G.; Berar, J. F.; Weigel, D.; Azokpota, C.; Pommier, C. *J. solid State Chem.* **1978**, *25*, 219.
(65) Chhor, K.; Pommier, C.; Berar, J. F.; Calvarin, G. *Mol. Cryst. Liq. Cryst.* **1981**, *71*, 3.
(66) Chhor, K.; Pommier, C.; Diot, M. *Mol. Cryst. Liq. Cryst.* **1983**, *100*, 193.
(67) Poizat, O.; Sourisseau, C.; Calvarin, G.; Chhor, K.; Pommier, C. *Mol. Cryst. Liq. Cryst.* **1981**, *73*, 159.
(68) Poizat, O.; Sourisseau, C.; Chhor, K.; Pommier, C. *J. Chim. Phys.* **1982**, *79*, 2.
(69) (a) Gilson, D. F. R.; Gomez, G. *J. Organomet. Chem.* **1982**, *240*, 41. (b) Balducci, G.; Bencivenni, L.; DeRosa, G.; Gigli, R.; Martini, B.; Nunziante Cesaro, S. *J. Mol. Struc.* **1980**, *64*, 163.
(70) Engelhardt, L. M.; Papasergio, R. I.; Raston, C. L.; White, A. H. *Organometallics* **1984**, *3*, 18.
(71) (a) Bailey, M. F.; Dahl, L. F. *Inorg. Chem.* **1965**, *4*, 1314. (b) Rees, B.; Coppens, P. *Acta Crystallogr., Sect. B* **1973**, *B29*, 2516. (c) Wang, Y.; Angermund, K.; Goddard, R.; Kruger, C. *J. Am. Chem. Soc.* **1987**, *109*, 587.
(72) Delise, P.; Allegra, G.; Mognaschi, E. R.; Chierico, A. *J. Chem. Soc., Faraday Trans. 2* **1975**, *71*, 207.
(73) Braga, D.; Grepioni, F. *Polyhedron* **1990**, *1*, 53.
(74) Chhor, K.; Lucazeau, G. *J. Raman Spect.* **1982**, *13*, 235.
(75) Howard, J.; Robson, K.; Waddington, T. C. *J. Chem. Soc., Dalton Trans.* **1982**, 967.
(76) Braga, D.; Bürgi, H. B.; Grepioni, F.; Raselli, A. *Acta Crystallogr.*, in press.
(77) Aime, S.; Gobetto, R. Personal communication.
(78) (a) Jellinek, F. *J. Organomet. Chem.* **1963**, *1*, 43. (b) Keulen, E.; Jellinek, F. *J. Organomet. Chem.* **1966**, *5*, 490. (c) Cotton, F. A.; Dollase, W. A.; Wood, J. S. *J. Am. Chem. Soc.* **1963**, *85*, 1543. (d) Ibers, J. A. *J. Phys. Chem.* **1964**, *40*, 3129. (e) Förster, E.; Albrecht, G.; Dürselen, W.; Kurras, E. *J. Organomet. Chem.* **1969**, *19*, 215.
(79) Anderson, S. E. *J. Organomet. Chem.* **1974**, *71*, 263.
(80) Campbell, A. J.; Fyfe, C. A.; Harold-Smith, D.; Jeffrey, K. R. *Mol. Cryst. Liq. Cryst.* **1976**, *36*, 1.
(81) Bailey, M. F.; Dahl, L. F. *Inorg. Chem.* **1965**, *4*, 1298.
(82) Aime, S.; Braga, D.; Gobetto, R.; Grepioni, F.; Orlandi, A. *Inorg. Chem.* **1991**, *30*, 951.
(83) Koshland, D. E.; Myers, S. E.; Chesick, J. P. *Acta Crystallogr., Sect. B* **1977**, *B33*, 2013.
(84) Braga, D.; Grepioni, F. *Organometallics* **1991**, *10*, 2563.
(85) van Meurs, F.; van Konigsveld, H. J. *J. Organomet. Chem.* **1977**, *131*, 423.
(86) (a) Wagner, G. W.; Hanson, B. E. *Inorg. Chem.* **1987**, *26*, 2019. (b) Wey, H. G.; Betz, P.; Topalovic, I.; Butenschön, H. *J. Organomet. Chem.* **1991**, *411*, 369.
(87) Braga, D.; Grepioni, F. *J. Chem. Soc., Dalton Trans.* **1990**, 3143.
(88) (a) Harvey, P. D.; Butler, I. S.; Gilson, D. F. R. *Inorg. Chem.* **1987**, *26*, 32. (b) Butler, I. S.; Gilson, D. F. R.; Harvey, P. D. *Spectroscopy* **1986**, *1*, 40. (c) Howard, J.; Graham, D. *Spectrochim. Acta, Part A* **1985**, *41A*, 815.
(89) Clark, G. R.; Palenik, G. J. *J. Organomet. Chem.* **1973**, *50*, 185.
(90) Benn, R.; Mynott, R.; Topalovic, I.; Scott, F. *Organometallics* **1989**, *8*, 2299.
(91) (a) Sayer, I. *J. Chem. Soc., Chem. Commun.* **1988**, 227. (b) Fitzsimmons, B. W.; Hume, A. R. *J. Chem. Soc., Dalton Trans.* **1980**, 180. (c) Fitzsimmons, B. W.; Sayer, I. *J. Chem. Soc., Dalton Trans.* **1991**, 2907.
(92) Dunitz, J. D.; Orgel, L. E.; Rich, A. *Acta Crystallogr.* **1956**, *9*, 373.
(93) Edwards, J. W.; Kington, G. L.; Mason, R. *J. Chem. Soc., Faraday Trans.* **1959**, *55*, 660.
(94) Willis, B. T. M. *Acta Crystallogr.* **1961**, *13*, 1088.
(95) Calvarin, G.; Berar, J. F. *J. Appl. Crystallogr.* **1975**, *8*, 380.
(96) Takusagawa, F.; Koetzle, T. F. *Acta Crystallogr., Sect. B* **1979**, *B35*, 1074.
(97) Seiler, P.; Dunitz, J. D. *Acta Crystallogr., Sect. B* **1979**, *B35*, 1068.
(98) Seiler, P.; Dunitz, J. D. *Acta Crystallogr., Sect. B* **1979**, *B35*, 2020.
(99) Ogasahara, K.; Sorai, M.; Suga, H. *Chem. Phys. Lett.* **1979**, *68*, 457.
(100) Bérar, J. F.; Calvarin, G.; Weigel, D.; Chhor, K.; Pommier, C. *J. Chem. Phys.* **1980**, *73*, 438.
(101) Seiler, P.; Dunitz, J. D. *Acta Crystallogr. Sect. B* **1982**, *B38*, 1741.
(102) Seiler, P.; Dunitz, J. D. *Acta Crystallogr. Sect. B* **1980**, *B36*, 2946.
(103) Takusagawa, F.; Koetzle, T. F. A. C. A. Symposium; Eufaula, AL, 1980; Abstract D4, p 16.
(104) Seiler, P.; Dunitz,, J. D. *Acta Crystallogr., Sect. B* **1980**, *B36*, 2255.
(105) Calvarin, G.; Weigel, D. *J. Appl. Crystallogr.* **1976**, *9*, 212.
(106) Braga, D.; Grepioni, F. *Organometallics* **1992**, *11*, 711.
(107) Holm, C. H.; Ibers, J. A. *J. Chem. Phys.* **1959**, *30*, 885.
(108) Mulay, L. N.; Attalla, A. *J. Am. Chem. Soc.* **1963**, *85*, 702.
(109) Haeberlen, U.; Kohlschütter, U. *Chem. Phys.* **1973**, *2*, 76.
(110) Gardner, A. B.; Howard, J.; Waddington, T. C.; Richardson, R. M.; Tomkinson, J. *Chem. Phys.* **1981**, *57*, 453.
(111) Kubo, A.; Ikeda, R.; Nakamura, D. *Chem. Lett.* **1981**, 1497.
(112) Chhor, K.; Lucazeau, G.; Sourisseau, C. *J. Raman Spectr.* **1981**, *11*, 183.
(113) Sourisseau, C.; Dianoux, A. J.; Poinsignon, C. *Mol. Phys.* **1983**, *48*, 367.
(114) (a) Spiess, H. W.; Zimmermann, H.; Haeberlen, U. *Chem. Phys.* **1976**, *12*, 123. (b) Levendis, D. C.; Boeyens, J. C. A. *J. Crystallogr. Spectr. Res.* **1985**, *15*, 1.
(115) (a) Haaland, A.; Nilsson, J. E. *Acta Chem. Scand.* **1968**, *22*, 2653. (b) Hedberg, L.; Hedberg, K. *J. Chem. Phys.* **1970**, *53*, 1228. (c) Carter, S.; Murrell, J. N. *J. Organomet. Chem.* **1980**, *192*, 399.
(116) Freyberg, D. P.; Robbins, J. L.; Raymond, K. N.; Swart, J. C. *J. Am. Chem. Soc.* **1979**, *101*, 892.
(117) Wemmer, D. E.; Ruben, D. J.; Pines, A. *J. Am. Chem. Soc.* **1981**, *103*, 28.
(118) Almenningen, A.; Haaland, A.; Samdal, S.; Brunvoll, J.; Robbins, J. L.; Smart, J. C. *J. Organomet. Chem.* **1979**, *173*, 293.
(119) Wrackmeyer, B.; Sebald, A.; Merwin, L. H. *Magn. Reson. Chem.* **1991**, *29*, 260.
(120) Makova, M. K.; Lenova, E. V.; Karimov, Yu. S.; Kochetkova, N. S. *J. Organomet. Chem.* **1973**, *55*, 1973.
(121) Sato, K.; Katada, M.; Sano, H.; Konno, M. *Bull. Chem. Soc. Jpn.* **1984**, *57*, 2361.
(122) (a) Daniel, M. F.; Leadbetter, A. J.; Mazid, M. A. *J. Chem. Soc., Faraday Trans.* **1981**, *77*, 1837. (b) Sato, K.; Iwai, M.; Sano, H.; Konno, M. *Bull. Chem. Soc. Jpn.* **1984**, *57*, 634.
(123) Daniel, M. F.; Leadbetter, A. J.; Meads, R. E.; Parker, W. G. *J. Chem. Soc., Faraday Trans.* **1978**, *74*, 456.
(124) Daniel, M. F.; Leadbetter, A. J.; Richardson, I. J. *J. Chem. Soc., Faraday Trans.* **1981**, *2*, 1851.
(125) Epstein, E. F.; Bernal, I.; Kopf, H. *J. Organomet. Chem.* **1971**, *26*, 229.
(126) Muller, E. G.; Petersen, J. L.; Dahl, L. F. *J. Organomet. Chem.* **1976**, *111*, 91.
(127) McCall, J. M.; Shaver, A. *J. Organomet. Chem.* **1980**, *193*, C37.
(128) Prout, K.; Cameron, T. S.; Forder, R. A.; Critchley, S. R.; Denton, B.; Rees, G. V. *Acta Crystallogr., Sect. B* **1974**, *B20*, 2290.
(129) Butler, I. S.; Fitzpatrick, P. J.; Gilson, D. F. R.; Gomez, G.; Shaver, A. *Mol. Cryst. Liq. Cryst.* **1981**, *71*, 213.
(130) Clearfield, A.; Warner, D. K.; Saldamaga-Molina, C. H.; Ropal, R.; Bernal, I. *Can. J. Chem.* **1975**, *53*, 1622.
(131) (a) Benn, R.; Grondey, H.; Erker, G.; Aul, R.; Reiner, N. *Organometallics* **1990**, *9*, 2493. (b) Benn, R.; Grondey, H.; Nolte, R.; Erker, G. *Organometallics* **1988**, *7*, 777.

(132) Braga, D.; Grepioni, F.; Parisini, E. *Organometallics* **1991**, *10*, 3735.
(133) Howie, R. A.; McQuillan, G. P.; Thompson, D. W.; Lock, G. A. *J. Organomet. Chem.* **1986**, *303*, 213.
(134) Erker, G.; Engel, K.; Krüger, C.; Chiang, A. *Chem. Ber.* **1982**, *115*, 3311.
(135) Erker, G.; Mühlenbernd, T.; Benn, R.; Rufinska, A.; Tsay, Y.; Krüger, C. *Angew. Chem., Int. Ed. Engl.* **1985**, *24*, 321.
(136) Erker, G.; Sosna, F.; Petersen, J. L.; Benn, R.; Grondey, H. *Organometallics* **1990**, *9*, 2462.
(137) (a) Campbell, A. J.; Fyfe, C. A.; Goel, R. G.; Maslowsky, E.; Senoff, C. V. *J. Am. Chem. Soc.* **1972**, *94*, 8387. (b) Campbell, A. J.; Cottrell, C. E.; Fyfe, C. A.; Jeffrey, K. R. *Inorg. Chem.* **1976**, *15*, 1326.
(138) (a) Bennett, M. J.; Cotton, F. A.; Davison, A.; Faller, J. W.; Lippard, S. J.; Morehouse, S. M. *J. Am. Chem. Soc.* **1966**, *19*, 4371. (b) Calderon, J. L.; Cotton, F. A.; DeBoer, B. G.; Takats, J. *J. Am. Chem. Soc.* **1971**, *93*, 3592.
(139) Fisher, B.; Van Mier, G. P. M.; Boersma, J.; Van Koten, G.; Smeets, W. J. J.; Spek, A. L. *Rec. J. R. Neth. Chem. Soc.* **1988**, *107*, 259.
(140) Heyes, S. J.; Dobson, C. M. *J. Am. Chem. Soc.* **1991**, *113*, 463.
(141) (a) Bryan, R. F.; Greene, P. T.; Newlands, M. J.; Field, D. J. *J. Chem. Soc. A* **1970**, 3068. (b) Bryan, R. F.; Greene, P. T. *J. Chem. Soc. A* **1970**, 3064.
(142) Dorn, H. C.; Hanson, B. E.; Motell, E. *J. Organomet. Chem.* **1982**, *224*, 181.
(143) Aime, S.; Botta, M.; Gobetto, R.; Orlandi, A. *Magn. Reson. Chem.* **1990**, *28*, S52.
(144) Braga, D.; Gradella, C.; Grepioni, F. *J. Chem. Soc., Dalton Trans.* **1989**, 1721.
(145) Mitschler, A.; Rees, B.; Lehmann, M. S. *J. Am. Chem. Soc.* **1978**, *100*, 3390.
(146) Altbach, M. I.; Hiyama, Y.; Wittebort, R. J.; Butler, L. G. *Inorg. Chem.* **1990**, *29*, 741.
(147) (a) Wilson, F. C.; Shoemaker, D. P. *J. Chem. Phys.* **1957**, *27*, 809. (b) Adams, R. D.; Collins, D. M.; Cotton, F. A. *Inorg. Chem.* **1974**, *13*, 1086.
(148) Nardin, G.; Delise, P.; Allegra, G. *Gazz. Chim. Ital.* **1975**, *105*, 1047.
(149) Allegra, G.; Tettamanti Casagrande, G.; Immizzi, A.; Pozzi, L.; Vitulli, G. *J. Am. Chem. Soc.* **1970**, *92*, 289.
(150) Allegra, G.; Colombo, A.; Immirzi, A.; Bassi, I. W. *J. Am. Chem. Soc.* **1968**, *90*, 4455.
(151) Allegra, G.; Colombo, A.; Mognaschi, E. R. *Gazz. Chim. Ital.* **1972**, *102*, 1060.
(152) (a) Carbonaro, A.; Segre, A. L.; Greco, A.; Tosi, C.; Dall'Asta, G. *J. Am. Chem. Soc.* **1968**, *90*, 4453. (b) Mann, B. E. *J. Chem. Soc., Dalton Trans.* **1978**, 1761.
(153) Rogers, D. M.; Wilson, S. R.; Girolami, S. *Organometallics* **1991**, *10*, 2419.
(154) Avdeef, A.; Raymond, K. N.; Hodgson, K. O.; Zalkin, A. *Inorg. Chem.* **1972**, *11*, 1083.
(155) McGarvey, B. R.; Nagy, S. *Inorg. Chem.* **1987**, *26*, 4198.
(156) Dickens, B. D.; Lipscomb, W. N. *J. Chem. Phys.* **1962**, *37*, 2084.
(157) Campbell, A. J.; Cottrell, C. E.; Fyfe, C. A.; Jeffrey, K. R. *Inorg. Chem.* **1976**, *15*, 1321.
(158) Campbell, A. J.; Fyfe, C. A.; Maslowsy, E. *J. Am. Chem. Soc.* **1972**, *94*, 2690.
(159) Fleischer, E. B.; Stone, A. L.; Dewar, R. B. K.; Wright, J. D.; Keller, C. E.; Pettit, R. *J. Am. Chem. Soc.* **1966**, *88*, 3158.
(160) Bennett, M. J.; Cotton, F. A.; Legzdins, P. *J. Am. Chem. Soc.* **1968**, *90*, 6335.
(161) Lyerla, J. R.; Fyfe, C. A.; Yannoni, C. S. *J. Am. Chem. Soc.* **1979**, *101*, 1351.
(162) Cottrell, C. E.; Fyfe, C. A.; Senoff, C. V. *J. Organomet. Chem.* **1972**, *43*, 203.
(163) Ladell, J.; Post, B.; Fankuchen, I. *Acta Crystallogr.* **1952**, *5*, 795.
(164) Spiess, H. W.; Grosescu, R.; Haeberlen, U. *Chem. Phys.* **1974**, *6*, 226.
(165) Donohue, J.; Caron, A. *Acta Crystallogr.* **1964**, *17*, 663.
(166) Gleeson, J. W.; Vaughan, R. W. *J. Chem. Phys.* **1983**, *78*, 5384.
(167) (a) Hanson, B. E. *Metal-Metal Bonds and Clusters in Chemistry and Catalysis*; Fackler, J. P., Ed.; Plenum: New York, 1989; p 231. (b) Hanson, B. E. *J. Am. Chem. Soc.* **1989**, *111*, 6442. (c) Hanson, B. E.; Whitmire, K. H. *J. Am. Chem. Soc.* **1990**, *112*, 974.
(168) Cotton, F. A.; Troup, J. M. *J. Chem. Soc., Dalton Trans.* **1974**, 800.
(169) (a) Sumner, G. G.; Klug, H. P.; Alexander, J. E. *Acta Crystallogr.* **1964**, *17*, 732. (b) Leung, P. C.; Coppens, P. *Acta Crystallogr., Sect. B* **1983**, *39*, 535.
(170) Hanson, B. E.; Sullivan, M. J.; Davis, R. J. *J. Am. Chem. Soc.* **1984**, *106*, 251.
(171) (a) Braga, D.; Grepioni, F. *Polyhedron* **1989**, *8*, 2237. (b) Braga, D.; Grepioni, F.; Sabatino, P.; Gavezzotti, A. *J. Chem. Soc., Dalton Trans.* **1992**, 1185.
(172) Anson, C. E.; Benfield, R. E.; Bott, A. W.; Johnson, B. F. G.; Braga, D.; Marseglia, E. A. *J. Chem. Soc., Chem. Commun.* **1988**, 889.
(173) (a) Wei, C. H.; Dahl, L. F. *J. Am. Chem. Soc.* **1969**, *91*, 1351. (b) Cotton, F. A.; Troup, J. M. *J. Am. Chem. Soc.* **1974**, *96*, 4155.
(174) (a) Dorn, H.; Hanson, B. E.; Motell, E. *Inorg. Chim. Acta* **1981**, *54*, L71. (b) Hanson, B. E.; Lisic, E. C.; Petty, J. T.; Iannacone, G. A. *Inorg. Chem.* **1986**, *25*, 4062.
(175) Walter, T. H.; Reven, L.; Oldfield, E. *J. Phys. Chem.* **1989**, *93*, 1320.
(176) Churchill, M. R.; Fettinger, J. C. *Organometallics* **1990**, *9*, 752.
(177) Grandjean, F.; Long, G. J.; Benson, C. G.; Russo, U. *Inorg. Chem.* **1988**, *27*, 1524.
(178) Adams, H.; Bailey, N. A.; Bentley, G. W.; Mann, B. E. *J. Chem. Soc., Dalton Trans.* **1989**, 1831.
(179) Churchill, M. R.; Hollander, F. J.; Hutchinson, J. P. *Inorg. Chem.* **1977**, *16*, 2655.
(180) Aime, S.; Botta, M.; Gobetto, R.; Osella, D.; Milone, L. *Inorg. Chim. Acta* **1988**, *146*, 151.
(181) Battiston, G. A.; Bor, G.; Dietler, U. K.; Kettle, S. F.; Rossetti, R.; Sbrignadello, G.; Stanghellini, P. L. *Inorg. Chem.* **1980**, *19*, 1961.
(182) Gilson, T. R.; Evans, J. *J. Chem. Soc., Dalton Trans.* **1984**, 155.
(183) Churchill, M. R.; DeBoer, B. G. *Inorg. Chem.* **1977**, *16*, 878.
(184) Hasselbring, L.; Lamb, H.; Dybowski, C.; Gates, B.; Rheingold, A. *Inorg. Chim. Acta* **1987**, *127*, L49.
(185) (a) Wei, C. H. *Inorg. Chem.* **1969**, *8*, 2384. (b) Carrê, F. H.; Cotton, F. A.; Frenz, B. A. *Inorg. Chem.* **1976**, *15*, 380.
(186) Hanson, B. E.; Lisic, E. C. *Inorg. Chem.* **1986**, *25*, 716.
(187) Aime, S.; Botta, M.; Gobetto, R.; Hanson, B. E. *Inorg. Chem.* **1989**, *28*, 1196.
(188) Churchill, M. R.; Hutchinson, J. P. *Inorg. Chem.* **1978**, *17*, 5328.
(189) Corey, E. R.; Dahl, L. F.; Beck, W. J. *J. Am. Chem. Soc.* **1963**, *85*, 1202.
(190) Braga, D.; Grepioni, F.; Johnson, B. F. G.; Lewis, J.; Housecroft, C. E.; Martinelli, M. *Organometallics* **1991**, *10*, 1260.
(191) Braga, D.; Grepioni, F.; Johnson, B. F. G.; Lewis, J.; Martinelli, M. *J. Chem. Soc., Dalton Trans.* **1990**, 1847.
(192) Gallop, M. A.; Johnson, Lewis, J.; Raithby, P. R. *J. Chem. Soc., Chem. Commun.* **1987**, 1809.
(193) Heyes, S. J.; Gallop, M. A.; Johnson, B. F. G.; Lewis, J.; Dobson, C. M. *Inorg. Chem.* **1991**, *30*, 3850.
(194) Braga, D.; Grepioni, F.; Johnson, B. F. G.; Lewis, J.; Martinelli, M.; Gallop, M. A. *J. Chem. Soc., Chem. Commun.* **1990**, 53.
(195) Braga, D.; Grepioni, F.; Johnson, B. F. G.; Parisini, E.; Martinelli, M.; Gallop, M. A.; Lewis, J. *J. Chem. Soc., Dalton Trans.* **1992**, 807.
(196) Chen, H.; Johnson, B. F. G.; Lewis, J.; Braga, D.; Grepioni, F.; Parisini, E. *J. Chem. Soc., Dalton Trans.* **1991**, 215.
(197) Braga, D.; Grepioni, F.; Johnson, B. F. G.; Chen, H.; Lewis, J. *J. Chem. Soc., Dalton Trans.* **1991**, 2559.
(198) Farrugia, L. J. *Acta Crystallogr., Sect. C* **1988**, *C44*, 997.
(199) Gomez-Sal, M. P.; Johnson, B. F. G.; Lewis, J.; Raithby, P. R.; Wright, A. H. *J. Chem. Soc., Chem. Commun.* **1985**, 1682.
(200) (a) Sanford, W. E.; Boyd, R. K. *Can. J. Chem.* **1976**, *54*, 2773. (b) Allen, P. S.; Cowking, A. *J. Chem. Phys.* **1967**, *47*, 4286.
(201) (a) Cox, E. G.; Cruickshank, D. W. J.; Smith, J. A. S. *Proc. R. Soc. London Ser. A* **1958**, *247*, 1. (b) Bacon, G. E.; Curry, N. A.; Wilson, S. A. *Proc. R. Soc. London Ser. A* **1964**, *279*, 98.
(202) (a) Adams, D. M.; Ekejiuba, I. O. C. *J. Chem. Phys.* **1982**, *77*, 4793. (b) Adams, D. M.; Hatton, P. D.; Shaw, A. C.; Tan, T. *J. Chem. Soc., Chem. Commun.* **1981**, 226. (c) Huang, Y.; Butler, I. S.; Gilson, D. F. R. *Inorg. Chem.* **1991**, *30*, 1098. (d) Adams, D. M.; Davey, L. M.; Hatton, P. D.; Shaw, A. C. *J. Mol. Struct.* **1982**, *79*, 415. (e) Adams, D. M.; Ekejiuba, I. O. C. *J. Chem. Phys.* **1983**, *78*, 5408.
(203) Kurihara, T.; Ohashi, Y.; Sasada, Y.; Ohgo, Y. *Acta Crystallogr., Sect. B* **1983**, *B39*, 243. (b) Kurihara, T.; Uchida, A.; Ohashi, Y.; Sasada, Y.; Ohgo, Y. *J. Am. Chem. Soc.* **1984**, *106*, 5718. (c) Sekine, A.; Sakay, Y.; Uchida, A.; Ohashi, Y.; Aray, Y.; Ohgo, Y.; Kamiya, N.; Iwasaki, H. *Acta Crystallogr., Sect. A* **1990**, *A46*, C179. (d) Ohashi, Y.; Tomotake, Y.; Uchida, A.; Sasada, Y. *J. Am. Chem. Soc.* **1986**, *108*, 1196. (e) Uchida, A.; Ohashi, Y.; Sasada, Y.; Ohgo, Y.; Baba, S. *Acta Crystallogr., Sect. B* **1984**, *B40*, 473. (f) Uchida, A.; Dunitz, J. D. *Acta Crystallogr., Sect. B* **1990**, *B46*, 45 and references therein.
(204) Miller, E. J.; Brill, T. B.; Rheingold, A. L.; Fultz, W. C. *J. Am. Chem. Soc.* **1983**, *105*, 7580.

(205) Bianchini, C.; Peruzzini, M.; Zanobini, F. *Organometallics* **1991**, *10*, 3415.
(206) (a) Bernstein, J. *Organic Solid State Chemistry*; Desiraju, G. R., Ed.; Elsevier: Amsterdam, 1987; pp 471. (b) Bernstein, J.; Hagler, A. T. *J. Am. Chem. Soc.* **1978**, *100*, 673.
(207) (a) Raston, C. L.; White, A. L. *J. Chem. Soc., Dalton Trans.* **1976**, 7. (b) Etter, M. C.; Siedle, A. R. *J. Am. Chem. Soc.* **1983**, *105*, 641.